

# Synbiot Production and Encapsulation

A Thesis Submitted to the College of  
Graduate Studies and Research  
in Partial Fulfillment of the Requirements  
for the Degree of Master of Science  
in the Department of Food and Bioproduct Sciences  
University of Saskatchewan  
Saskatoon, SK

By

Kimberly Anne Wood

© Copyright Kimberly Anne Wood, June 2010. All rights reserved.

## **PERMISSION TO USE**

In presenting this thesis/dissertation in partial fulfillment of the requirements for a Postgraduate degree from the University of Saskatchewan, I agree that the Libraries of this University may make it freely available for inspection. I further agree that permission for copying of this thesis/dissertation in any manner, in whole or in part, for scholarly purposes may be granted by the professor or professors who supervised my thesis/dissertation work or, in their absence, by the Head of the Department or the Dean of the College in which my thesis work was done. It is understood that any copying or publication or use of this thesis/dissertation or parts thereof for financial gain shall not be allowed without my written permission. It is also understood that due recognition shall be given to me and to the University of Saskatchewan in any scholarly use which may be made of any material in my thesis/dissertation.

Requests for permission to copy or to make other uses of materials in this thesis/dissertation in whole or part should be addressed to:

Head of the Department of Food and Bioproduct Sciences

University of Saskatchewan

Saskatoon, Saskatchewan S7N 5A8

Canada

## ABSTRACT

The use of probiotics and prebiotics has become a popular trend in the food industry. The main goal of this study was to produce a synbiotic by encapsulating a probiotic and a prebiotic within a matrix that would provide sufficient protection to the probiotic against simulated gastric juice (SGJ). The ability of the probiotic, *Bifidobacterium adolescentis*, to grow on short chain fructooligosaccharides (FOS; DP 2-8, P95), inulin (DP 2-60, ST), and FOS/inulin mixture (DP 2-60, Syn), as well as glucose and a glucose-free maltooligosaccharide (MOS), were evaluated. *Bifidobacterium adolescentis* had a significantly higher specific growth rate on P95 ( $0.47\text{ h}^{-1}$ ), than glucose ( $0.40\text{ h}^{-1}$ ). Examination of the growth medium containing P95 and MOS by high performance anion exchange with pulsed amperometric detection (HPAE-PAD) revealed that *B. adolescentis* utilised the oligosaccharides to the same extent as the monosaccharides.

*Bifidobacterium adolescentis* was successfully encapsulated with and without P95 using extrusion and emulsion methods, at cell concentrations of 8-9 log colony forming units (CFU)  $\text{mL}^{-1}$ . Capsules formed by the extrusion method with 1.0% alginate (AL), 4.0% pea protein isolate (PPI) + 0.5% AL, and 4.0% whey protein isolate (WPI) + 0.5% AL ranged in geometric mean diameter from 2.0 to 2.2 mm. Capsules formed by emulsion with 4.0% WPI + 0.5% AL had geometric mean diameter of 53  $\mu\text{m}$ . Extrusion-based encapsulated probiotics in either PPI + AL or WPI + AL showed improved survival in SGJ at pH 2.0 for 2.0 h with log CFU  $\text{mL}^{-1}$  reductions of 3.6 and 1.1, respectively. Free cells, AL extrusion-based and WPI + AL emulsion-based encapsulated probiotics showed no survival after 30 min in SGJ at pH 2.0. The addition of 1.0% (w/w) P95 to the PPI + AL capsules improved probiotic survival such that 1.0 log CFU  $\text{mL}^{-1}$  reduction was observed. The amount of P95 encapsulated ranged from 4.0 to 4.4 mg per gram of capsules.

The external surface of the PPI + AL capsules as examined by cold stage scanning electron microscopy (cryo-SEM) and atomic force microscopy (AFM) was smooth with the presence of pores ranging in diameter from 0.25 to 1.00  $\mu\text{m}$ . The addition of P95 to

the capsules had no significant effect on surface roughness as measured by AFM, but significantly increased the external capsule thickness. The internal structure of the PPI + AL capsules examined by cryo-SEM revealed a porous honeycomb-like structure, with inner pore diameters ranging between 13.0 and 21.9  $\mu\text{m}$ . Probiotic cells were found to be randomly dispersed on the surface and in the interior of the honeycomb pores. In contrast, the prebiotic was found to be distributed throughout the capsule as observed by confocal laser scanning microscopy (CLSM), indicating that it would be readily available to the probiotic as a carbon source.

## **ACKNOWLEDGEMENTS**

I would like to sincerely thank my supervisors Drs. Nicholas Low and Michael Nickerson for their leadership, patience and support during my studies. They allowed me to have a lot of independence in my project which I am very thankful for. They were very approachable, funny and easy to get along with. I want to thank them for giving me the opportunity to travel to many scientific conferences where I was able to learn exciting new research in the area of food science. Lastly I want to thank them for allowing me the time to discover my true calling and the support they gave me while pursuing that dream, which I am glad to say, has become a reality.

To all of my co-workers in Drs. Nicholas Low and Michael Nickerson lab I want to thank you for creating a very positive and enjoyable work environment. Our conversations and laughs made lab work something I looked forward to. In particular, I would like to thank Yuanlong Cao and Kelci Ottenbreit for all their help in the first year of my degree, their input was invaluable.

All the cryo-SEM work was performed by George Braybrook at the University of Alberta. Jason Maley at the Saskatchewan Structural Sciences Centre helped me with the AFM work. I would also like to thank Dr. Art Davis for all his input on sample preparation for CLSM and SEM.

I would also like to thank that Department of Food and Bioproduct Sciences, the Canadian Dairy Commission, NSERC and the Advanced Food and Materials Network for the financial support they all provided me during my studies. I appreciated the opportunity to work as a teaching assistant for Food Chemistry and Food Analysis classes. The funding provided from these sources was very helpful to me.

To my parents, Barbara and Derek Wood, I owe much gratitude. They were there through all of it, the good and the bad, giving me advice, support and love. Thanks to my brothers, David and Christopher, and my sister-in-law, Alina, for listening when mom and dad were not available.

Lastly, to my friends, you are the people that helped me get away from my school life and whom I experienced what else life had to offer. To the people I go shopping with, played sports with and otherwise enjoyed the subtleties of life with, I thank you. I hope you are all successful in your future.

## TABLE OF CONTENTS

PERMISSION TO USE.....	i
ABSTRACT.....	ii
ACKNOWLEDGEMENTS.....	iv
TABLE OF CONTENTS.....	vi
LIST OF TABLES.....	x
LIST OF FIGURES .....	xi
LIST OF ABBREVIATIONS.....	xv
1. Introduction .....	1
2. Literature Review .....	3
2.1 Probiotics .....	3
2.1.1 Definition.....	3
2.1.2 Classified probiotics .....	3
2.1.2.1 <i>Lactobacillus spp.</i> .....	3
2.1.2.2 <i>Bifidobacterium spp.</i> .....	4
2.1.2.3 <i>Streptococcus spp.</i> .....	4
2.1.3 Health benefits.....	5
2.1.4 Challenges associated with probiotic use .....	7
2.2 Prebiotics.....	9
2.2.1 Definition.....	9
2.2.2 Ingredients used as prebiotics.....	9
2.2.2.1 Fructooligosaccharides.....	10
2.2.2.2 Galactooligosaccharides.....	12
2.2.2.3 Maltooligosaccharides.....	12
2.2.2.4 Pectin.....	14
2.2.3 Health benefits.....	14
2.2.4 Challenges associated with prebiotic use .....	17

2.3	Synbiots.....	17
2.3.1	Benefits of synbiots .....	17
2.4	Encapsulation .....	17
2.4.1	Extrusion.....	18
2.4.2	Emulsion.....	20
2.4.3	Wall materials.....	21
2.4.3.1	Alginate .....	21
2.4.3.2	Whey protein isolates .....	23
2.4.3.3	Pea protein isolates .....	25
2.5	Imaging techniques .....	25
2.5.1	Scanning electron microscopy.....	25
2.5.2	Cold stage scanning electron microscopy (cryo-SEM) .....	28
2.5.3	Atomic force microscopy (AFM).....	29
2.5.4	Confocal laser scanning microscopy (CLSM).....	31
2.5.4.1	Fluorescence.....	34
3.	Material and Methods.....	38
3.1	Materials.....	38
3.2	Study 1: Investigation on the effects of wall material and capsule size on the survivability of encapsulated <i>B. adolescentis</i> in simulated gastric juice (SGJ).....	39
3.2.1	Microorganisms.....	39
3.2.2	Comparison of the growth profile of <i>B. adolescentis</i> in MRS and RCM broths .....	39
3.2.3	Preparation of <i>B. adolescentis</i> for encapsulation.....	40
3.2.4	Encapsulation of <i>B. adolescentis</i> in protein and/or alginate.....	40
3.2.4.1	Extrusion .....	41
3.2.4.2	Emulsion.....	41
3.2.5	Analysis of capsule morphology, geometric mean and percent distribution.....	42
3.2.6	Survival of free and encapsulated <i>B. adolescentis</i> in SGJ.....	42
3.3	Study 2: Investigation of the growth potential of <i>B. adolescentis</i> on a selection of carbohydrates, and the effect of the encapsulated synbiot on probiotic survival in SGJ.....	43
3.3.1	Preparation of glucose-free maltooliogaccharide (MOS).....	43
3.3.2	Comparison of <i>B. adolescentis</i> specific growth rates in a semi-synthetic medium containing different carbohydrates.....	44



3.3.3	Carbohydrate profile analysis of the semi-synthetic medium containing FOS and MOS .....	44
3.3.3.1	High performance anion exchange – pulsed amperometric detection (HPAE-PAD).....	45
3.3.3.2	Synbiot encapsulation with FOS (P95) and its effect on the survival of <i>B. adolescentis</i> in SGJ.....	45
3.3.4	Examination of the concentration and type of FOS (P95) encapsulated .....	46
3.3.5	Enumeration of <i>B. adolescentis</i> before and after drying .....	46
3.4	Study 3: Investigation of the external and internal morphology of the pea protein-alginate capsules and determination of the spatial distribution of fluorescently-labelled glucose and <i>B. adolescentis</i> within these capsules.....	47
3.4.1	Derivatization of glucose.....	47
3.4.2	Labelling of <i>B. adolescentis</i> with propidium iodide (PI) .....	48
3.4.3	Production of pea protein-alginate capsules containing GLU-FA .....	48
3.4.4	Production of pea protein-alginate capsules containing PI-labelled <i>B. adolescentis</i> .....	48
3.4.5	Preparation of capsules for confocal laser scanning microscopy .....	48
3.4.6	Confocal laser scanning microscopy .....	49
3.4.7	Cold stage scanning electron microscopy .....	50
3.4.8	Atomic force microscopy .....	50
3.5	Statistics .....	51
4.	Results and Discussion.....	52
4.1	Study 1: Investigation on the effects of wall material and capsule size on the survivability of encapsulated <i>B. adolescentis</i> in SGJ.....	52
4.1.1	Comparison of the growth profile of <i>B. adolescentis</i> in MRS and RCM broths .....	52
4.1.2	Capsule geometric mean, surface morphology and size distribution ....	54
4.1.3	Survival of free and encapsulated <i>B. adolescentis</i> in SGJ.....	57
4.1.4	Summary and conclusions .....	60
4.2	Study 2: Investigation of the growth potential of <i>B. adolescentis</i> on a selection of carbohydrates, and the effect of the encapsulated synbiot on probiotic survival in SGJ.....	62
4.2.1	Comparison of <i>B. adolescentis</i> specific growth rates in a semi-synthetic media containing different carbohydrates.....	62
4.2.2	HPAE-PAD analysis of the carbohydrate profile of the medium containing P95 (FOS) and MOS before and after incubation with <i>B. adolescentis</i> .....	65

4.2.3	Synbiot encapsulation with FOS (P95) and its effect on the survival of <i>B. adolescentis</i> in SGJ .....	68
4.2.4	Enumeration of <i>B. adolescentis</i> before and after drying .....	72
4.2.5	Summary and conclusions .....	73
4.3	Study 3: Investigation of the external and internal structures, size and shapes of the pea protein-alginate capsules, and determination of the spatial distribution of prebiotics and probiotics within these capsules .....	75
4.3.1	Examination of the external surface, size and shape of capsules .....	75
	that external pores were present but the cryo-SEM images failed to show them. The external wall thickness of the AL capsules was not determined as freeze fracturing was unsuccessful in producing a clean edge. ....	82
4.3.2	Examination of the internal structure of the capsules .....	82
4.3.3	Prebiotic and probiotic distribution within the capsules .....	85
4.3.4	Summary and conclusions .....	93
5.	Conclusions .....	94
6.	Future Directions .....	97
7.	References .....	99

## LIST OF TABLES

Table 4-1	Geometric mean diameter of capsules produced by extrusion and emulsion methods determined by PSA.....	57
Table 4-2	Percent change in carbohydrate abundance in P95 after 24 h of <i>B. adolescentis</i> cell growth in a basal media containing P95 as the carbon source.....	66
Table 4-3	Percent P95 in extrusion-based capsules and supernatant.....	69
Table 4-4	Internal and external wall and pore sizes for AL and PPI + AL capsules...	80

## LIST OF FIGURES

Figure 2-1	Structure of fructooligosaccharide with a terminal glucose, $n = 1 - 9$ (adapted from Gibson & Roberfroid, 1995).....	11
Figure 2-2	Structure of galactooligosaccharides, $n = 1-9$ (adapted from Roberfroid, 2000).....	13
Figure 2-3	Structure of pectin (adapted from Walter, 1991).....	15
Figure 2-4	Process flow diagram for the encapsulation of probiotics by extrusion (A) and emulsion-based (B) techniques (adapted from Krasaekoopt et al., 2003).....	19
Figure 2-5	Structure of alginate: composed of $\beta$ -D-mannuronic acid (M) and $\alpha$ -L-guluronic acid (G) (adapted from Sabra & Deckwer, 2005). ....	22
Figure 2-6	Schematic of an SEM showing the Wehnelt assembly with filament (A), anode aperture (B), electron beam (C), condenser lenses (D), deflector coils (E), deflector coils (L), cathode ray tube (CRT) (M), specimen (F) on stage (G), and electrons (I), striking collector (H), amplifier (J), and feeding voltage (K) (adapted from Dykstra, 1992).....	27
Figure 2-7	Block diagram of a laser deflection contact AFM (adapted from Kaupp, 2006).....	30
Figure 2-8	Schematic of an AFM probe (adapted from Rugar & Hansma, 1990).....	32
Figure 2-9	Simple diagram of how an image is acquired by CLSM (adapted from Hibbs, 2004a).....	33
Figure 2-10	Reductive amination of glucose using fluoresceinamine I and $\text{NaCNBH}_3$ (adapted from Borch et al., 1971).....	36
Figure 4-1	Optical density (A) and cell numbers (B) for growth curves of <i>B. adolescentis</i> in (○) MRS-cys and (●) RCM-cys broths. Data points represent the mean value and the range is represented by the bars. ....	53
Figure 4-2	Particle size distribution (%) determined by particle size analysis of capsules produced by extrusion and emulsion methods.....	55

Figure 4-3	SEM micrographs of freeze- (A, D, and E) and air-dried (B, C, and F) extrusion based capsules produced with AL (A, B); PPI + AL (C, D); WPI + AL (E, F). Magnification at 9.3x. ....	56
Figure 4-4	Survival of free- and extrusion-based encapsulated <i>B. adolescentis</i> cells in SGJ at pH 6.0 (A), pH 3.0 (B) and pH 2.0 (C), detection limit of 1.3 and 2.6 log CFU mL <sup>-1</sup> for free and encapsulated cells, respectively. Data represents the mean value ± one standard deviation (n = 3). ....	58
Figure 4-5	Survival of free- and emulsion-base encapsulated <i>B. adolescentis</i> cells in SGJ at pH 6.0 (A), pH 3.0 (B) and pH 2.0 (C), detection limit of 1.3 and 2.6 log CFU mL <sup>-1</sup> for free and encapsulated cells, respectively. Data represents the mean value ± one standard deviation (n = 3). ....	61
Figure 4-6	Specific growth rates of <i>B. adolescentis</i> on different carbohydrate samples; Glu (10.0 g L <sup>-1</sup> glucose); ST (10.0 g L <sup>-1</sup> Orafti® ST); P95 (10.0 g L <sup>-1</sup> Orafti® P95); Syn (10.0 g L <sup>-1</sup> Orafti® Synergy1); Neg (no carbohydrate); Min Glu (0.85 g L <sup>-1</sup> glucose); MOS (10.0 g L <sup>-1</sup> glucose free maltooligosaccharide). Data represents the mean value ± one standard deviation (n = 3). Notations (*) and (**) represent a significant change in specific growth rate from glucose and minimal glucose, respectively (p < 0.05). ....	63
Figure 4-7	HPAE-PAD carbohydrate elution patterns present at time 0 (A) and after 24 h of <i>B. adolescentis</i> growth (B). DP 2 = maltose, DP 3 = maltotriose, DP 4 = maltotetraose, DP 5 = maltopentaose, DP 6 = maltohexaose (glucose relative retention time ~ 6 min). ....	67
Figure 4-8	HPAE-PAD carbohydrate profiles for the P95 standard and the homogenized 1.0% AL + P95 extrusion-based capsules. (F= fructose, DP 2-6 = [βF-1→2]n, n = 2-6). ....	70
Figure 4-9	Survival of free- and encapsulated <i>B. adolescentis</i> cells with and without P95 in SGJ at pH 2.0 for 1.0%AL (A), 4.0% WPI + 0.5% AL (B) 4.0% PPI + 0.5% AL (C). Data represents the mean value ± one standard deviation (n = 3). ....	71

Figure 4-10	<i>B. adolescentis</i> cell counts before and after drying in the extrusion-based capsules containing P95. Data represents the mean value $\pm$ one standard deviation (n = 3).	74
Figure 4-11	Cryo-SEM micrographs of the external surface of 4.0% PPI + 0.5% AL capsules in the absence (A, B) and presence (C, D) of <i>B. adolescentis</i> . Rectangles indicate the areas in A and C that are magnified in B and D, respectively, and white arrows indicate pores.	76
Figure 4-12	AFM topographical images (5.0 x 5.0 $\mu$ m) of 4.0% PPI + 0.5% AL capsules in the absence (A), and presence (B) of P95. Arrows indicate possible external pores.	77
Figure 4-13	Cryo-SEM micrographs showing the exterior surface of: 4.0% PPI + 0.5% AL + <i>B. adolescentis</i> (A); and 4.0% PPI + 0.5% AL + <i>B. adolescentis</i> + P95 (B) capsules. White arrows indicate presumptive <i>B. adolescentis</i> cells.	78
Figure 4-14	Cryo-SEM micrographs showing the exterior surface of 1.0% AL capsules.	81
Figure 4-15	Cryo-SEM micrographs of the internal structures of 1.0% AL capsules illustrating the large hollow (A) and small filamentous containing (B) honeycomb pores. The rectangle indicates the area in A magnified in B.	83
Figure 4-16	Cryo-SEM micrographs showing the internal structures of capsules composed of: 4.0% PPI + 0.5% AL + <i>B. adolescentis</i> (A, B); and 4.0% PPI + 0.5% AL + <i>B. adolescentis</i> + P95 (C, D).	84
Figure 4-17	Cryo-SEM micrographs showing the presence of bacteria in capsules composed of: 4.0% PPI + 0.5% AL + <i>B. adolescentis</i> (A,B); and 4.0% PPI + 0.5% AL + <i>B. adolescentis</i> + P95 (C). White arrows indicate <i>B. adolescentis</i> cells.	87

Figure 4-18	CLSM images of: <i>B. adolescentis</i> labelled with PI (A); 4.0% PPI + 0.5% AL capsules (B); and 4.0% PPI + 0.5% AL + <i>B. adolescentis</i> labelled with PI (C) capsules. Images taken with a 40x objective lens, attenuation, brightness and contrast for all images were the same. $\lambda_{\text{ex}} = 488 \text{ nm}$ $\lambda_{\text{em}} = 573\text{-}647 \text{ nm}$ .....	88
Figure 4-19	CLSM images of capsules comprised of: 4.0% PPI + 0.5% AL + impure GLU-FA (A); 4.0% PPI + 0.5% AL + 0.005 M FA (B) and 4.0% PPI + 0.5% AL + DMSO (C). Attenuation, brightness and contrast for all images were the same. $\lambda_{\text{ex}} = 488 \text{ nm}$ $\lambda_{\text{em}} = 495\text{-}525 \text{ nm}$ . ....	89
Figure 4-20	CLSM images of 4.0% PPI + 0.5% AL + DMSO + GLU-FA capsules showing carbohydrate distribution in centre cross-sections (A, B, and D) and peripheral cross-section (C) of the capsules. Images were taken with a 10x objective lens. $\lambda_{\text{ex}} = 488 \text{ nm}$ $\lambda_{\text{em}} = 495\text{-}525 \text{ nm}$ .....	91
Figure 4-21	Cryo-SEM micrographs showing the porous external surface of 4.0% PPI + 0.5% AL + DMSO + GLU-FA (A) and the flattening of the internal pores of 4.0% PPI + 0.5% AL + DMSO (B), capsules. ....	92

## LIST OF ABBREVIATIONS

AFM	Atomic Force Microscopy
AL	Alginate
CFU	Colony Forming Unit
CLSM	Confocal Laser Scanning Microscopy
Cryo-SEM	Cold Stage Scanning Electron Microscopy
°C	Degrees Celcius
DE	Dextrose Equivalent
DMSO	Dimethyl Sulfoxide
DP	Degree of Polymerization
FA	Fluoresceinamine Isomer I
FOS	Fructooligosaccharides
HPAE-PAD	High Performance Anion Exchange Chromatography with Pulsed Amperometric Detection
M	Molar
mg	Milligram
ml	Milliliter
mM	Millimolar
MOS	Glucose-Free Maltooligosaccharides
MRS	De man, Rogosa Sharpe Media
N.A.	Numerical Aperture
NaCNBH <sub>3</sub>	Sodium Cyanoborohydride
nm	Nanometer
P95	Short Chain FOS, Orafti® P95
PBS	Phosphate Buffer Saline
PI	Propidium Iodide
PPI	Pea Protein Isolate
PS	Peptone Saline
PSA	Particle Size Distribution Analyzer



RCM	Reinforced Clostridial Media
Rf	Retention Factor
RI	Refractive Index
SEM	Scanning Electron Microscopy
SGJ	Simulated Gastric Juice
SHIME	Simulator of the Human Intestinal Microbial Ecosystem
ST	Inulin, Orafti® ST
SYN	FOS and Inulin Mixture, Orafti® Synergy 1
TLC	Thin Layer Chromatography
WPI	Whey Protein Isolate

## 1. Introduction

The consumption of probiotics has become widely popular with health conscious consumers. Probiotics are a live microbial supplement that improves the host's health by altering its intestinal flora (Fuller, 1989). Probiotics have been reported to have several health benefits associated with their consumption such as, a decrease in lactose malabsorption, a decrease in intestinal infection via competitive exclusion, suppression of cancer and a reduced risk of coronary heart disease (Gibson & Wang, 1994a; Kulkarni & Reddy, 1994; Agerbaek et al., 1995; Fooks et al., 1999). Although probiotics have been purported as having many health benefits, they must maintain viability during their transit through the gastrointestinal tract to reach the colon in a concentration of  $10^7$  live cells per gram of intestinal contents for the host to experience any of these benefits (Bouhnik, 1993). Classified as a probiotic, *Bifidobacteria*, are very sensitive to the low pH of the stomach (pH 2.0) and their viability tends to be lost after 30 min of exposure. Several strategies have been investigated to improve probiotic survival such as the use of prebiotics, which act as a probiotic growth promoter, along with encapsulation. Prebiotics are non-digestible carbohydrates that stimulate the growth of the probiotics present in the colon (Gibson & Roberfroid, 1995). The administration of prebiotics to the diet has been proven to increase probiotic numbers when the organisms are already present in the colon (Gibson et al., 1995). There are health benefits associated with prebiotic consumption such as the ability to decrease the number of detrimental bacteria and increase the number of beneficial bacteria found in the gastrointestinal tract, reduce plasma triacylglycerols and provide constipation relief (Delzenne & Roberfroid, 1994; Tomomatsu, 1994; Fiordaliso et al., 1995; Gibson & Roberfroid, 1995). However, prebiotics will only increase the number of probiotics already present in the colon. Therefore, to increase the survival of supplemented probiotics, encapsulation techniques have been studied (Krasakoopt et al., 2003). Encapsulation is the process by which a bioactive ingredient(s) (e.g., probiotics) is entrapped or coated with a matrix material (e.g., protein and/or polysaccharide; Risch, 1995). Alginate (AL), a linear

heteropolysaccharide of D-mannuronic and L-guluronic acid, is the most popular material used in the encapsulation of probiotics because it is biocompatible, inexpensive, and easy to use (Krasaekoopt et al., 2004). However, studies have shown that AL capsules do not significantly increase probiotic survival in the presence of simulated gastric juice (SGJ; Lee & Heo, 2000; Sultana et al., 2000; Truelstrup-Hansen et al., 2002). Encapsulation offers much promise to the probiotic industry as probiotics are generally selected for their ability to survive the low pH of the stomach, however, through successful encapsulation the industry can select probiotics based on their health effects.

The overall goal of this research project was to encapsulate the probiotic, *Bifidobacterium adolescentis*, and a prebiotic within a protein and/or AL mixture that could provide sufficient protection to the probiotic against SGJ. Several objectives were established to meet this goal. The first objective of this research project was to investigate the effect of wall materials, AL, WPI and PPI (individually and in combination) and the size of the microcapsules on the survival of *B. adolescentis* in SGJ as a function of pH. The second objective was to investigate the growth potential of *B. adolescentis* on a commercial oligosaccharide (prebiotic) mixture and to incorporate the prebiotic with the best growth potential into the capsules to produce a synbiot. The final objective was to investigate the external and internal structures of the designed capsule and to determine the spatial distribution of the prebiotic and probiotic within that design.

## **2. Literature Review**

### **2.1 Probiotics**

#### **2.1.1 Definition**

Probiotics were first defined in 1971 as “organisms and substances which contribute to the intestinal microbial balance” (Sperti, 1971). However, this definition includes substances such as antibiotics, so in 1989 a more refined definition was established for probiotics as a live microbial supplement which beneficially affects the host by improving its intestinal microbial balance (Fuller, 1989). This definition suggests that the organism must be viable in order to be classified as a probiotic. Fuller (1992), suggested this definition be modified such that for an organism to be classified as a probiotic it must have the following characteristics:

1. they retain their viability after being processed on an industrial scale;
2. they must be stable and viable during use and during long periods of storage;
3. they must be able to survive the gastrointestinal tract; and
4. they must create a beneficial affect for the host.

#### **2.1.2 Classified probiotics**

There are three main genera of bacteria used as probiotics; *Lactobacillus*, *Bifidobacterium* and *Streptococcus* (Fuller, 1992). Other less common bacteria used as probiotics belong to the genera *Leuconostoc*, *Pediococcus*, *Propionibacterium* and *Bacillus*. Some yeasts, *Saccharomyces cerevisiae* and *Candida pintolopesii*, and moulds, *Aspergillus niger* and *Aspergillus oryzae*, have also been used as probiotics in animal feed.

##### **2.1.2.1 *Lactobacillus* spp.**

Lactobacilli bacteria are large, non-spore forming, gram-positive rods, that have anaerobic or microaerophilic respiration (Fooks et al., 1999). Gram-positive bacteria have a thick peptidoglycan layer as part of their cell wall whereas gram-negative bacteria

have a thin layer (Alcamo, 1997). Anaerobic bacteria will not grow in the presence of oxygen and therefore an atmosphere devoid of oxygen must be present in order for growth. Microaerophilic organisms are organisms that require a lower concentration of oxygen than that found in air. Lactobacillus bacteria are microaerophilic and are commonly used as a starter culture in yogurt production and are the most commonly used probiotics in foods (Fuller, 1992). Lactobacillus species used as probiotics include *L. delbreuckii* subspecies *bulgaricus*, *L. acidophilus*, *L. casei*, *L. germentum*, *L. plantarum*, *L. brevis*, *L. cellobious*, *L. lactis* and *L. reuteri*.

#### **2.1.2.2 *Bifidobacterium* spp.**

*Bifidobacteria* are large, gram-positive branch shaped rods that are microaerophilic (Fuller, 1992). The use of *Bifidobacteria* as probiotics started with work done by Tisser, in 1905. He showed that infants who were breast-fed had *Bifidobacteria* as the dominant organisms in their feces, and he implied that formula-fed infants did not (Fuller, 1992). *Bifidobacterium* spp. can make up to 25% of the total colonic microflora in adults and 95% in infants with the predominant species being *B. adolescentis* and *B. longum* in adults and *B. infantis* and *B. breve* in infants (Gibson & Roberfroid, 1995; Gibson et al., 1997). Recent studies showed that there was no difference in the amount of *Bifidobacteria* present in breast-fed and formula-fed infants (Penders et al., 2005). However, there was a difference in the amount of pathogenic bacteria present in these two infant groups. Breast-fed infants had 15% less *Clostridium difficile* and 14% less pathogenic *Escherichia coli*, two organisms known to cause diarrhea. The difference in microflora between the two infant groups may be explained by the type of bifidobacteria present (Fuller, 1992). The bifidobacteria species classed as probiotics are very important when assessing the beneficial health effects of these organisms. Bifidobacteria classed as probiotics include, *B. adolescentis*, *B. animals*, *B. bifidum*, *B. infantis*, *B. longum* and *B. thermophilum* (Fuller, 1992).

#### **2.1.2.3 *Streptococcus* spp.**

Streptococci are small gram-positive cocci that are usually found in pairs or short chains (Fooks et al., 1999). These organisms are facultative anaerobes, meaning they can grow in the presence or absence of oxygen (Alcamo, 1997). *Streptococcus salivarius*

subspecies *thermophilus*, was first used as a probiotic in sour milk and yogurt, and is still commonly used as a started culture for yogurt (Fuller, 1992). Other Streptococci that are classed as probiotics include, *S. lactis*, *S. cremoris*, *S. diatilactis* and *S. intermedius* (*S. anginosus*) (Fuller, 1992).

### **2.1.3 Health benefits**

Many potential health benefits have reportedly been associated with the use of probiotics. Benefits that have been reported with the ingestion of probiotics include a decrease in lactose malabsorption, a reduced risk of coronary heart disease, a decrease in intestinal and vaginal infections, suppression of cancer, and the production of B vitamins (Gibson & Roberfroid, 1995; Fooks et al., 1999; Reid, 2002). Although these are significant health claims, there is much scepticism in this area with research turning towards proving efficacy.

Lactose malabsorption is very common, as it affects over half of the world's population (Fooks et al., 1999). This condition results from an insufficient activity of lactase ( $\beta$ -galactosidase) in the human gut. Lactase hydrolyzes lactose into glucose and galactose. Without this conversion an individual will experience abdominal distension, increased flatulence and/or diarrhea. Lactic acid bacteria produce lactase which has the ability to hydrolyze lactose into its monosaccharide components, which are more efficiently digested. Fermented dairy products, such as yogurt, that contain probiotics are more easily digested by the majority of the population than non-fermented products, such as milk.

It has been reported that dairy products fermented by probiotics have the ability to reduce LDL-cholesterol in humans, and reduce the risk of coronary heart disease development (Fooks et al., 1999). In one case, 58 healthy Danish men were subjected to a six week feeding trial where half ingested a fermented milk product that contained the probiotic, *S. thermophilus*, and the other half ingested a placebo (Agerbaek et al., 1995). The LDL-cholesterol levels in the probiotic fed group were reduced by 10% when compared to the control. The HDL-cholesterol and triacylglycerol levels were similar for both groups.

The administration of probiotics has been reported to reduce pathogenic bacteria populations in the colon, which may result in a reduction of intestinal infections. The

gastrointestinal tract contains up to  $10^{12}$  live bacteria cells per gram of intestinal content, therefore, competition arises between microbial species for nutrients and colonization (Gibson & Wang, 1994a). Some bacteria can produce an inhibitory effect against others in order to increase their chances of survival. Several Bifidobacteria spp. have been proven to have such an effect. In a study by Gibson & Wang (1994a), it was shown that eight species of *Bifidobacteria*, *B. bifidum*, *B. adolescentis*, *B. angulatum*, *B. catenulatum*, *B. breve*, *B. infantis*, *B. longum* and *B. pseudolongum* were able to inhibit the growth of the following pathogenic bacteria *in vitro*: *Vibrio cholera*, *Shigella sonnei*, *Listeria monocytogenes*, *E. coli*, *Campylobacter* spp., *Salmonella* spp., *Clostridium perfringens* and *Bacteroides fragiles*.

Colon cancer is one of the leading causes of cancer deaths in the United States. Probiotics have been associated with the prevention of this disease. In a study by Kulkarni & Reddy (1994), *B. longum* was fed to rats in order to observe its effect against azoxymethane-induced preneoplastic lesions such as aberrant crypt foci, which have been associated with colon cancer. The study concluded that the feeding of *B. longum* inhibited aberrant crypt foci formation by 53%, indicating preventative potential. In another study, the feeding of *B. longum* to humans for five weeks resulted in a decrease in the proportion of bacteriodes and lecithinase-negative clostridia found in the participant's feces (Benno & Mitsuoka, 1992). Lecithinase-negative clostridia species have been found to constitute a high proportion of fecal microflora in colon cancer patients and have been implicated in the formation of carcinogens from bile acids. These two studies (Kulkarni & Reddy, 1994; Benno & Mitsuoka, 1992) indicate that there is definite potential for some probiotic species to aid in the prevention of colon cancer.

Bifidobacteria have the ability to produce water-soluble vitamins such as thiamine, nicotinic acid, folic acid, vitamin B<sub>12</sub> and biotin (Deguchi et al., 1985; Noda et al., 1994). *Bifidobacterium bifidum* and *B. infantis* were able to synthesize thiamine, nicotinic acid and folic acid in significantly higher concentrations whereas other species, such as *B. breve* and *B. longum* produced these vitamins in lower concentrations (Deguchi et al., 1985). In contrast, *B. adolescentis* was not able to produce any of these vitamins. *B. bifidum* and *B. adolescentis* were able to produce a large amount of biotin

extracellularly, 158.0 and 27.4  $\mu\text{g L}^{-1}$  respectively, when grown in media containing isomaltooligosaccharides.

There are many potential health benefits associated with the use of probiotics, most being preventative in nature. However, more research must be conducted in order to confirm these health claims and understand the roles of probiotics in the human diet.

#### **2.1.4 Challenges associated with probiotic use**

There are documented challenges associated with the consumption of probiotics because viability must be maintained in order for them to have a beneficial effect. For this to occur they must arrive at the colon at a concentration of  $10^7$  live cells per gram of intestinal content (Bouhnik, 1993). However, the human body is designed to prevent illness by reducing the amount of foreign bacteria present in the gastrointestinal tract. The low pH of the stomach can negatively affect the amount of viable probiotics that can reach the colon. One study using a dynamic model of the stomach and small intestine indicated that after 110 min in the gastric compartment, viable counts for *S. thermophilus* and *L. bulgaricus* were less than 1%, 60% for *L. acidophilus* and 80% for *B. bifidum* (Marteau et al., 1997). Bile salts in the small intestine can also play a destructive role with viable counts reaching the colon of less than 10% for *S. thermophilus* and *L. bulgaricus*, 15% for *L. acidophilus* and 30% for *B. bifidum*. The majority of bifidobacteria are especially sensitive to acidic conditions. When initial counts of 8 log CFU  $\text{mL}^{-1}$  of *B. breve* and *B. longum* were exposed to SGJ at a pH between 1.5 and 2.0 for 30 min the bacteria experienced a 6 and 7 log CFU  $\text{mL}^{-1}$  reduction in numbers, respectively (Lee & Heo, 2000; Picot & Lacroix, 2004). In contrast, *B. bifidum* cell counts decreased by 4.75 log units after exposure to SGJ at pH 2.5 for 1 h and showed no survival after 2 h (Guerin et al., 2003). *Bifidobacterium adolescentis*, *B. breve*, *B. lactis* and *B. longum* were exposed to SGJ at pH 2.0 for 30 min and all strains were reduced by 5 log CFU  $\text{mL}^{-1}$ , where initial counts were approximately 8 log CFU  $\text{mL}^{-1}$  (Truelstrup-Hansen et al., 2002). The acid resistance of *B. lactis* decreased only 1 log unit after being exposed to SGJ at pH 2 for 2.0 h, but did not survive after being exposed to SGJ at pH 1.0 for 1 h (Favaro-Trindade & Grosso, 2002). Lorca & de Valdez (2001) found that *L. acidophilus* grown in a media with an uncontrolled pH (4.5) in comparison to a controlled pH (pH 6.0) had increased acid tolerance when the bacteria reached their



stationary phase. Protein profiles of the more acid tolerant strain showed an over expression of 16 proteins, 7 were expressed as a result of the stationary phase and 9 were expressed as a result of a drop in culture pH. This approach could help determine acid resistant strains by their protein profiles in response to the stationary phase of growth. Because probiotics are sensitive to the low pH of the stomach, they must be protected in some fashion in order to reach the colon in sufficient numbers to exert a beneficial effect.

Probiotic viability also decreases during product processing and storage (Mattila-Sandholm et al., 2002). When probiotics are subjected to freeze drying or spray drying their viability decreases. Therefore, the selection of a strain that will withstand processing is also very important. In yogurt, a 78% decline in the population *B. longum* after 30 d of storage at 4 °C has been reported (Adhikari et al., 2000). Another problem associated with probiotics is their ability to adhere to the intestinal wall. Bouhnik et al. (1992), showed that the recovery rate of *Bifidobacterium spp.* in the feces of human volunteers was consistent with their percent survival (approximately 30%) during transit through the gastrointestinal system, indicating that the bifidobacteria were not effectively adhering to the intestinal wall. The authors observed that after ending probiotic administration their presence in feces also stopped. If the bacteria do not adhere to the colon wall their ability to produce beneficial health effects may be compromised. These problems can be strain specific and can be mitigated with screening in order to find a suitable strain. However, health benefits are also strain specific, therefore the identification of resistant and health promoting probiotic may be difficult, and different methods to increase probiotic survival are investigated. Using different methods other than strain selection for probiotic survival will allow researchers to incorporate strains that have greater associated health properties. Prebiotics can be used to increase the growth potential of the probiotic in the gastrointestinal system and increase its viability during storage. Encapsulation provides an additional means for improving the viability of probiotics, due to the protective effect of their wall materials.

## **2.2 Prebiotics**

### **2.2.1 Definition**

Prebiotics were defined by Gibson & Wang (1994b) as “a non-digestible food ingredient that beneficially affects the host by selectively stimulating the growth and/or activity of one or a limited number of bacteria in the colon, and thus improves host health”. Food ingredients that pass through the upper part of the digestive system without being absorbed or hydrolysed by human enzymes are referred to as colonic foods. Colonic foods act as nutrients for endogenous colonic bacteria and indirectly provide the host with energy, metabolic substrates (short chain fatty acids), and essential minerals. Prebiotics are colonic foods but not all colonic foods are prebiotics.

For a food ingredient to be classified as a prebiotic it must meet the following criteria (Gibson & Roberfroid, 1995):

1. it cannot be hydrolysed or absorbed in the upper part of the digestive system;
2. it must cause the growth and/or activation of one or a limited number of beneficial colonic bacteria by being a selective substrate;
3. it must be able to change the microflora of the colon to a healthier composition; and
4. it must induce beneficial luminal or systemic effects to the health of the host.

### **2.2.2 Ingredients used as prebiotics**

Food ingredients considered to have prebiotic qualities are some non-digestible carbohydrates (oligo and polysaccharides), some peptides and proteins, and some lipids (Gibson & Roberfroid, 1995). Non-digestible carbohydrates are the most commonly used prebiotic because they are naturally occurring and some are able to fulfill all of the aforementioned criteria. Non-digestible carbohydrates include: resistant starch (starch which is not hydrolysed in the small intestine), non-starch polysaccharides (hemicellulose, pectins, gums), and oligosaccharides (galactooligosaccharides, fructooligosaccharides [FOS]) (Gibson & Roberfroid, 1995; van Dokkum & van den Heuvel, 2001).

Oligosaccharides are generally characterized to be comprised of 2-9 monosaccharides covalently linked together, whereas polysaccharides are more than 9 monosaccharides in length (Roberfroid, 2000). However, there are very few naturally

occurring polysaccharides that contain less than 25 to 30 monosaccharides, therefore the term oligosaccharide is given to carbohydrate polymers ranging in size from 2 to 20-25 monosaccharides (Lin et al., 1988). Oligosaccharides are water-soluble and have relatively low sweetness values of 0.3 to 0.6, where sucrose has a value of 1.0 (Crittenden & Playne, 1996). Their sweetness depends on their monosaccharide composition and structure. Oligosaccharides are considered to be good bulking agents because they have a low relative sweetness, and their high molecular weight improves product viscosity and mouthfeel. Oligosaccharides are commonly used in the production of low caloric and diabetic foods.

Methods used to produce non-digestible oligosaccharides are: (1) hot water extraction of roots (Roberfroid, 2000), such as inulin extraction from chicory root; (2) enzyme hydrolysis of oligosaccharides or polysaccharides such as xylooligosaccharide production by the action of xylanase on pectin; and (3) the use of osyl-transferases, which can be used to synthesize oligosaccharides from a mixture of disaccharides such as FOS production from sucrose.

#### **2.2.2.1 Fructooligosaccharides**

Fructooligosaccharides or oligofructose is the only oligosaccharide that meets all prebiotic criteria (Gibson & Roberfroid, 1995). FOS consists of  $\beta$ -(1 $\rightarrow$ 2) glycosidic bonded  $\beta$ -D-fructose moieties (Figure 2-1; Roberfroid, 2000) that can have two structures, one consisting of all fructose moieties and the other having a terminal D-glucose  $\alpha$ -(1 $\rightarrow$ 2) linked to a fructose molecule. Inulin is the main polysaccharide for FOS production and is naturally found in chicory and Jerusalem artichoke roots (Roberfroid, 2000). FOS can be produced by inulin hydrolysis with acid or inulase and from sucrose using osyl-transferases.

The growth of most bifidobacteria species are found to be improved when FOS was used as the carbohydrate source but not when inulin was used. In a study by Rossi et al. (2005), it was observed that of the 55 strains of bifidobacteria studied, the majority (52) were able to utilize FOS as a carbon source whereas only 8 could utilize inulin. Species belonging to *B. longum*, and *B. animalis* had increased growth rates when cultured in media containing 1.0% (w/v) FOS (degree of polymerization, DP 2-4) and Raftilose™ (DP 2-8, glucose + fructose + lactose < 6.8%), when compared to their

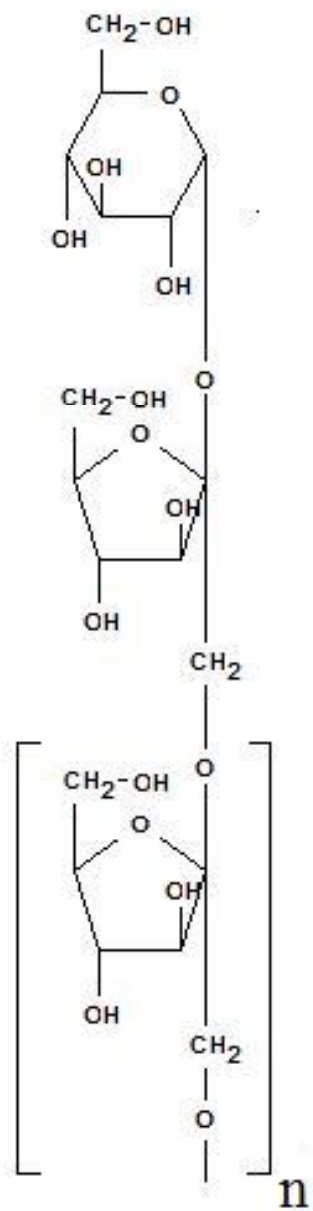


**Figure 2-1** Structure of fructooligosaccharide with a terminal glucose,  $n = 1 - 9$  (adapted from Gibson & Roberfroid, 1995).

growth rates with inulin (Bielecka et al., 2002). Eight species of bifidobacteria, *B. infantis*, *B. catenulatum*, *B. pseudolongum*, *B. longum*, *B. angulatum*, *B. breve*, *B. bifidum* and *B. adolescentis* were grown in media containing branched FOS (average DP = 13, 8% branching), FOS (average DP = 4), inulin (average DP = 10) and glucose. Each of the organisms preferred FOS over the other carbon sources with the exception of *B. bifidum* which grew best in the presence of glucose (Gibson & Wang, 1994b). The inability of *B. bifidum* to ferment FOS was reported by Kaplan & Hutkins (2000). In their study the growth rate of *B. adolescentis*, *B. breve*, *B. bifidum*, *B. infantis*, and *B. longum* on De man, Rogosa Sharpe plates (MRS) containing 2.0% (w/v) FOS and 30 mg bromocresol purple per liter (which creates a yellow zone around the colonies if the carbohydrate was fermented) showed that only *B. bifidum* was not a FOS fermentor.

#### 2.2.2.2 Galactooligosaccharides

Galactooligosaccharides (Figure 2-2) are composed of  $\beta$ -D-galactose units that are bonded through  $\beta$ -(1 $\rightarrow$ 6) glycosidic linkages with a terminal  $\alpha$ -(1 $\rightarrow$ 4) linked glucose (Roberfroid, 2000). This group of oligosaccharides are produced from lactose with osyl-transferases.

*Bifidobacterium infantis*, *B. lactis* and *B. longum* were found to have higher growth rates (0.131 h<sup>-1</sup>, 0.091 h<sup>-1</sup> and 0.116 h<sup>-1</sup>, respectively) when galactooligosaccharides were used as the main carbon source when compared to those for glucose of 0.058 h<sup>-1</sup>, 0.075 h<sup>-1</sup> and 0.095 h<sup>-1</sup>, respectively (Vernazza et al., 2006).

#### 2.2.2.3 Maltooligosaccharides

Maltooligosaccharides or glucooligosaccharides are composed of  $\alpha$ -D glucose molecules bonded through  $\alpha$ -(1 $\rightarrow$ 4) glycosidic linkages (Crittenden & Playne, 1996). They are produced by treating starch molecules with isoamylase or pullanase to destroy the branch points followed by treatment with  $\alpha$ -amylase to hydrolyze the  $\alpha$ -1-4 linkages to produce oligosaccharides of various lengths.

Maltooligosaccharides are generally considered to have the ability to promote the growth of bifidobacteria in the human colon (Crittenden & Playne, 1996). Research has shown that a diet rich in a maltotetraose enriched corn syrup reduced the level of *Clostridium perfringens* in the colon (Crittenden & Playne, 1996). In a study observing

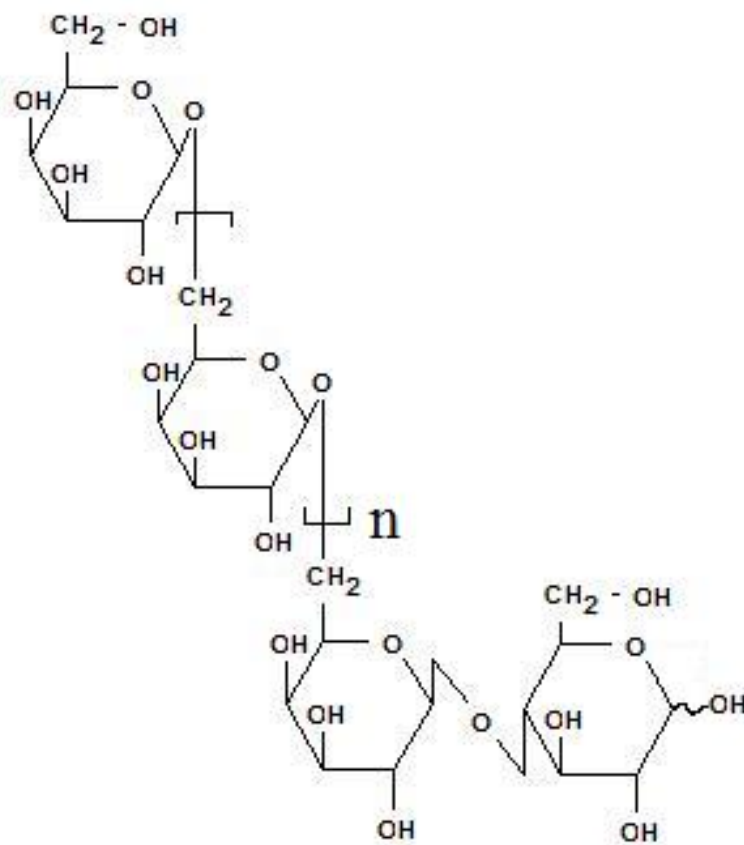


**Figure 2-2** Structure of galactooligosaccharides,  $n = 1-9$  (adapted from Roberfroid, 2000).

the growth of five Bifidobacteria strains (*B. adolescentis*, *B. infantis*, *B. lactis*, and two strains of *B. longum*) where maltooligosaccharides were used as the sole carbon source, only *B. lactis* showed growth ( $0.041 \text{ h}^{-1}$ ), whereas all others showed minimal ( $0.009 \text{ h}^{-1}$ ) or no growth (Vernazza et al., 2006). However, to be considered a prebiotic, oligo/polysaccharides must be able to reach the colon, and maltooligosaccharides are generally digested in the small intestine.

#### **2.2.2.4 Pectin**

Pectin is composed of  $\alpha$ -(1, 4)-linked D-galacturonic acid and its methyl ester (Figure 2-3). Pectin can be classified as high or low methoxy depending on the degree of esterification (Walter, 1991). High methoxy pectin has a degree of esterification greater than 50%, whereas low methoxy pectin has less than 50%. Pectin is a major byproduct from the juice industry, however little research on the prebiotic effect of this carbohydrate has been conducted. Some bifidobacteria are able to grow on low methoxy (8% degree of esterification) pectin but not on high methoxy (66% degree of esterification) pectin (Olano-Matrin et al., 2002; Guerin et al., 2003).

#### **2.2.3 Health benefits**

Prebiotics have been associated with several health benefits. Some of the more scientifically studied include an increase of beneficial bacteria and a decrease in detrimental bacteria located in the gastrointestinal tract, increased absorption of minerals/cations, reduced plasma triacylglycerols, and constipation relief (Delzenne & Roberfroid, 1994; Tomomatsu, 1994; Fiordaliso et al., 1995; Gibson et al., 1995).

Fructooligosaccharides and inulin have been found to increase bifidobacteria numbers and to reduce those of harmful bacteria in the human colon (Gibson et al., 1995). As an example, eight participants were subjected to a 45 d study where they consumed 15 g of sucrose per day for 15 d, then 15 g of FOS (Raftilose, DP 2-8) or inulin (Raftiline, average DP of 10) was administered for the next 15 d. For the last 15 d of the trial, FOS or inulin was substituted with 15 g of sucrose per day. The subjects' bowel habits, transit time, stool composition and predominant genera of stool bacteria were measured. The authors found that both FOS and inulin increased stool frequency by 14%

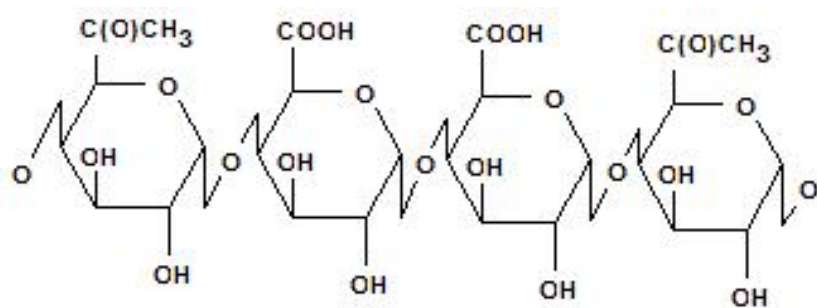


**Figure 2-3** Structure of pectin (adapted from Walter, 1991).



and 34%, respectively. The participant's stool microflora was measured, and the authors found that both FOS and inulin increased bifidobacteria numbers from 8.8 to 9.5 log g stool<sup>-1</sup> to 9.2 to 10.1 log g stool<sup>-1</sup>, while bacteroides, clostridia and fusobacteria numbers decreased. The authors concluded that the consumption of dietary FOS or inulin could improve intestinal health and help prevent constipation (Gibson et al., 1995). Roberfroid (2000) reported that in a large majority of studies where prebiotic oligosaccharides were administered, increases in bifidobacteria numbers rarely exceeded 0.5 of a log unit, with the average population in the feces before treatment ranging from 9.5 to 10 log CFU g<sup>-1</sup>, and reaching a maximum of 10.5 log CFU g<sup>-1</sup> after treatment. This observation questions the physiological significance of prebiotic consumption.

The use of prebiotics has also been associated with better absorption of divalent cations in the colon (Gibson & Roberfroid, 1995). This was confirmed in rat studies, where a diet that contained FOS or inulin was found to improve intestinal uptake of the minerals Ca<sup>2+</sup>, Mg<sup>2+</sup> and Fe<sup>2+</sup> by 60–65% (Delzenne & Roberfroid, 1994). If the same results could be observed in humans, then a diet rich in FOS or inulin could possibly increase the efficiency of mineral absorption, alleviating Fe<sup>2+</sup> and Ca<sup>2+</sup> deficiencies.

High plasma triacylglycerols and cholesterol increase an individual's risk of developing coronary heart disease, a leading cause of death in North America. FOS has been shown to have a positive effect in reducing plasma triacylglycerols, phospholipids and cholesterol (Fiordaliso et al., 1995). As an example, rats on a diet containing 10% FOS showed reduced plasma triacylglycerols (25% decrease), phospholipids (15% decrease) and cholesterol (15% decrease). Therefore, a diet rich in FOS may lower plasma triacylglycerol levels, reducing the risk of developing coronary heart disease. Although, FOS and inulin have been associated with health benefits, very little work has been done with other prebiotic oligosaccharides. More research is needed in this area to clearly establish the health benefits of these compounds and to determine if the health effects observed in animal studies are also found in humans.

#### **2.2.4 Challenges associated with prebiotic use**

There are a few documented problems associated with prebiotic consumption. The major one is that over consumption of FOS can cause diarrhea, flatulence and abdominal discomfort (Crittenden & Playne, 1996). It has been reported that the minimum dose of FOS that causes diarrhea is 40 – 50 g per day (Crittenden & Playne, 1996).

### **2.3 Synbiotics**

Synbiotics are defined as “a mixture of probiotics and prebiotics that beneficially affect the host by improving the survival and implantation of live microbial dietary supplements in the gastrointestinal tract, by selectively stimulating their growth and/or by activating the metabolism of one or a limited number of health-promoting bacteria and thus improving welfare” (Gibson & Roberfroid, 1995). Probiotics and prebiotics can be administered as separate entities or they can be combined (synbiotic) in forms such as microcapsules.

#### **2.3.1 Benefits of synbiotics**

The combination of prebiotics with probiotics could produce several nutritional benefits (Gibson & Roberfroid, 1995; Poo-Zobel et al., 2002; Rastall & Maitin, 2002) including: an increase in the survival rate of live bacteria in food products, increased protection against colon cancer, an increase in the number of viable bacteria that reach the colon, increased growth and implantation of the bacteria in the colon and an increase in the metabolic activation of these bacteria. In Japan, a legal standard of  $10^7$  viable probiotic cells per milliliter is required in fresh dairy products such as yogurt (Krasaekoopt et al., 2003). The pH of yogurt ranges from 4.2 to 4.6, which is too low for most bifidobacteria to remain viable, and they will lose their viability within the first week of storage (Adhikari et al., 2000).

### **2.4 Encapsulation**

Encapsulation is the process by which a bioactive ingredient(s) is entrapped or coated with a wall material (Risch, 1995). If the particle size formed by encapsulation is

between 0.2 to 5000  $\mu\text{m}$  then the process is referred to as microencapsulation (Risch, 1995). However, the definition of what makes a capsule a microcapsule is not well defined, and all capsules, microcapsules and not will be referred to as capsules. The material to be coated or entrapped can be a liquid, solid or gas, can be either living or non-living and is referred to as the core material or active ingredient, such as the probiotic. The material that forms the coat is referred to as the wall material, membrane or coating. Wall materials most commonly used for encapsulation of food ingredients are hydrocolloids (Roberfroid, 2000; Anal & Singh, 2007). Hydrocolloids from natural sources are used in the food industry and include starch, maltodextrins, gum Arabic, celluloses, agar, gelatin, carrageenans, alginates, low methoxy pectin, whey protein and gellan gum (Risch, 1995).

A common step in the microencapsulation process is spray drying; however it is not commonly used for probiotics because it causes high cell injury and death. For example, *L. rhamnosus* encapsulated by spray drying in a media that contained 10% (w/v) polydextrose resulted in a viability loss of >90% (Corcoran et al., 2003). However, Picot & Lacroix (2004) developed a procedure whereby probiotics were embedded in milk fat and then spray dried with only minimal loss of cell viability.

Two techniques commonly used for the encapsulation of probiotics are extrusion (droplet method) and emulsion (two-phase system) (Krasaekoopt et al., 2003). In these methods the hydrocolloids commonly used are anionic and include carrageenan, alginate, low methoxy pectin and gellan gum (Risch, 1995).

#### **2.4.1 Extrusion**

This method is the oldest and most commonly used technique to make capsules with hydrocolloids (Krasaekoopt et al., 2003). Extrusion is the most popular technique used for the encapsulation of probiotics because of its ease, simplicity, low cost and gentle formulation conditions that ensures a high retention of viable cells. The method (Figure 2-4 A) involves the preparation of a hydrocolloid solution to which the active ingredient is added, and then extruded through a syringe (forming droplets) into a setting (cross-linking) solution (Risch, 1995; Krasaekoopt et al., 2003). Gel spheres form

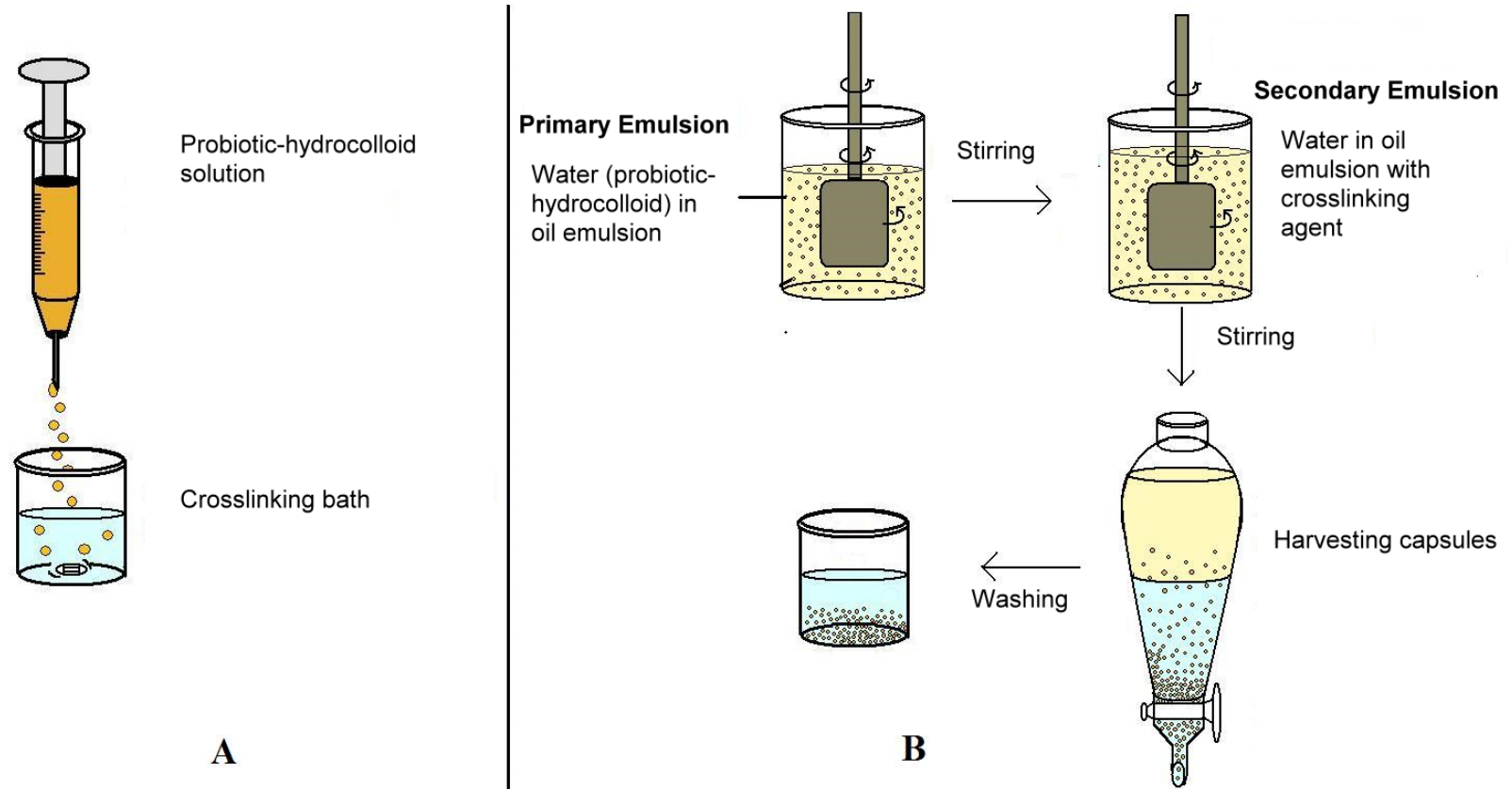


**Figure 2-4** Process flow diagram for the encapsulation of probiotics by extrusion (A) and emulsion-based (B) techniques (adapted from Krasaekoopt et al., 2003).

immediately upon the droplets coming into contact with the cross-linking solution, entrapping the core material within a three-dimensional lattice (Krasaekoopt et al., 2003). Prebiotics can be incorporated into the capsules by adding them into the hydrocolloid solution along with the probiotic and therefore entrapping them together, or by applying an additional coating post-capsule formation. The diameter of the capsules depends on the diameter of the syringe, hydrocolloid concentration, solution viscosity and the distance between the syringe and the cross linking solution.

#### **2.4.2 Emulsion**

This technique involves two phases, a discontinuous and a continuous phase (Krasaekoopt et al., 2003). The discontinuous phase contains both the probiotic and the hydrocolloid polymer in which the probiotic will be encapsulated, and the continuous phase consists of a large volume of vegetable oil such as soybean, canola or corn (Figure 2-4 B). The discontinuous phase is added to the continuous phase and the two are homogenized to form a water-in-oil emulsion. Tween 80 or another emulsifier is usually added to the continuous phase at concentrations of 0.2 and 0.5% to ensure homogeneity (Sultana et al., 2000; Truelstrup-Hansen et al., 2002; Krasaekoopt et al., 2003; Muthukumarasamy et al., 2006). Once the emulsion has formed, a cross-linking solution is added to precipitate the water-soluble hydrocolloids to form gel particles within the oil (Krasaekoopt et al., 2003) and the capsules are phase separated. The size of the capsules is controlled by the speed of agitation and the concentration of the hydrocolloid, and typically has a wide distribution range of 25  $\mu\text{m}$  to 2 mm.

Probiotics encapsulated in alginate (AL) by the emulsion technique have not generally been shown to significantly improve survivability. *Lactobacillus acidophilus* and *Bifidobacterium* spp. encapsulated in 2% AL and 2% Hi-maize™ starch formed by the emulsion method ranged in size from 0.5 to 1 mm and did not improve probiotic survival as the viability numbers for the encapsulated cells were similar to those of the free cells (Sultana et al., 2000). Four bifidobacteria species were microencapsulated in 1% AL using the emulsion technique (Truelstrup-Hansen et al., 2002) to produce two capsule sizes with geometric means of 19 and 67  $\mu\text{m}$ . The capsules contained

approximately 8 log viable CFU mL<sup>-1</sup> bacteria cells and were subjected to SGJ at pH 2.0, 3.0 and 6.0 for 2 h. The study concluded that encapsulation did not improve the survival of the bacteria, as the numbers of surviving cells for the encapsulated bacteria were similar to those for free cells. Whereas, *Bifidobacterium infantis* and *B. bifidum* were encapsulated in 3% sodium AL by the emulsion method and were protected when incorporated in mayonnaise (Khalil & Mansour, 1998). Encapsulated cell counts remained stable in the mayonnaise for 8 to 10 weeks where numbers reached 5.8 and 5.7 log CFU g<sup>-1</sup> for *B. bifidum* and *B. infantis*, respectively, whereas free cells decreased to 4 log CFU g<sup>-1</sup> after 1 week of storage at 5°C.

### **2.4.3 Wall materials**

#### **2.4.3.1 Alginate**

Alginate is the wall material most commonly used for the extrusion capsule formation method (Krasaekoopt et al., 2003). AL is a polysaccharide extracted from various brown algae and is comprised of monomeric units of  $\alpha$ -L-guluronic acid (G) and  $\beta$ -D-mannuronic acid (M) (Figure 2-5; Sabra & Deckwer, 2005). AL can be composed of G and M units in three different ways: a) homopolymeric G blocks, b) homopolymeric M blocks, or c) heteropolymeric G-M blocks where G and M sequences are randomly arranged either as alternating G-M units or as short interchanging G and M blocks interspersed by individual G and M units. All three blocks types may be present within a single AL molecule. The gel forming properties of AL is largely dependent on the block structure and chain length of the molecule. AL gels are formed by the addition of cation such as Ca<sup>2+</sup> in the form CaCl<sub>2</sub>. Calcium is the preferred cation and binds preferentially to the G units, which creates crosslinks within and between the AL molecules and forms what is known as an egg-box model (Sabra & Deckwer, 2005). Alginates rich in G units form strong, dense, and brittle gels whereas ALs rich in M units form soft elastic gels

Alginate-based capsules formed by extrusion increase the survival of probiotics as the polysaccharide concentration and capsule size increase (Chandramouli et al., 2004; Lee & Heo, 2000). *Lactobacillus acidophilus* was encapsulated by a modified extrusion method, where the capsules were formed by syringe injection using compressed air

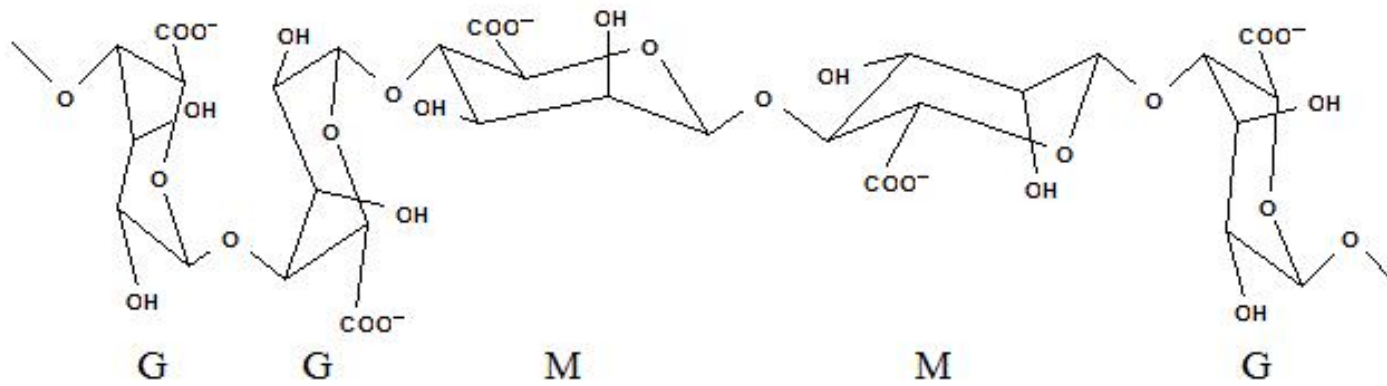
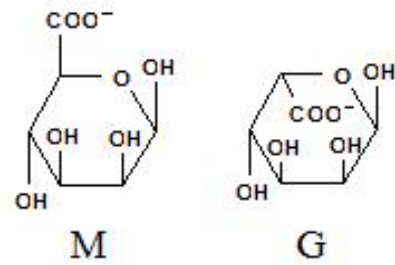


**Figure 2-5** Structure of alginate: composed of  $\beta$ -D-mannuronic acid (M) and  $\alpha$ -L-guluronic acid (G) (adapted from Sabra & Deckwer, 2005).

(Chandramouli et al., 2004). Different AL concentrations, capsule sizes and  $\text{CaCl}_2$  concentrations were investigated to determine optimal conditions for the survival of *L. acidophilus*. This study concluded that cell viability increased as AL concentration (0.75-2.0%) and capsule size (200, 450, and 1000  $\mu\text{m}$ ) increased. There was no significant increase in the survivability of encapsulated cells as the concentration of  $\text{CaCl}_2$  (0.1, 0.2 and 1.0 M) increased. Encapsulated *L. acidophilus* (1.8% AL with a capsule size of 450  $\mu\text{m}$ ) experienced a 3 log reduction in numbers, whereas the free cells experienced a 5 log reduction when exposed to SGJ at pH 2.0 for 3 h when initial cell counts were 9 log CFU  $\text{mL}^{-1}$ . Lee & Heo (2000) performed a similar study where *B. longum* was encapsulated by extrusion using syringe/compressed air; AL concentrations (2, 3 and 4%) and capsule size (1.03, 1.75 and 2.62 mm) were studied in order to observe their effects on probiotic survival in SGJ. Free cells and cells entrapped in 2% AL, with initial cell numbers of 9 and 6 log CFU  $\text{mL}^{-1}$  respectively, were all dead after 2 h, whereas cells entrapped with 3% AL were reduced to 2 log CFU bead $^{-1}$  (initial count 6.5 log CFU bead $^{-1}$ ) and 7 log CFU bead $^{-1}$  for cells entrapped in 4% AL (initial count 7.5 log CFU bead $^{-1}$ ), under the same conditions. Although the extrusion method is capable of increasing the survival of probiotics in numbers high enough to produce a beneficial health effect, it is not practical on an industrial scale because the beads produced are too large to be incorporated into foods as they can or may adversely affect texture (Truelstrup-Hansen et al., 2002).

#### **2.4.3.2 Whey protein isolates**

Whey protein isolate (WPI), on average, consists of 90-92% protein, 0.5-1.0% lactose, 0.5-1.0% lipid, 2-3% ash and 4-5% moisture (Kilara & Vaghela, 2004). The most abundant protein found in whey is  $\beta$ -lactoglobulin, and it comprises about 58% of the total protein content and has a molecular weight of 18.3 kDa. The second most prevalent whey protein is  $\alpha$ -lactalbumin with a molecular weight of 14.1 kDa. Other proteins found in WPI are bovine serum albumin, immunoglobulins and proteose peptones. Proteose peptones are defined as the proteins that remain soluble after the milk has been heated at 95°C for 2 h and acidified to pH 4.7.



The formation of a gel (or wall matrix) with whey protein first involves, the unfolding of protein molecules followed by the formation of a three-dimensional ordered aggregate (Jost, 1993). Whey proteins are heated at 80-85°C for 15-30 min at pH 7 to induce denaturation and polymerization into higher molecular weight soluble aggregates, creating a turbid and low viscosity solution (whey protein concentration of ~4%). The heat-denatured solution is cooled to room temperature, and the addition of NaCl or CaCl<sub>2</sub> results in gel formation (Hongprabhas & Barbut, 1997). The cations bind to the pre-heated whey proteins causing further protein modification, which causes the aggregates to form a network or a gel. Gelation of the heat-treated whey protein occurs more slowly with the use of NaCl than with CaCl<sub>2</sub> (Bryant & McClements, 2000). A possible reason for this is that Ca<sup>2+</sup> ions are more effective at screening protein electrostatic interactions than Na<sup>+</sup>, and that Ca<sup>2+</sup> ions are capable of forming ion-bridges between negatively charged amino acids on protein molecules.

Whey protein isolates have been shown to increase the survival of probiotics in SGJ by either the addition of the isolate to the bacterial culture or as a wall material for encapsulation. *Bifidobacterium infantis* was subjected to SGJ at pH 2.0 for 3 h in the presence of 1 g L<sup>-1</sup> WPI (Charteris et al., 1998). The presence of WPI significantly improved survivability when compared to bacteria incubated in SGJ without WPI. *Lactobacillus rhamnosus* was encapsulated by extrusion using a 70:30 mixture of 12% WPI:bacteria via injection through a 23 gauge needle into a setting solution (16.7% CaCl<sub>2</sub>, 0.1% peptone and 0.04% Tween 20). The capsules were droplet-shaped, opaque and had a diameter of 2.8 mm. This material was subjected to a dynamic gastrointestinal model which varied in pH from 4.4 to 2.0 over 90 min (Reid et al., 2005). Entrapped cells experienced a 2.4 log CFU mL<sup>-1</sup> reduction in viability when initial numbers were 6.2 log CFU mL<sup>-1</sup> and the free cells experienced a 4 log CFU mL<sup>-1</sup> reduction. *Bifidobacterium breve* and *B. longum* were encapsulated in 10% WPI by spray drying (Picot & Lacroix, 2004). Free cells and encapsulated cells were subjected to SGJ at pH 1.9 for 30 min where initial cell counts were around 8 log CFU mL<sup>-1</sup>. Cell numbers for encapsulated and free cells for *B. breve* after 30 min were 2 and 1 log CFU mL<sup>-1</sup>, respectively, and less than 1 log CFU mL<sup>-1</sup> for both the encapsulated and free *B. longum*

cells. Although these processes increased probiotic survival they did not do so at numbers sufficient to likely create a beneficial health effect to the host.

#### **2.4.3.3 Pea protein isolates**

Pea protein isolate (PPI) is composed of 88-92% protein, 0.5% lipid, 4-6% ash, and 4-5% carbohydrate (Franco et al., 2000). The major globular proteins in pea protein isolate are legumin (11S) and vicilin (7S) (Ducel et al., 2004). Legumin has a molecular weight of 330 kDa and an isoelectric point (pI) of 4.8 (Derbyshire et al., 1976), whereas vicilin has a molecular weight of 150 kDa and a pI of 5.5 (Bastista et al., 2005). For pea proteins to form a gel structure they must unfold exposing functional groups, such as sulfhydryl or hydrophobic moieties (Batista et al., 2005). No research results have been published using pea protein as a wall material for probiotic/synbiotic encapsulation.

### **2.5 Imaging techniques**

To gain a better understanding of how the process of encapsulation improved probiotic protection to SGJ, researchers have used capsule/core material imaging employing microscopy techniques such as scanning electron microscopy (SEM), atomic force microscopy (AFM), and confocal laser scanning microscopy (CLSM). These techniques offer the visualization of the external and internal structure and substructures of the capsules. In the following sections these imaging techniques are briefly reviewed, along with selected applications related to their use in elucidating capsule morphology.

#### **2.5.1 Scanning electron microscopy**

Scanning electron microscopy offers advantages over other microscopy techniques such as transmission electron microscopy (TEM) as the sample size can be much larger and images have a greater depth of field. SEM uses electrons to create an image, therefore the specimen under investigation must be conductive. However, most biological materials are good insulators and will build up charge if not coated, thus creating a distorted image (Dykstra, 1992). To make a specimen conductive it is coated with a very thin layer (100 Å) of gold or palladium using a sputter coater (Dykstra, 1992). A sputter coater consists of a vacuum chamber, a noble-metal-plated cathode (gold or

palladium) and an anode. The specimen is placed on the anode and a vacuum is created within the chamber. Once the vacuum ( $10^{-3}$  Torr) has been achieved a high voltage field is created between the cathode and the anode. For the current to pass between the cathode and the anode an inert gas, such as argon, is released into the chamber. The electron flow results in ionization of the argon gas and these ions are accelerated by the electron field and travel towards the cathode. The argon ions hit the cathode at high speed dislodging metal atoms that collect on the surfaces inside the chamber, coating the specimen. Once the specimen is conductive it can be imaged using SEM. A SEM system is comprised of an electron gun, condenser lenses, deflector coils, a detector and an amplifier (Figure 2-6; Dykstra, 1992). The electron gun produces an electron beam by applying a voltage to a filament, such as tungsten, causing it to heat up and release electrons. The electrons accelerate towards an anode, producing a beam of electrons. The condenser lenses are electromagnetic and focus the electron beam on a small surface segment of the specimen. The deflector coils cause this electron beam to move across the specimen's surface. When the electron beam hits the specimen's surface secondary electrons are dislodged and travel to the striking collector. The collector counts these electrons and sends a signal to an amplifier and a final image is created by the number of electrons emitted from each segment of the specimen via a cathode ray tube (CRT). The more electrons produced the brighter the image, indicating height, and the fewer electrons produced the darker the image, indicating depth.

When imaging with conventional SEM the specimen is imaged under a vacuum and must be free of water. Therefore, a specimen must be dried prior to analysis by conventional SEM. Unfortunately, drying can result in structural changes to a specimen. Moss et al. (1989) found that when wood fibres present in paper pulp were air-dried prior to SEM they completely collapsed, and underwent shrinkage and distortion. In another study, calcium-AL microcapsules fixed with glutaraldehyde followed by dehydration in an ethanol series were examined (Allan-Wojtas et al., 2008). Results showed that these microcapsules were not comparable to those that were not dehydrated. Therefore

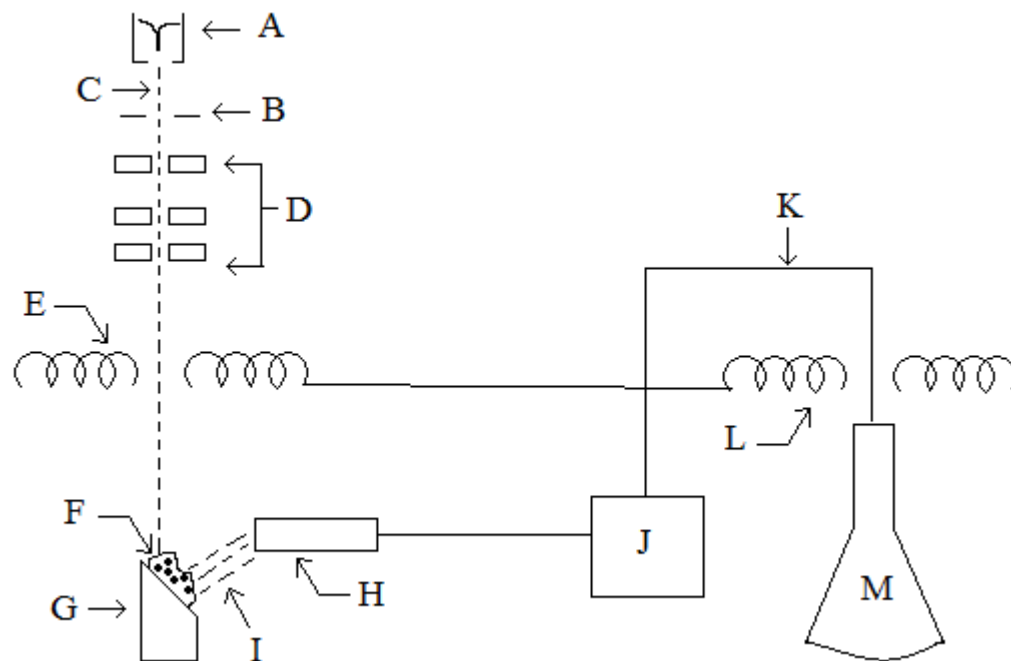


**Figure 2-6** Schematic of an SEM showing the Wehnelt assembly with filament (A), anode aperture (B), electron beam (C), condenser lenses (D), deflector coils (E), deflector coils (L), cathode ray tube (CRT) (M), specimen (F) on stage (G), and electrons (I), striking collector (H), amplifier (J), and feeding voltage (K) (adapted from Dykstra, 1992).

conventional SEM makes it difficult to observe a specimen's natural structure in an aqueous state.

### **2.5.2 Cold stage scanning electron microscopy (cryo-SEM)**

Cold stage or low temperature scanning electron microscopy can be used to image a specimen in an aqueous environment. This technique involves the rapid diffusion of heat out of a specimen, instantaneously stopping biological activity (fixing the sample) by subjecting the specimen to extremely cold ( $<-150^{\circ}\text{C}$ ) temperatures (Dykstra, 1992). However, when freezing, damage to the specimen's cellular structure can occur when water crystallizes. Ice crystal growth begins with a nucleation point where water from the surrounding medium migrates towards it. Solute concentrations in regions between ice crystals increase as they grow and continue until solute concentrations are sufficient to prevent it. Ice crystal development in cells are bounded by the cell membrane, meaning they will not grow larger than the cell (Hagler, 1988). Ice crystal formation is thought to occur in living organism between  $-2$  and  $-80^{\circ}\text{C}$  (Dykstra, 1992); however, in cryo-SEM water within the specimen is rapidly frozen with liquid nitrogen ( $-196^{\circ}\text{C}$ ), eliminating the ability for ice crystals to grow. One can view the specimen in its entirety or the interior of a specimen by fracturing it with a microtome which is referred to as freeze-fracture (Dykstra, 1992). Once the frozen specimen is placed in the SEM chamber under a vacuum ( $10^{-5}$  Torr) the ice sublimates off the specimen's surface. The sample is then coated with gold or palladium as in the case for conventional SEM, and imaged under vacuum at cold temperatures ( $<-150^{\circ}\text{C}$ ).

Cold stage SEM imaging of calcium-AL capsules containing probiotics allowed for detailed observation of the microcapsules in their frozen hydrated state (Allan-Wojtas et al., 2008). Results showed that the microcapsules were spherical in shape and had a relatively smooth external surface. Because cryo-SEM involves the sublimation of ice in order to reveal the structure/surface of a specimen, any soluble but non-volatile substance may create an artifact. These solute artifacts were observed by Moss et al. (1989) when examining nylon fibres in solutions containing different carbohydrates (D-glucose, D-xylose and L-arabinose) at different concentrations (50-0.03 mM). When imaging the

nylon fibers using cryo-SEM, those in the carbohydrate solutions showed the presence of fibrillar or sheet-like materials, whereas those in distilled water did not. The presence of fibrillar like materials were found to increase as the carbohydrate concentration increased. Miller et al. (1983) used cryo-SEM to examine chloroplasts in distilled water, 140 mM sucrose and 100 mM NaCl. They found that the chloroplast's membrane was completely obscured in sucrose but was clearly visible in distilled water. In addition, the chloroplasts in NaCl appeared to be embedded in a network of microfilaments. These results indicate that the presence of microfilaments in a specimen analysed by cryo-SEM may be a process artifact.

### **2.5.3 Atomic force microscopy (AFM)**

Atomic force microscopy produces topographical images of a sample in a non-destructive way, making it suitable for studying biological samples (Hansma et al., 1988). AFM is a technique that works by scanning a sample with a tip/probe very close to its surface (Kaupp, 2006). While the tip is scanned over the surface of the sample, the AFM records interatomic forces between the apex of the tip and the atoms in the sample (Hansma et al., 1988). The major forces created between the moving tip and the sample surface are created from van der Waals, electrostatic, hydrophobic, hydrophilic, and capillary interactions (Kaupp, 2006). It measures the attractive or repulsive forces between the probe and the sample in either a constant height or force mode (Hansma et al., 1988). When AFM measures repulsive forces the tip is in contact with the sample. When AFM measures the attractive forces the tip is close to the surface of the sample but not in contact.

All AFM instruments have five essential components: a sharp tip mounted on a soft cantilever, a system to sense the cantilever's deflection, a feedback system to monitor and control the deflection of the cantilever, a scanning system that will move the sample in a raster pattern with respect to the tip, and a display system that converts the data into an image (Rugar & Hansma, 1990). A simple block diagram of an AFM system is shown in Figure 2-7. The sample to be analysed is mounted on the xyz piezo scanner under the probe (Kaupp, 2006). The probe is a micromachined cantilever with a sharp

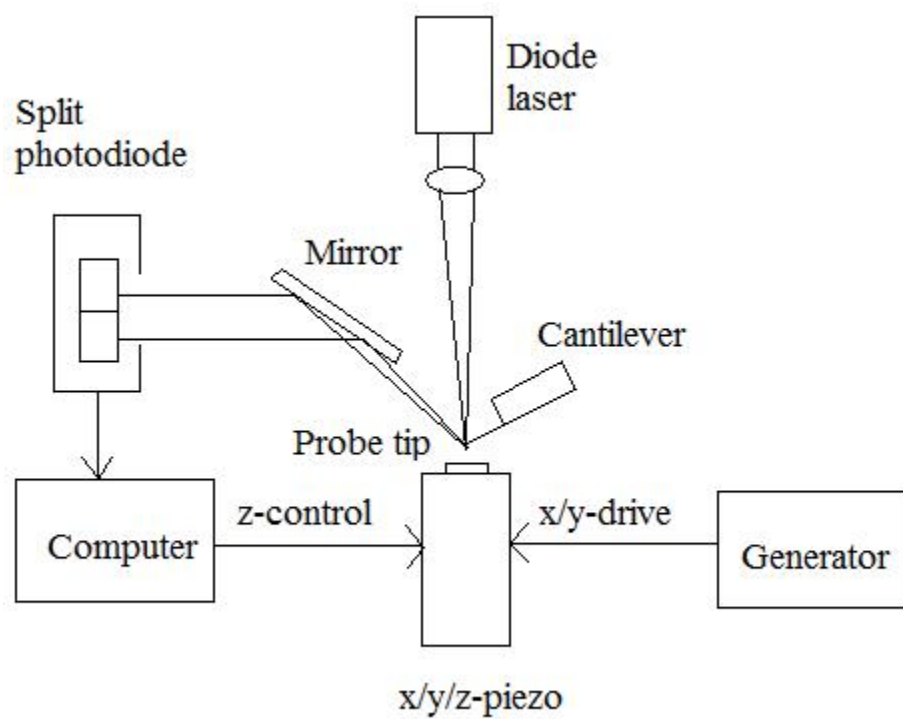


**Figure 2-7** Block diagram of a laser deflection contact AFM (adapted from Kaupp, 2006).

pyramidal tip at one end that is brought into contact with the sample surface (Rugar & Hansma, 1990; Figure 2-8). Probes made from  $\text{Si}_3\text{N}_4$  are thinner and softer and are usually used for studying soft biological samples with the contact mode in air and under between it and the sample will deviate from the constant force applied creating an error signal. This signal is amplified to generate height images that reflect the surface configuration. The height image represents the vertical translations ( $z$ ) of the piezo scanner needed to eliminate the error signal created as the probe is moved from one place to another, elevated surfaces are assigned a brighter contrast relative to lower lying surfaces.

The topography and surface roughness of extrusion-based AL capsules (800  $\mu\text{m}$  in diameter) crosslinked with  $\text{BaCl}_2$  were examined using non-contact AFM (Zimmermann et al., 2003). The AFM images showed that AL capsules that were stored in the cross-linking solution had a rougher surface than those washed three times with a  $\text{NaCl}$  solution. A variety of different extrusion AL-based beads and capsules crosslinked with either  $\text{BaCl}_2$  or  $\text{CaCl}_2$  were examined using contact AFM (Lekka et al., 2004). It was observed that the  $\text{Ba}^{2+}$ -AL beads had a sponge-like surface which was not observed for the  $\text{Ca}^{2+}$ -AL beads. It was also observed that the  $\text{Ca}^{2+}$ -AL capsules had much less variation in their surface profile than the  $\text{Ba}^{2+}$ -AL capsules.

#### **2.5.4 Confocal laser scanning microscopy (CLSM)**

The principle of laser scanning microscopy is to scan a segment on an object with a finely focused laser to create an image while using a ‘pinhole’ to remove any light that is out of focus (Hibbs, 2004a) thereby creating an optical thin section. With this technology one can create images of exceptional resolution and create a 3-dimensional representation by collecting optical slices of an object at different focal depths. CLSM is composed of several parts, a conventional light microscope, a laser, a scan head, a controller box and a computer (Figure 2-9). The conventional light microscope produces the image by using an objective lens, therefore the quality and resolution of the final image depends on the quality of the objective lens (i.e. high numerical aperture lenses result in thinner optical sections). The scan head moves the laser across the sample in a



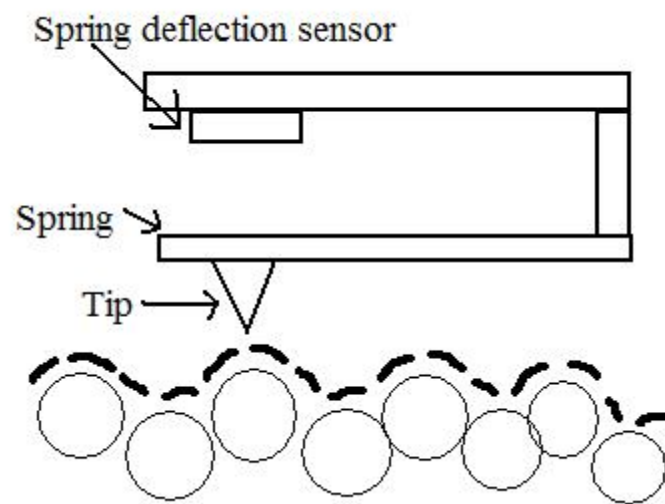


**Figure 2-8** Schematic of an AFM probe (adapted from Rugar & Hansma, 1990).

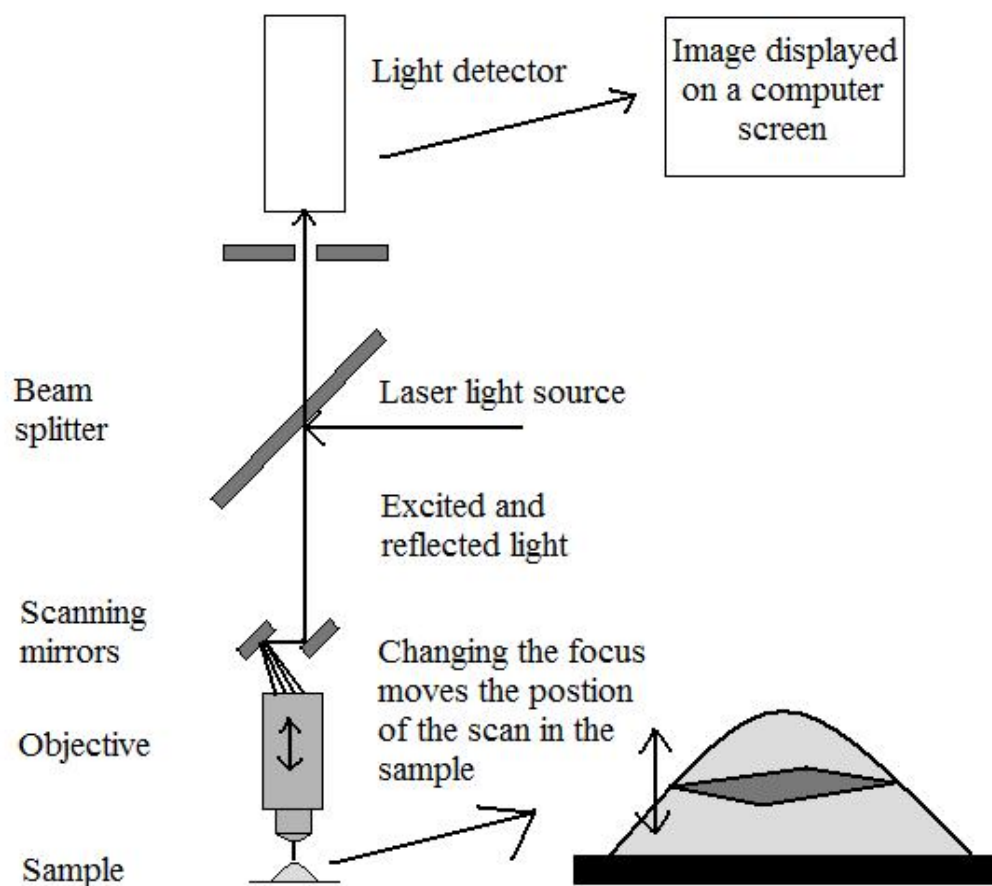


**Figure 2-9** Simple diagram of how an image is acquired by CLSM (adapted from Hibbs, 2004a).

rastering motion while the controller or optics box is used to separate light of different wavelengths. The 'pinhole' located in the scan head is a crucial part of the CLSM as it allows only the in-focus light through, physically rejecting any out-of-focus light. The light is detected by photomultiplier tubes. The computer and the controller box are required for capturing the image and microscope.

Confocal laser scanning microscopy creates an image by scanning across the sample with a diffraction-limited point of excited light (created by the laser) in a rastering motion (Hibbs, 2004a; Figure 2-9). The scanning pattern is achieved using two mirrors, one that scans at a high speed in the x-axis direction and the other scans at a slower speed in the y-axis direction. The irradiated light will excite the naturally or applied fluorophores within the sample that match at the wavelength of the laser. Fluorescent light emitted back towards the objective from the sample is separated from the light of a second fluorophore or unwanted reflected excited light by dichroic mirrors. Dichroic mirrors are designed to allow the passage of light of a specific wavelength, or range of wavelengths. Therefore, with the use of dichroic mirrors a researcher can choose which wavelength to image if a sample contains two or more fluorophores, or to eliminate background fluorescence. The in-focus light that passes through the dichroic mirrors will pass through the 'pinhole' and be detected by the photomultiplier tube. The signal created by the detector is converted to a digital form, and the image is displayed in greyscale but can be suitably coloured.

#### **2.5.4.1 Fluorescence**

To view samples with CLSM they must contain a fluorophore that can be excited with a laser. There are many commercially available fluorescent tags that allow one to label a large array of chemical and biological compounds (Hibbs, 2004b). Reactive fluorophores, for example fluoresceinamine (FA) and Texas red sulphonyl chloride, are commonly used to label antibodies, proteins, lipids and carbohydrates. There are also fluorophores, such as acridine orange and propidium iodide (PI), for labelling nucleic acids. Due to the large variety of fluorescent tags available it is important for the

researcher to understand what they are trying to image and choose the appropriate compound.

#### **2.5.4.1.1 Fluoresceinamine I (FA)**

Fluoresceinamine I is a fluorophore that is excited at 490 nm and emits at 530 nm, and is commonly used to label carbohydrates (Arnosti et al., 2000; Figure 2-10). Fluoresceinamine I has been used to label polysaccharides such as alginic acid, xylan, and maltodextrins (De Belder & Granath, 1973; Arnosti et al., 2000; Arnosti, 2003). Carbohydrates with reducing ends can be derivatized with FA to create a fluorescently labelled molecule. A method for derivatizing a reducing carbohydrate with FA is the reductive amination reaction (Borch et al., 1971). This method involves the reaction of the carbonyl group on a reducing carbohydrate with the primary amino group of FA to form a Schiff's base (Figure 2-10). The resulting Schiff's base is reduced to a secondary amine with sodium cyanoborohydride ( $\text{NaCNBH}_3$ ).

#### **2.5.4.1.2 Propidium Iodide (PI)**

Propidium iodide is nucleic acid stain that binds to DNA and RNA (Truernit & Haseloff, 2008). Once the dye is bound to the nucleic acids of the sample its fluorescence is increased 20-30 fold and the fluorescence excitation and emission wavelengths shift 30-40 nm to the red and 15 nm to the blue, respectively (Arndt-Jovin & Jovin, 1989). When PI is bound to nucleic acids its excitation maximum is 535 nm and the emission maximum is 617 nm, and can be accomplished with a xenon or mercury-arc lamp or with the 488 nm line of an argon-ion laser.

Propidium iodide stains cells where their cellular membrane has been compromised or is permeable, therefore the cells must not be viable in order for the stain to move across the cellular membrane and stain the nucleic acids. Cells can be killed by employing a mild chemical/heat treatment in order to ensure that they do not lyse releasing their nucleic acids into solution. Subjecting bacteria to 70% ethanol at 4°C has been used in the case of *E. coli* (Hahn et al., 2008), however in the case of *Bifibacterium*, simply exposing the cells to oxygen (21%) is sufficient to induce death (Simpson et al.,

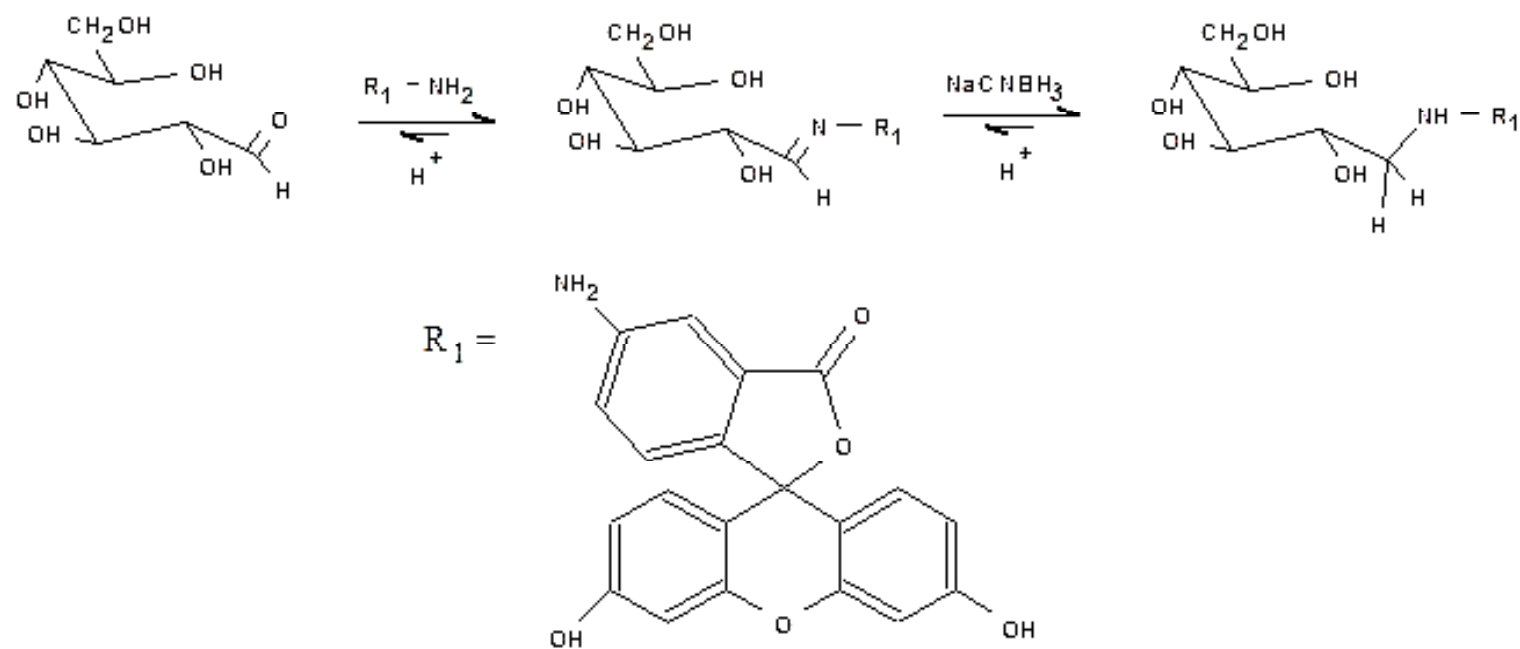


Figure 2-10 Reductive amination of glucose using fluoresceinamine I and NaCNBH<sub>3</sub> (adapted from Borch et al., 1971).

2005). Researchers have used PI to enumerate the number of dead microbes within bacterial suspensions (Apajalahti et al., 2003).

### 3. Material and Methods

#### 3.1 Materials

The following materials were generously supplied for this research project. Dextrose equivalent syrup (DE-36) was provided by Archer Daniels Midland (Decatur, GA). Orafti® P95 (P95) [FOS, DP 2-8 (6.8% D-glucose + D-fructose + sucrose)]; Orafti® ST (ST) inulin [DP 2-60 (1.3% glucose + fructose, 5.7% sucrose)]; and Orafti® Synergy1 (Syn) [FOS/inulin mixture, DP 2-60 (8.3% D-glucose + D-fructose + sucrose)] were supplied by ORAFTI S.A. (Oreye, Belgium). Pea protein isolate (PPI) [82% protein, 2.5% fat, <4.0% ash, values reported by supplier] was supplied by Nutri-Pea Limited (Portage la Prairie, MB). Whey protein isolate (WPI) [97.7% protein, 0.4% lipid, 1.8% ash, values reported by supplier] was supplied by Davisco (Le Sueur, MN).

The following materials and chemicals were purchased from Sigma-Aldrich (Oakville, ON): alginic acid sodium salt from brown alginate (AL) medium viscosity (batch # 035K0205), dimethyl sulfoxide (DMSO), fluoresceinamine I (FA), D-fructose (fructose), D-glucose (glucose), L-cysteine hydrochloride monohydrate (cys), magnesium sulfate, maltotriose, maltotetraose, maltopentaose, maltohexaose, maltoheptaose, propidium iodide (PI), sodium acetate anhydrous, sodium cyanoborohydride ( $\text{NaCNBH}_3$ ), Tween 80, and vitamin K1.

N-butanol, ethyl acetate, glacial acetic acid, potassium dihydrogen orthophosphate ( $\text{KH}_2\text{PO}_4$ ), di-potassium hydrogen orthophosphate ( $\text{K}_2\text{HPO}_4$ ), and sodium bicarbonate ( $\text{NaHCO}_3$ ) were purchased from BDH Inc. (Toronto, ON).

Calcium chloride dihydrate ( $\text{CaCl}_2$ ), hydrochloric acid (HCl), potassium chloride (KCl) and sodium phosphate dibasic heptahydrate ( $\text{Na}_2\text{HPO}_4$ ) were purchased from EMD Chemicals (Darmstadt, Germany).

Reinforced clostridial media (RCM), De man, Rogosa, Sharpe (MRS) media and yeast extract were purchased from Oxoid Ltd. (Basingstroke, England).

Activated carbon, sodium chloride (NaCl) and sodium hydroxide solution (NaOH, 50% w/w), were purchased from Fischer Scientific (Fair Lawn, NJ).

Ethanol, 95 and 100% anhydrous, were purchased from Commercial Alcohols Inc. (Brampton, ON).

*Bifidobacterium adolescentis* ATCC 15703 was purchased from American Type Culture Collection (Manassas, VA).

Bile salts were purchased from Difco Laboratories (Detroit, MI).

Hemin was purchased from Fluka (Buchs, Switzerland).

Granulated Difco agar and Bacto™ peptone was purchased from BD (Sparks, MD).

ProLong was purchased from Invitrogen (Eugene, OR).

The water used in this research, labelled as ddH<sub>2</sub>O was produced from a Millipore Milli-Q™ water system (Millipore Corporation, Milford, MA) unless otherwise stated.

### **3.2 Study 1: Investigation on the effects of wall material and capsule size on the survivability of encapsulated *B. adolescentis* in simulated gastric juice (SGJ)**

#### **3.2.1 Microorganisms**

*Bifidobacterium adolescentis* was chosen for this research project because of its low acid intolerance and ability to utilise FOS. *Bifidobacterium adolescentis* was stored at -70 °C in a 1:1 (v:v) suspension of glycerol and MRS broth. Cultures were streaked onto RCM supplemented with 0.05% (v/v) L-cysteine HCl (RCM-cys) plates at 37 °C under anaerobic conditions (80% N<sub>2</sub>, 10% CO<sub>2</sub> and 10% H<sub>2</sub>) using an anaerobic chamber (Forma Scientific Inc., Marietta, GA).

#### **3.2.2 Comparison of the growth profile of *B. adolescentis* in MRS and RCM broths**

Growth experiments were conducted on MRS and RCM broths to determine when *B. adolescentis* reached its stationary growth phase as well as the corresponding cell concentration. Side arm flasks containing 100 mL of MRS or RCM broth were prepared according to the manufacturer's instructions. Flasks were autoclaved at 121 °C for 15 min, supplemented with L-cysteine to 0.05% (v/v) and placed in the anaerobic



chamber to equilibrate overnight. Culture tubes containing 5 mL of sterile MRS or RCM broth supplemented with 0.05% L-cysteine (v/v) were inoculated with two isolated colonies of *B. adolescentis* and incubated at 37 °C under anaerobic condition) for 24 h. A 100 µL aliquot was used to inoculate the side arm flasks which were incubated under anaerobic conditions for 30 h at 37 °C. The optical density (600 nm) of the suspensions were measured every 40 min for 0-20 h and then every 30 min for 20-30 h by spectrophotometry (Novaspec, Biochrom Ltd., Cambridge, England). Aliquots (100 µL) were removed from the flasks, serially diluted with peptone saline (PS; 8.5 g L<sup>-1</sup> NaCl and 1.0 g L<sup>-1</sup> Bacto™ Peptone), and spread plated to determine cell counts. Experiments were conducted in duplicate.

### **3.2.3 Preparation of *B. adolescentis* for encapsulation**

Two isolated colonies of *B. adolescentis* were transferred into RCM-cys broth held at 37 °C under anaerobic conditions. Cells were harvested after 24 h (stationary phase) by centrifugation (1900 x g, 15 min at 4 °C), washed once with phosphate buffer saline (PBS; 0.01 M NaH<sub>2</sub>PO<sub>4</sub>, 0.137 M NaCl, 2.68 mM KCl, pH 7.0) and resuspended in PS to a final cell concentration of 8-9 log CFU mL<sup>-1</sup> determined by pour plate.

### **3.2.4 Encapsulation of *B. adolescentis* in protein and/or alginate**

Wall material solutions prepared for the encapsulation of *B. adolescentis* included: 1.0% (w/w) AL, 4.0% WPI + 0.5% (w/w) AL, and 4.0% PPI + 0.5% (w/w) AL. Preliminary work creating capsules with the emulsion method showed that 4.0% WPI produced capsules with a mean diameter of less than 100 µm, where other concentrations (6.0, 8.0 and 10.0%) did not (greater than 400 µm). Protein isolate concentrations lower than 4.0% did not form a stable gel. AL was added along with the protein isolates in order for the capsules to form via the extrusion method. With AL concentrations greater than 1.0% it becomes increasingly difficult to eject the solution through the syringe and to bring AL completely into solution. One percent AL and 4% WPI + 0.5% AL were prepared by dissolving 0.8 g AL and 3.2 g WPI + 0.4 g AL, respectively, in 80.0 g ddH<sub>2</sub>O. Solutions were heated at 80 °C for 30 min in order to denature the protein and bring AL into solution and then cooled to 40 °C in a water bath. The 4.0% PPI + 0.5%

AL was prepared by dissolving 3.2 g PPI in 0.1 M NaOH (~pH 10, required to bring PPI into solution) followed by heating at 80 °C for 30 min in order to denature the protein and cooled to 40 °C in a water bath. Once cooled, the solution was neutralized to pH 7.0 with 1.0 M HCl and 0.8 g AL was added. AL was added after neutralization to prevent gelation. The resulting solution was heated at 80 °C for another 30 min and then cooled to 40 °C in a water bath. The weights of the final solutions were corrected for water loss during heating.

#### **3.2.4.1 Extrusion**

The capsules were prepared using a modification of the method by Krasaekoopt et al. (2003). A mixture containing 1.0 g (8-9 log CFU mL<sup>-1</sup>, section 3.2.3) washed *B. adolescentis* cells was mixed with 18.0 g of the 1.0% AL solution and injected through a 20G needle (2.0 cm in length) into a filter sterilized cross-linking solution (5.0% (w/v) CaCl<sub>2</sub> + 1.0% (w/v) Tween 80). The resulting capsules were allowed to harden in the cross-linking solution for 30 min, and were then washed three times with PS. The capsules were either used immediately, freeze dried using a vacuum freeze-dryer (Labconco Corp., Kansas City, MO), or left to air-dry overnight (15 h). Percent encapsulation of *B. adolescentis* was ~ 100%. Experiments were repeated with 4.0% WPI + 0.5% AL and 4.0% PPI + 0.5% AL.

#### **3.2.4.2 Emulsion**

Microcapsules were produced using a modification of the emulsion method of Truelstrup-Hansen et al. (2002). One gram of (8-9 log CFU mL<sup>-1</sup>) washed *B. adolescentis* cells was mixed with 18.0 g of 4.0% WPI + 0.5% (w/w) AL and was added to 100.0 g of canola oil (NoName, Calgary, AB) containing 1.0% (w/v) Tween 80. The solution was stirred at 900 rpm for 20 min using an overhead stirrer equipped with a square blade paddle (Caframon Ltd., Wiarton, ON) to create a water-in-oil emulsion. Thirty-two millilitres of a second emulsion containing 85.0 g of canola oil, 1.0 g Tween 80, and 17.0 g of 63 mM CaCl<sub>2</sub> was added to the first emulsion and stirred (900 rpm) for an additional 20 min. The resulting solution was transferred to a separatory funnel and 40.0 mL of a filter sterilized 5.0% (w/v) CaCl<sub>2</sub> solution was added to break the emulsion.

The microcapsules produced were allowed to separate from the oil phase, removed, washed three times with PS and adjusted to approximately a 1:1 (v/v) ratio of WPI-AL capsules to PS.

Capsules produced by the emulsion method composed of PPI + AL was tried. PPI has difficulty separating from the water-oil interface due to the hydrophobic groups interacting strongly with the oil phase.

### **3.2.5 Analysis of capsule morphology, geometric mean and percent distribution**

Air and freeze-dried extrusion-based capsules were examined by SEM for their surface morphologies (Philips, Eindhoven, Netherlands) at 20.0 kV. The capsules were specimen mounted using double-sided adhesive tape and coated with gold using a sputter coater (Edwards and Philips, West Sussex, England) under vacuum with argon purging.

Wet microcapsules were sized using a laser scattering particle size distribution analyzer (PSA) (Horiban Instruments Inc., Irvine, CA) for size and size distribution. The geometric mean diameter of the capsules was recorded instead of arithmetic mean due to the non-uniform distribution. Experiments were performed in triplicate.

### **3.2.6 Survival of free and encapsulated *B. adolescentis* in SGJ**

The survival of free and encapsulated *B. adolescentis* in SGJ (0.08 M HCl with 0.2 % (w/v) NaCl; Rao et al., 1989) were studied at pH values (adjusted via the use of 1.0 and 0.1 M NaOH and HCl) of 6.0, 3.0 and 2.0. Aliquots of 0.5 mL of the free and wet encapsulated cells ( $8-9 \log \text{CFU mL}^{-1}$ ) in PS was added to 9.5 mL of SGJ and incubated at 37 °C. Aliquots of SGJ at pH 6.0 were removed at 20 min time intervals for 2 h, whereas for SGJ at pH 3.0 and 2.0, aliquots were removed at 5 min time intervals for the first 30 min then at 30 min time intervals until 2 h. Simulated gastric juice at pH 3.0 and 2.0 were neutralized with 0.1 M and 1.0 M NaOH, respectively, after being removed from the incubator. Samples containing the encapsulated cells were homogenized (Omni Macro Homogenizer, Omni International Inc., Marietta, GA) at a setting of 4.5 for 30 sec before being assayed. Preliminary work showed that there was no adverse effect of homogenization on cell survival. Samples were assayed for their cell concentration by

serial dilution in PS and pour plating with RCM-cys agar. The plates were incubated under anaerobic conditions at 37 °C for 48 h. Detection limit of 1.3 and 2.6 log CFU mL<sup>-1</sup> were established for the free and encapsulated cells respectively, due to the dilution of the cells by the addition of the SGJ and the process of encapsulation. Experiments were conducted in triplicate.

### **3.3 Study 2: Investigation of the growth potential of *B. adolescentis* on a selection of carbohydrates, and the effect of the encapsulated synbiot on probiotic survival in SGJ**

#### **3.3.1 Preparation of glucose-free maltooliogaccharide (MOS)**

A MOS sample was prepared from a DE-36 syrup by charcoal-Celite chromatography. Five grams of the DE-36 syrup was dissolved in ddH<sub>2</sub>O and added to 200 g of activated carbon in 600 mL of ddH<sub>2</sub>O and stirred for 2 h. The solution was vacuum filtered and the carbohydrate-bound carbon was washed with ddH<sub>2</sub>O until the eluted glucose peak area recorded by HPAE-PAD was less than 500,000 mV (corresponding to ~2.5% glucose). Glucose levels were further reduced by washing with 10% (v/v) ethanol until the peak area of glucose recorded by HPAE-PAD was less than 50,000 mV (~0.16% glucose).

The carbohydrate-bound carbon was placed into a 1L beaker containing 900 mL of 50% (v/v) ethanol and stirred for 1 h and then vacuum filtered. The filtered solution was evaporated (Buchi, Postfach, Switzerland) and reconstituted with 25 mL of ddH<sub>2</sub>O. Trace glucose was removed by ion exchange chromatography (78 x 300 mm Supelcogel<sup>TM</sup> Ca column; Supelco, Torrance, CA) employing an Agilent 1100 gradient chromatography system in series with a refractive index (RI) detector (Agilent Technologies Inc., Palo Alto, CA). The mobile phase was ddH<sub>2</sub>O at a flow rate of 0.5 mL min<sup>-1</sup> and the sample injection volume was 100 µL. Oligosaccharides eluting from 7.0 to 10.5 min (relative retention time for glucose was 12.0 min) were pooled and evaporated to produce MOS (<0.007% glucose w/w). Data collection and analysis were performed using ChemStation<sup>TM</sup> software (Rev. A.08.03).

### **3.3.2 Comparison of *B. adolescentis* specific growth rates in a semi-synthetic medium containing different carbohydrates**

The fermentation of carbohydrates by *B. adolescentis* was examined in a semi-synthetic media (Vernazza et al., 2006) which contained the following (in g L<sup>-1</sup>): 2.0 Bacto™ peptone, 2.0 yeast extract, 0.1 NaCl, 0.04 K<sub>2</sub>HPO<sub>4</sub>, 0.04 KH<sub>2</sub>PO<sub>4</sub>, 0.01 MgSO<sub>4</sub> 7H<sub>2</sub>O, 0.01 CaCl<sub>2</sub> 2H<sub>2</sub>O, 2.0 NaHCO<sub>3</sub>, 0.005 hemin, 0.5 bile salts, 2.0 mL L<sup>-1</sup> Tween 80 and 10 µL L<sup>-1</sup> Vitamin K. The media was adjusted to pH 7.0 with 0.1 M NaOH, dispensed into screw cap culture tubes (9.0 mL) and autoclaved at 121 °C for 15 min. Media was supplemented with 0.05% (v/v) L-cysteine HCl.

Two isolated colonies of *B. adolescentis* were used to inoculate 5 mL of RCM-cys broth and then incubated under anaerobic conditions at 37 °C for 12 h to produce cell concentrations of approximately 9 log CFU mL<sup>-1</sup>. Aliquots (100 µL) of this cell suspension were used to inoculate the semi-synthetic medium, which contained filter sterilized 10 g L<sup>-1</sup> solutions of glucose, MOS, P95, ST, SYN, or 0.85 g L<sup>-1</sup> glucose (Min Glu). Tubes were incubated under anaerobic conditions at 37 °C for 24 h. Microbial growth was monitored hourly by measuring sample optical density at 600 nm until the log phase (~3 h) was reached, at which time readings were taken every 30 min. Once the stationary phase (~7 h) was reached, readings were taken every two hours. At each reading an aliquot of the sample was removed and assayed by serial dilution with PS using RCM-cys agar. Plates were incubated under anaerobic conditions at 37 °C for 48 h. The specific growth rates (µ) were calculated as the slope of the linear/exponential (2 to 6 h) phase of growth on the log CFU mL<sup>-1</sup> vs. time (h) graphs. Experiments were performed in triplicate.

### **3.3.3 Carbohydrate profile analysis of the semi-synthetic medium containing FOS and MOS**

The carbohydrate profile of the semi-synthetic medium containing P95 and MOS were analysed by HPAE-PAD before (0 h) and after (24 h) incubation with *B. adolescentis* as outlined above. The relative retention times of the oligosaccharides

present in the samples were determined by comparison those with a maltooligosaccharide standard (DP 2-7; 100 mg L<sup>-1</sup>). Experiments were performed in triplicate.

### **3.3.3.1 High performance anion exchange – pulsed amperometric detection (HPAE-PAD)**

A Dionex Bio LC 4000 gradient high performance liquid chromatography system equipped with a Dionex PAD (Dionex, Sunnyvale, CA) was used for sample carbohydrate analysis. A Dionex CarboPac PA1 [4 x 250 mm] anion exchange column was used in series with a Dionex CarboPac Guard PA-1 [4 x 50 mm] column for carbohydrate separation. Carbohydrate detection was afforded by PAD using the following potentials and durations: E<sub>1</sub> = 50 mV, T<sub>1</sub> = 0.299 s; E<sub>2</sub> = 600 mV, T<sub>2</sub> = 0.299s; E<sub>3</sub> = -800 mV, T<sub>3</sub> = 0.499 s. All samples were filtered through a nylon syringe filter (13 mm diameter, 0.2 µm pore size; Chromatographic Specialties Inc., Brockville, ON) prior to analysis. The injection volume for all analyses was 50.0 µL. Data analysis was accomplished using WMSP Chromatography Manager software WML-2010 (Nangning Weimalong Chromatograph Science Technology Co. LTD, China). The mobile phase consisted of three solvents; solvent A, 100 mM NaOH, solvent B; 100 mM NaOH and 250 mM Na<sup>+</sup>CH<sub>3</sub>COO<sup>-</sup> and solvent C, 300 mM NaOH. The gradient program was 100% solvent A and after 8 min the percentage of solvent B increased linearly to 100% after 60 min, followed by a rapid change to 100% solvent C at 61 min. From 90 to 91 min a rapid change to 100% solvent A occurred and was held until 120 min. The flow rate was maintained at 1.0 mL min<sup>-1</sup> and the column pressure was approximately 1200 psi.

### **3.3.3.2 Synbiot encapsulation with FOS (P95) and its effect on the survival of *B. adolescentis* in SGJ**

Capsules prepared by extrusion were produced as outlined section 3.2.4.1 with the addition of 0.19 g P95 to the wall material solution. The resulting capsules were subjected to SGJ at pH 2.0 for 2.0 h under the same reaction conditions as described in section 3.2.6. Capsules were also examined by PSA as described in section 3.2.5. Experiments were performed in triplicate.

### 3.3.4 Examination of the concentration and type of FOS (P95) encapsulated

The amount of P95 encapsulated was determined by acid hydrolysis of the cross-linking solution, the PS wash and the capsules. Washed capsules (6 g) were added to 15 mL of 6.0 N HCl, whereas 1.0 mL of the cross-linking solution and the PS wash were added separately to 0.5 mL of 6.0 N HCl. Each of these three solutions were stirred overnight (15 h) at room temperature (21 °C). The capsule slurry was gravity filtered and washed (15 mL ddH<sub>2</sub>O) and the supernatant, as well as the hydrolyzed cross-linking and PS solutions, were individually neutralized to approximately pH 7.0 with 1.0 M NaOH. Neutralized solutions were individually analyzed by HPAE-PAD, with an isocratic mobile phase of 100 mM NaOH. The amount of P95 encapsulated was determined by comparing the amount of fructose produced by acid hydrolysis (supernatant + cross-linking + PS wash solutions) to the amount of fructose produced by the acid hydrolysis of a range (0.4 to 0.01% w/v) of P95 (correlation coefficient of 0.9964). Experiments were performed in triplicate.

To examine the type of FOS encapsulated, capsules were gravity filtered and washed three times with PS. The filtered capsules were homogenised (setting 4.5 for 30 sec) in 30 mL of 1.0 M phosphate buffer, pH 7.0, for 30 sec. The resulting slurry was syringe filtered (0.2 µm) and analysed by HPAE-PAD to determine the type of FOS encapsulated.

### 3.3.5 Enumeration of *B. adolescentis* before and after drying

Capsules containing P95 and live *B. adolescentis* cells were produced as described in section 3.2.4.1. Counts of *B. adolescentis* in the wet capsules were determined by the homogenisation of 0.5 mL of capsules in 9.5 mL PS, followed by serial dilution in PS and pour plating with RCM-cys agar. For each wall material, the equivalent number of air dried (25 °C for 15 h) or freeze dried (-40 °C for 15 h) capsules in 0.5 mL of wet capsules were used for analysis. Capsules were added to 9.5 mL aliquots of PS and were allowed to resuspend for 1 hr. The samples were homogenised at a setting of 4.5 for 30 sec and plated using pour plating with RCM-cys agar after serial dilution with PS. Plates

were incubated under anaerobic conditions at 37 °C for 48 h. Experiments were performed in triplicate.

### **3.4 Study 3: Investigation of the external and internal morphology of the pea protein-alginate capsules and determination of the spatial distribution of fluorescently-labelled glucose and *B. adolescentis* within these capsules**

#### **3.4.1 Derivatization of glucose**

Glucose was fluorescently labelled with FA using a modified reductive amination procedure (Guttman & Pritchett, 1995). In brief, 10  $\mu\text{L}$  of a 100  $\text{mg mL}^{-1}$  glucose solution was placed in a 500  $\mu\text{L}$  microcentrifuge tube and lyophilized for 1 h. The resulting dried glucose was derivatized by the addition of 100  $\mu\text{L}$  of a 0.4 M FA and 1.0 M  $\text{NaCNBH}_3$  mixture in 70:30 (v/v) dimethyl sulfoxide (DMSO):glacial acetic acid solution. The mixture was vortexed for 30 s and placed in a heating block (IncuBlock, Denville Scientific Inc, South Plainfield, NJ) at 70 °C overnight (15 h). Following derivatization, the sample was diluted with 800  $\mu\text{L}$  of a 1:1 (v/v) solution of ethanol and ethyl acetate and the FA labelled glucose (GLU-FA) was separated from the free FA using thin layer chromatography (TLC). The sample was placed on a preparatory TLC plate (20x20 cm, 500  $\mu\text{m}$  thickness, Whatman Int. Ltd., Maidstone, England), developed using a mobile phase of 1:1:8 (v/v/v) ethanol:acetic acid:ethyl acetate and visualised by UV (200 – 400 nm). The GLU-FA with a retention factor ( $R_f$ ) of 0.21 was removed from the plate with a sharp knife separating it from the free FA with a  $R_f$  of 0.95. The GLU-FA was eluted from the silica with 50 mL of a 3:7 (v/v) ethanol:ethyl acetate solution by gravity filtration. The solvent was evaporated (Buchi, Postfach, Switzerland) and the resulting solid/liquid was dissolved in 2 mL of a 1:1 (v/v) ethanol:ethyl acetate solution, and placed in 2 mL pre-weighed centrifuge tubes. The solvent was then allowed to evaporate in a fume hood (~72 h). Approximately 4 mg of GLU-FA was recovered. Samples were checked for purity using TLC with the aforementioned mobile phase and stored in the dark at 4°C until used for encapsulation studies.



### **3.4.2 Labelling of *B. adolescentis* with propidium iodide (PI)**

*Bifidobacterium adolescentis* were labelled with PI in order to observe cell location/distribution within the PPI + AL capsules. Five millilitres of *B. adolescentis* cells ( $\sim 8 \log \text{ CFU mL}^{-1}$ ) in PBS were fixed overnight at 37°C in an oxygenated environment to permeabilize the bacterial cell membrane. Cells were then pelleted by centrifugation (1900 x g, 15 min) and resuspended in an aqueous solution of PI (15 nmol) for 2 h at room temperature, and then washed with PS (1.0 mL) by centrifugation three times to remove any unbound PI.

### **3.4.3 Production of pea protein-alginate capsules containing GLU-FA**

Capsules composed of the wall materials 1.0% AL and 4.0% PPI + 0.5% AL were prepared as described in section 3.2.4.1. For examination of carbohydrate distribution, 7 mg of GLU-FA dissolved in 0.40 g of DMSO was added to the PPI + AL wall material solution. The concentration of the PPI + AL solution was adjusted to account for the addition of DMSO to ensure the wall material concentrations were maintained at 4.0% PPI + 0.5% AL. Examinations of prebiotic distribution within the capsules were measured in the absence of probiotics.

### **3.4.4 Production of pea protein-alginate capsules containing PI-labelled *B. adolescentis***

Capsules composed of the wall materials 1.0% AL and 4.0% PPI + 0.5% AL were prepared as described in section 3.2.4.1. For examination of probiotic distribution PI, labeled *B. adolescentis* were encapsulated. Capsules produced were stored at 4°C until analyzed.

### **3.4.5 Preparation of capsules for confocal laser scanning microscopy**

Capsules studied or examined by CLSM were, PPI + AL, PPI + AL + DMSO, PPI + AL + DMSO + 0.005 M FA, PPI + AL + DMSO + GLU-FA, PPI + AL + PI-labeled *B. adolescentis*. DMSO was added to the capsules in order to solubilise the GLU-FA. Capsules (1.5 g) were prepared for CLSM imaging by subjecting them to an ethanol dehydration series, followed by embedding in paraffin wax, cross-sectioning at 8  $\mu\text{m}$  and

mounting on a glass slide as described by Jensen (1962). The ethanol dehydration series consisted of several solution changes with each subsequent solution containing a slightly higher concentration of ethanol. The capsules (1.5 g) were dehydrated in an ethanol dehydration series which started with a 10% (V/V) ethanol solution (2.0 mL) followed by increases of 10% to a final ethanol concentration of 100% which was repeated three times. Capsules were maintained in each solution for 40 min before a dehydration change was made, leaving sufficient solution to cover the capsules. The resulting capsules were left overnight in 100% ethanol. Dehydrated capsules were incubated at 60°C and 3-4 chips of paraffin wax were added. Over the course of 1 d, paraffin wax chips (2-3) were added periodically (every 2 h) to increase the liquid volume two fold. Samples were incubated at 60°C overnight without lids (3 mL total volume) to afford ethanol evaporation. The wax was decanted and replaced three times with fresh molten wax (2.0 mL) to ensure removal of residual ethanol. The capsules plus wax were poured into ceramic dishes (3x5x1 cm) and were allowed to cool and harden at room temperature for 48 h. The capsules were then sectioned at 8 µm using a rotary microtome (Ernst Leitz GMBH, Weztlar, Germany) and mounted onto glass slides (75x25x1 mm) coated with Myer's solution (albumin and glycerol, 1:1, v/v). The sectioned capsules were allowed to adhere to the slides overnight. The slides were then placed in xylene overnight to dissolve the wax; this step was repeated with fresh xylene. Coverslips were mounted onto the glass slides using ProLong and were imaged by CLSM.

#### **3.4.6 Confocal laser scanning microscopy**

A Zeiss LSM 410 Confocal Laser Scanning Microscopy system (Zeiss, Thornwood, NY), equipped with an argon multiline ion laser (Uniphase 2214-25ML) was used to investigate the location and distribution of the GLU-FA and probiotics within the PPI + AL capsules. All confocal fluorescence images were taken with a 10x (numerical aperture [N.A.] 0.3 Epiplan-Neofluar) or 40x (N.A. 1.3 Plan-Neofluar) objective. The software used for CLSM imaging was Carl Zeiss LSM version 3.99 (Zeiss). The laser was adjusted to an excitation wavelength of 488 nm. Emission filter blocks Chroma

D515/20 and HQ610/75 were used for the GLU-FA and probiotic imaging, respectively. Scale bars were added to the images using ImageJ version 1.38w.

### **3.4.7 Cold stage scanning electron microscopy**

One or two capsules of each wall material (AL and PPI + AL) were randomly selected and imaged. Data was reported using 10-20 measurements from an individual capsule from 2-3 images and represent as an average measurement  $\pm$  standard error of measurement. Individual capsules were placed into 2 mm cavities machined into 2x1x0.5 cm custom made copper mounts which were then plunge-frozen in nitrogen slush at -210°C. The samples were placed in the Emitec K1250 cryo preparation chamber (Emitec, Ashford, UK) at -170°C and fractured with a precooled sharp blade. Samples were transferred under vacuum to the SEM chamber (JEOL, Field Emission SEM, Tokyo, Japan) where the temperature was raised to -40°C and surface ice was allowed to sublime for approximately 30 min. Samples were then cooled to -150°C and transferred back to the cryo preparation chamber where they were sputter coated with about 100 Å of gold and transferred to the SEM chamber maintained at -160°C with an acceleration voltage of 5kV. Images were recorded digitally.

Pore sizes were determined by measuring the long and short internal axis. The aspect ratio of the pores was determined by dividing the long internal axis by the short internal axis.

### **3.4.8 Atomic force microscopy**

Capsules (1.5 g) were dehydrated in an n-butanol series prior to examination by AFM. The n-butanol series consisted of several solution changes with each subsequent solution containing a slightly higher concentration of n-butanol. The n-butanol dehydration solutions were as follows and in order of addition: A (50 ml H<sub>2</sub>O/40 mL 95% EtOH/10 mL n-butanol), B (30 mL H<sub>2</sub>O/50 mL 95% EtOH/20 mL n-butanol), C (15 mL H<sub>2</sub>O/50 mL 95% EtOH/35 mL n-butanol), D (45 mL 95% EtOH/75 mL n-butanol), E (35 mL 95% EtOH/75 mL n-butanol) and F (100% n-butanol). The capsules were maintained in each solution for 1 h before a dehydration change was made, leaving

sufficient solution to keep the capsules covered. The final 100% n-butanol dehydration was repeated three times and samples were maintained at 4°C until imaged.

Atomic force microscopy was performed using a PicoSPM Iinstrument (Molecular Imaging Corp. Tempe, AZ). Imaging was carried out using oxide-sharpened silicon nitride AFM probes with a tip radius of ca. 10 nm (cantilever nominal spring constant = 0.12 N m<sup>-1</sup>; resonance frequency of approximately 26 Hz; Veeco Probes, Camarillo, CA) in the contact mode. The scanning force constant was 60-80 nN and scan rates were approximately 1 Hz. Image areas of 5.0 by 5.0 µm were collected. The stored images were analyzed using PicoScan software, version 5.3.3. (Molecular Imaging Corp.) to determine capsule surface roughness. Six areas of 2.0 by 2.0 µm were selected from each capsule image and analyzed to determine the root mean squared surface roughness of the capsule. Data was obtained from two randomly selected capsules of each type.

The root mean squared roughness ( $R_{rms}$ ) is calculated from the equation:

$$R_{rms} = \sqrt{\frac{\sum_{i=1}^n (Z_i - \bar{Z})^2}{n}}$$

where  $Z_i$  is the height value of each single data point in the image,  $\bar{Z}$  is the mean value of all the height values in the image, and  $n$  is the number of data points in the image.

### 3.5 Statistics

Sample data are presented as the mean  $\pm$  standard deviation, unless otherwise stated. Statistical significance between samples was determined using the Student's T-test ( $p < 0.05$ ).

## 4. Results and Discussion

### 4.1 Study 1: Investigation on the effects of wall material and capsule size on the survivability of encapsulated *B. adolescentis* in SGJ

#### 4.1.1 Comparison of the growth profile of *B. adolescentis* in MRS and RCM broths

*Bifidobacterium adolescentis* reached stationary growth phase more rapidly in the RCM-cys broth than in the MRS-cys broth (Figure 4-1 A, B). The optical densities of the cells indicated that the stationary phase for RCM-cys was reached after 20 h of growth, whereas 30 h was required for MRS-cys (Figure 4-1 A). The viable cell count data indicated that *B. adolescentis* reached the target growth value of approximately  $9 \log \text{CFU mL}^{-1}$  at 20 h of growth for both RCM-cys and MRS-cys broth; these cell numbers were maintained for up to 27 h (Figure 4-1 B). Viable cell count experiments were halted after 27 h of growth as numbers had not changed between 20 and 27 h. For RCM-cys broth, the entry into the stationary phase resulted in cell numbers close to the target growth value of approximately  $9 \log \text{CFU mL}^{-1}$ .

The importance of producing a cell concentration of approximately  $9 \log \text{CFU mL}^{-1}$  was based on the delivery of sufficient bacteria to transverse the GI tract and reach the colon in numbers large enough to produce a beneficial affect to the host (Bouhnik, 1993). It is also important for the bacteria to be in their stationary growth phase as it has been shown that the acid tolerance of probiotics increases after entry into this growth phase and therefore would have some natural resistance to the acidic environment of the stomach (Hartke et al., 1996). In this study, the stationary growth phase for *B. adolescecentis* was reached at 20 and 30 h for RCM-cys and MRS-cys broths respectively. Entry into the stationary phase for both media differed between the measurements taken using optical density and cell concentration (Figure 4-1 A,B). The discrepancy was thought a result of the increased sensitivity of the cell concentration assay in comparison to the optical density assay. Because the target cell numbers of

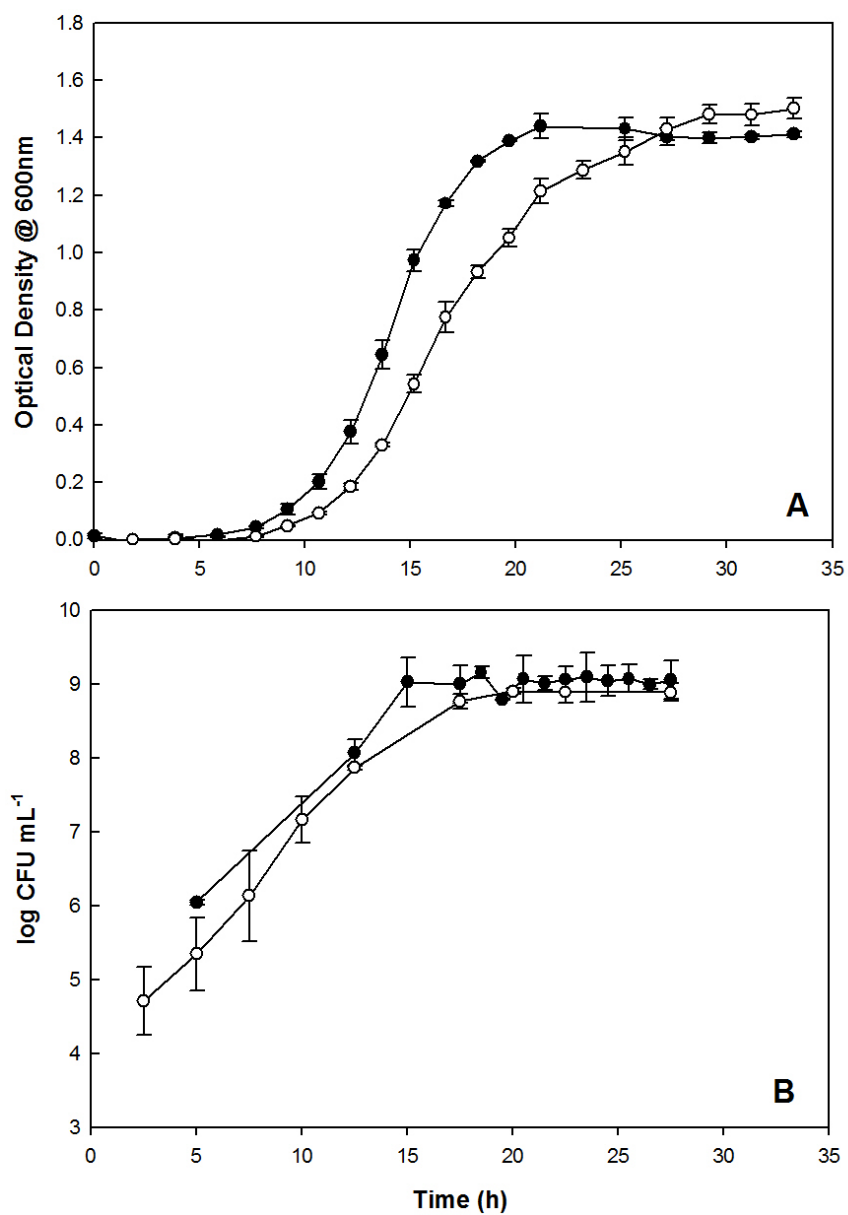


**Figure 4-1** Optical density (A) and cell numbers (B) for growth curves of *B. adolescentis* in (○) MRS-cys and (●) RCM-cys broths. Data points represent the mean value and the range is represented by the bars.

approximately 9 log CFU mL<sup>-1</sup> was reached in the RCM-cys stationary phase of growth more rapidly (~20 h) it was used as the growth medium for all further studies.

#### **4.1.2 Capsule geometric mean, surface morphology and size distribution**

*Bifidobacterium adolescentis* was successfully encapsulated using the modified extrusion method of Krasaekoopt et al. (2003), with encapsulated cell numbers averaging  $8.7 \pm 0.4$  log CFU mL<sup>-1</sup> (number of cells added to capsule suspension) or  $7.4 \pm 0.2$  log CFU g<sup>-1</sup> wet capsules. Capsule size and percent size distribution were determined using PSA and the geometric mean and variance of the capsules, and percent distribution are shown in Table 4-1 and Figure 4-2, respectively. Capsules produced via extrusion using 1.0% AL had a geometric mean diameter of 2.3 mm, and were spherical in shape and colourless. The 4.0% WPI + 0.5% AL capsules had a geometric mean diameter of 2.2 mm, had a tear drop shape and a white opaque colour (Figure 4-3 F). The 4.0% PPI + 0.5% AL were the smallest capsules produced (geometric mean diameter = 2.0 mm) and also exhibited the tear dropped shape and had a pale tan opaque colour. SEM images of the freeze- and air-dried capsules revealed that the AL capsules exhibited a rougher, more porous-appearing external structure (Figure 4-3 A, B), whereas the WPI and PPI capsules had a smoother, less porous external appearance (Figure 4-3 C-F). *Bifidobacterium adolescentis* was also successfully encapsulated by the emulsion method of Tuelstrup-Hansen et al. (2002) using AL only, yielding an average number of viable cells of  $8.3 \pm 0.2$  log CFU mL<sup>-1</sup> (section 3.2.3). This method was successful in reducing the size of the capsules to less than 100 µm, with a mean geometric diameter of 53.38 µm and had a size distribution ranging from approximately 10 to 350 µm (Table 4-1, Figure 4-2).

The extrusion method afforded the production of capsules of consistent size and relatively uniform size distribution (Table 4-1 and Figure 4-2). According to literature, capsules produced by this method vary in size from 2 to 5 mm in diameter, which is controlled by the concentration of the wall material solution, the needle diameter of the syringe, and the distance between the syringe and the cross linking solution (Krasaekoopt et al., 2003; Anal & Singh, 2007). The non-spherical tear-drop shape of the protein-

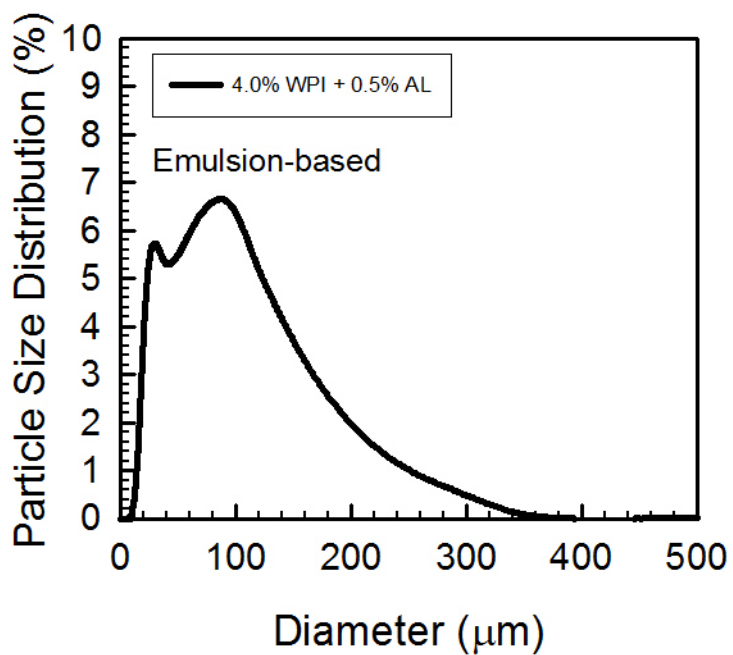
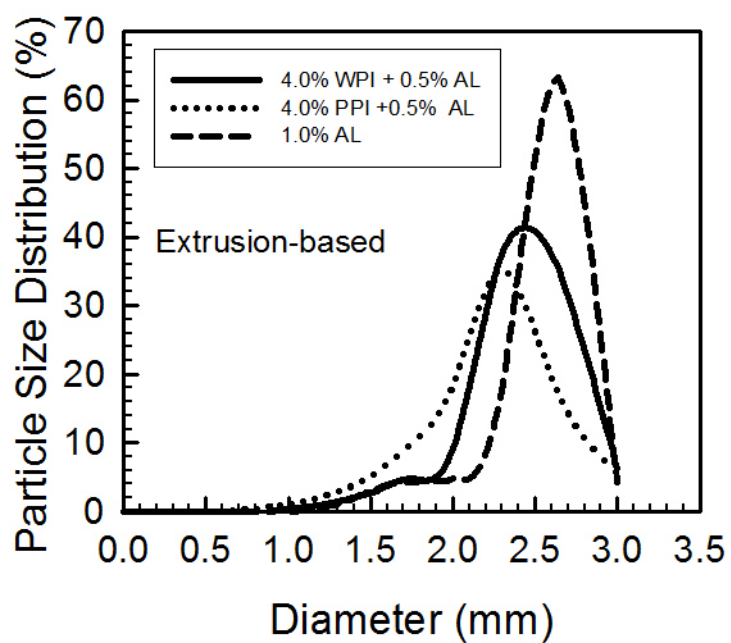


**Figure 4-2** Particle size distribution (%) determined by particle size analysis of capsules produced by extrusion and emulsion methods.



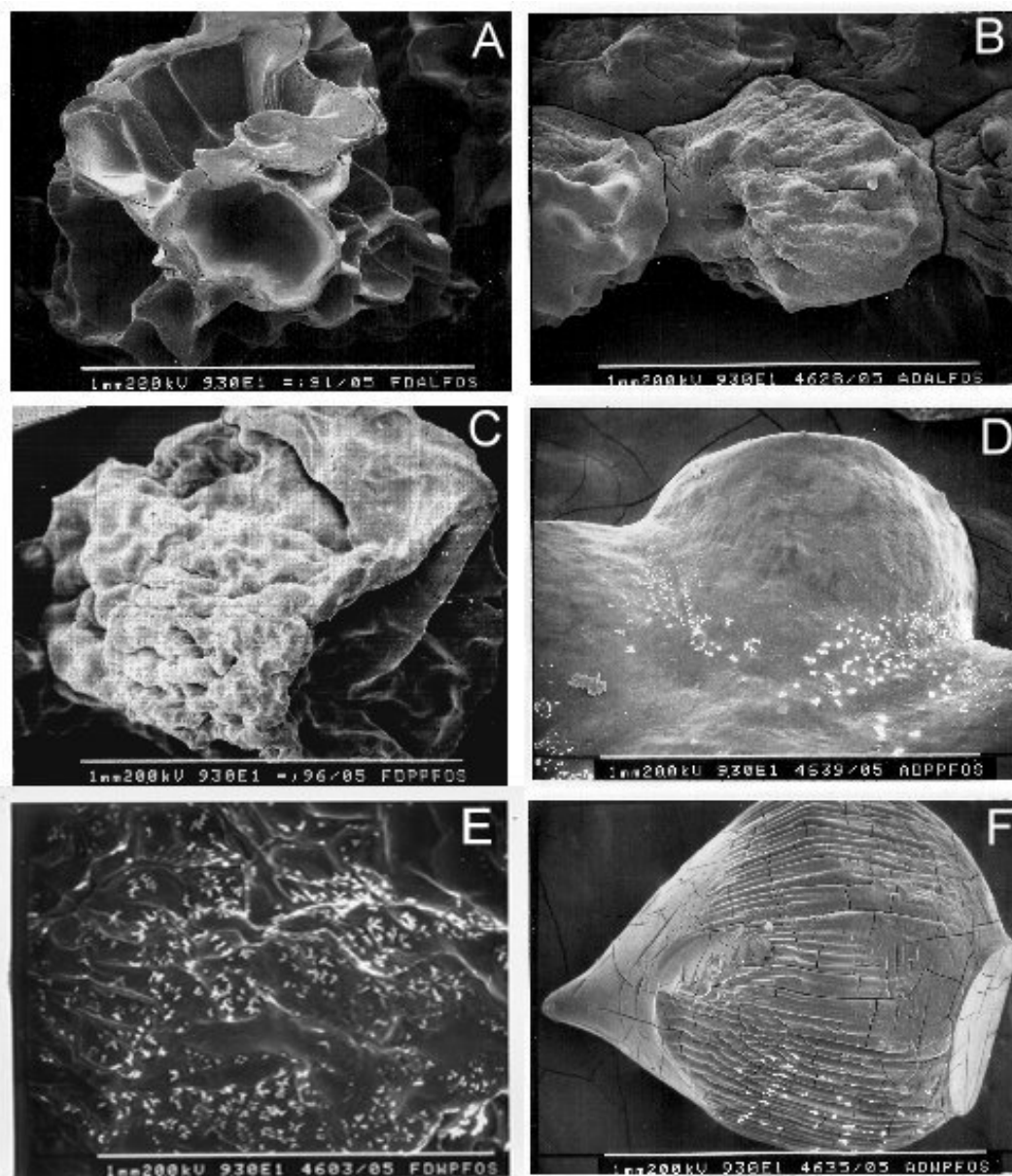


**Figure 4-3** SEM micrographs of freeze- (A, D, and E) and air-dried (B, C, and F) extrusion based capsules produced with AL (A, B); PPI + AL (C, D); WPI + AL (E, F). Magnification at 9.3x.

**Table 4-1 Geometric mean diameter of capsules produced by extrusion and emulsion methods determined by PSA.**

Technique	Materials <sup>a</sup>	Geometric Mean (μm)
Extrusion	1.0% AL	2254
	1.0% AL with 1.0% P95	2018
	4.0% WPI + 0.5% AL	2150
	4.0% WPI + 0.5% AL with 1.0% P95	2054
	4.0% PPI + 0.5% AL	1990
	4.0% PPI + 0.5% AL with 1.0% P95	1769
Emulsion	4.0% WPI + 0.5% AL	53.38

<sup>a</sup> alginate (AL), whey protein isolate (WPI), pea protein isolate (PPI)

based capsules (Figure 4-3 F) can be explained by the slower gelation properties of this material when compared to AL (Reid et al., 2005). In order to decrease the diameter of the capsules to <100 μm, a modification of the emulsion method of Truelstrup-Hansen et al. (2002) was used. The wall material concentration (4.5%) was higher compared to the capsules created by Truelstrup-Hansen et al. (2002). To reduce the size of the capsules the rpm of the stirrer was increased to 900 rpm to decrease the droplet size within the emulsion to <100 μm. The size of these microcapsules (~53μm) was below that of 100 μm which is reported to not adversely affect the texture of foods (Truelstrup-Hansen et al., 2002).

#### **4.1.3 Survival of free and encapsulated *B. adolescentis* in SGJ**

Free *B. adolescentis* cells were able to survive for 2 h in SGJ at pH 3.0 and 6.0 with little (a decline of 1.2 log CFU mL<sup>-1</sup> from initial cell numbers), or no reduction in cell viability, respectively (Figure 4-4 A, B). However, free cells were not able to survive in SGJ at pH 2.0, as indicated by the rapid drop (7 log CFU mL<sup>-1</sup>) in cell viability after only 10 min (Figure 4-4 C). Encapsulating *B. adolescentis* in 1.0% AL by the extrusion method did not result in improved cell survival in SGJ at pH 2.0, as cell counts were similar to those observed for the free cells (Figure 4-4 C). Capsules produced using either 4.0% WPI or PPI + 0.5% AL aided the survival of *B. adolescentis* in SGJ at pH 2.0

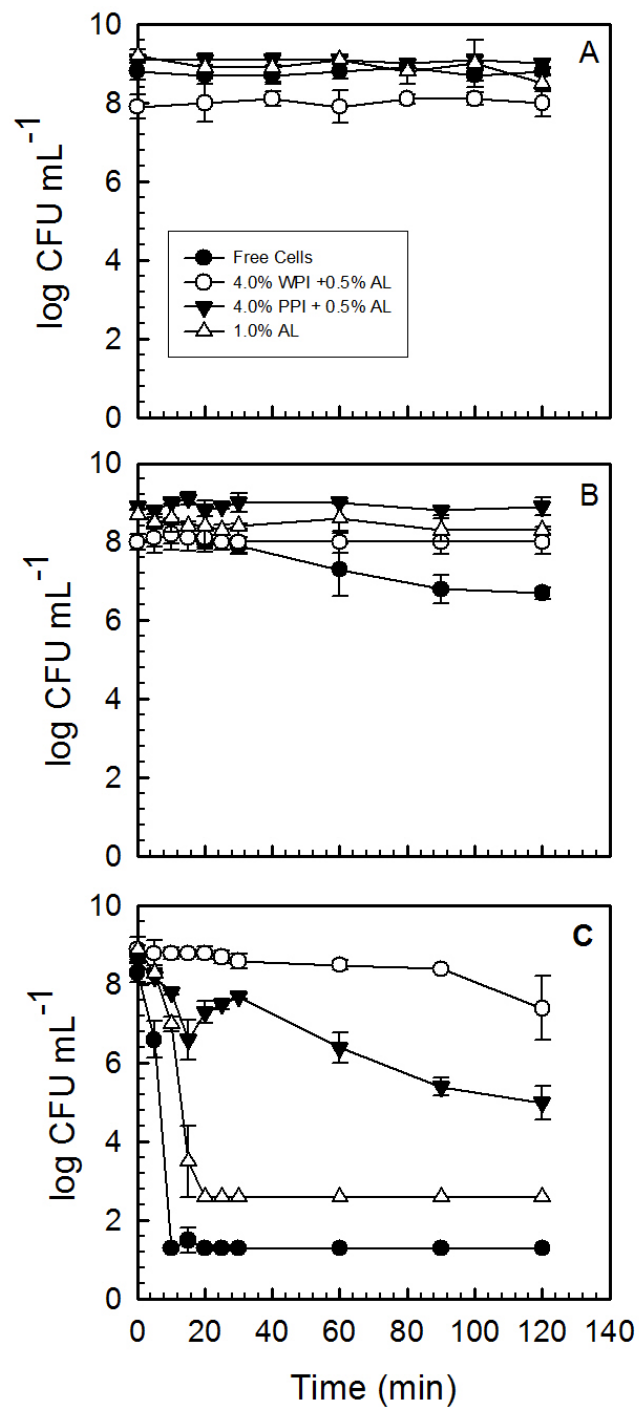


**Figure 4-4** Survival of free- and extrusion-based encapsulated *B. adolescentis* cells in SGJ at pH 6.0 (A), pH 3.0 (B) and pH 2.0 (C), detection limit of 1.3 and 2.6  $\log \text{CFU mL}^{-1}$  for free and encapsulated cells, respectively. Data represents the mean value  $\pm$  one standard deviation ( $n = 3$ ).

(Figure 4-4 C). After 2 h of exposure to SGJ at pH 2.0, *B. adolescentis* experienced a 1.5 and 3.6 log CFU mL<sup>-1</sup> reduction in numbers for 4.0% WPI + 0.5% AL and 4.0% PPI + 0.5% AL, respectively.

The increase in probiotic survival exhibited by the capsules produced by the extrusion method may be explained by several factors. First, structural differences between the AL capsules and the protein + AL capsules could help to explain the increase in probiotic survival for the protein + AL capsules. SEM of the AL capsules produced in this study showed a very porous and rough external surface (Figure 4-3 A, B). With these large pore sizes (~400 µm; Figure 4-3 A), SGJ could readily diffuse into the AL capsules resulting in decreased probiotic survival. Both of the protein-based capsules had a smoother, less porous external surface than the AL capsules (Figure 4-3 C-F). The smoother, less porous external surface of the protein-based capsules may have resulted in a slower diffusion of SGJ into the capsules resulting in higher probiotic survival rates.

Second, the observed increase in probiotic survival for the protein + AL capsules may be related to the higher concentration of wall materials used when compared to the AL capsules. The AL capsules were prepared using 1.0% (w/w) AL, whereas the protein + AL capsules were prepared using 4.0% protein + 0.5% AL. This difference in concentration of the wall materials would result in a more dense capsule structure, which would be expected to retard the diffusion of SGJ into the protein-based capsules when compared to the less dense structure of the AL capsules. The observed higher survival rate for the probiotic in the WPI + AL versus PPI + AL capsules may be explained by the higher concentration of protein per gram of wall material for WPI (97%) when compared to PPI (82%). It has been shown that an increase in wall material concentration improves probiotic survival for AL (Lee & Heo, 2000).

Finally, the protein-based capsules in this research were produced using a high (0.45 M) CaCl<sub>2</sub> concentration which resulted in opaque capsules. Barbut (1995), found that WPI gels produced with a high (>180 mM) CaCl<sub>2</sub> concentrations were opaque and had lower water holding capacity, when compared to those produced with low (<180 mM) CaCl<sub>2</sub> concentrations which were transparent. These differences in water

holding capacity could explain the increased survival of the probiotic in protein-based (lower SGJ absorption) versus AL (higher SGJ absorption) capsules.

The emulsion-produced capsules employing 4.0% WPI + 0.5% AL as wall materials were unable to provide any protection to the probiotic against SGJ at pH 2.0, as the results obtained were similar to those of the free cells (Figure 4-5 C). By decreasing the size of the capsules the surface area to volume increases which increases the exposure of the capsules to the environment. Therefore, as the surface area to capsule size decreases the ability of the SGJ to diffuse into the capsules increases, decreasing probiotic survival. These results agree with those reported in literature, where alginate capsules showed no protection for encapsulated *B. longum* and *B. lactis* at pH 2.0 (Truelstrup-Hansen et al., 2002). The emulsion-produced capsules could exhibit structural differences to the extrusion-produced capsules that may increase the ability of SGJ to infiltrate the capsules. However, no structural studies of the emulsion-produced capsules was conducted.

#### **4.1.4 Summary and conclusions**

The use of RCM broth supplement with L-cysteine was able to produce cell concentrations of *B. adolescentis* of approximately  $9 \log \text{CFU mL}^{-1}$  in their stationary growth phase. This was important because *B. adolescentis* in their stationary growth phase have the highest acid tolerance, and would be in sufficient concentration to produce a beneficial effect to their host upon arrival to the large intestine.

The type of wall materials used in capsule production was found to have an effect on probiotic survival. The use of pea and whey proteins in combination with AL resulted in increased probiotic survival in SGJ at pH 2.0, whereas AL alone showed no added protection. Images of the freeze- and air-dried capsules showed the AL capsules to be more porous than the protein-AL capsules. The use of protein in the wall material solution resulted in a smoother, less porous capsule which may have inhibited the movement of SGJ into the capsule resulting in increased probiotic survival. The higher wall material concentration in the protein + AL capsules increased probiotic survival as

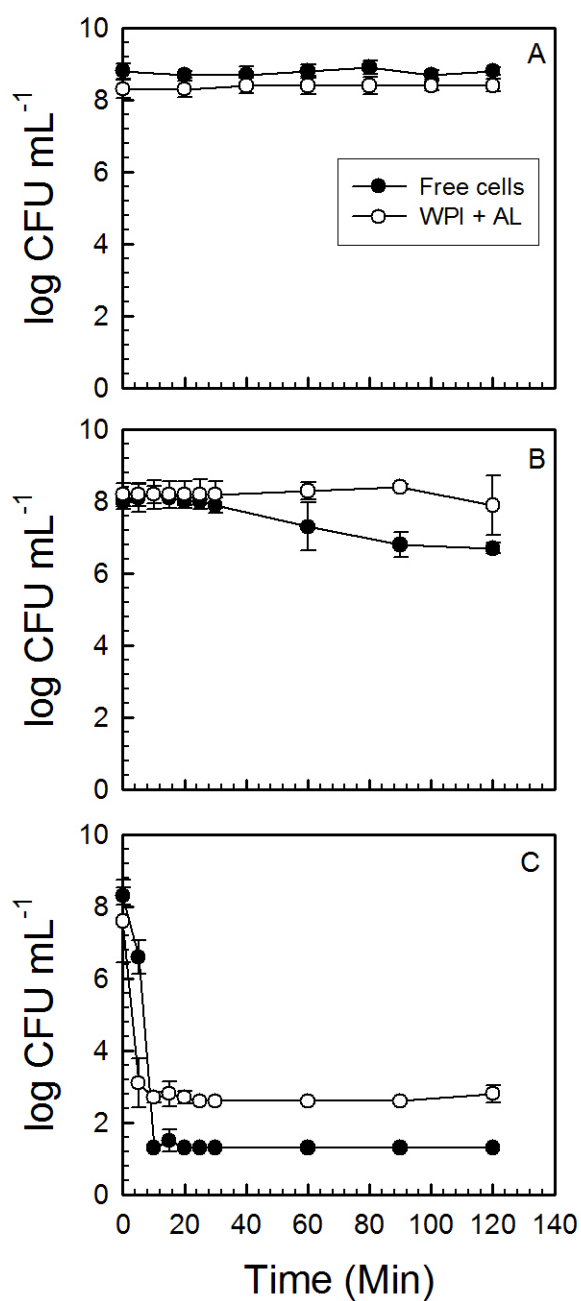


**Figure 4-5** Survival of free- and emulsion-base encapsulated *B. adolescentis* cells in SGJ at pH 6.0 (A), pH 3.0 (B) and pH 2.0 (C), detection limit of 1.3 and 2.6  $\log \text{CFU mL}^{-1}$  for free and encapsulated cells, respectively. Data represents the mean value  $\pm$  one standard deviation ( $n = 3$ ).

these capsules had a total polymer concentration of 4.5% compared to just 1.0% for Al capsules.

Capsule size was also found to effect probiotic survival. Capsules produced with 4.0% WPI + 0.5% AL by emulsion and extrusion had geometric means of 0.054 and 2.2 mm respectively. No increase in probiotic survival in SGJ (over free cells) was observed for the small capsules, whereas only a 1.0 log CFU mL<sup>-1</sup> reduction was observed for the larger capsules. However, structural differences between the emulsion and extrusion produced capsules could also help to explain decreases in probiotic survival.

## **4.2 Study 2: Investigation of the growth potential of *B. adolescentis* on a selection of carbohydrates, and the effect of the encapsulated synbiot on probiotic survival in SGJ**

### **4.2.1 Comparison of *B. adolescentis* specific growth rates in a semi-synthetic media containing different carbohydrates**

The specific growth rate of *B. adolescentis* was studied on glucose, two different FOS samples (P95 and Syn), and an inulin sample (ST). As shown in Figure 4-6, *B. adolescentis* was able to utilize inulin and FOS as a carbon source and had a significantly ( $p < 0.05$ ) higher specific growth rate with P95 when compared to glucose. However, all of these commercial samples contained appreciable levels of glucose, fructose and sucrose. For example, 1.3% and 5.7% of the total carbohydrate content (as per supplier data) of ST was glucose/fructose and sucrose, respectively. Therefore, a growth study employing the maximum amount of these carbohydrates (8.5%) was conducted with glucose (0.85 g L<sup>-1</sup>). *Bifidobacterium adolescentis* was able to grow in this medium with a specific growth rate that was not significantly different ( $p > 0.05$ ) from those observed for Glu, ST or Syn.

A glucose-free maltooligoaccharide (MOS) sample was prepared from a DE-36 syrup employing both HPAE-PAD and Ca<sup>+2</sup> ion exchange chromatography with a final monosaccharide content of <0.007%. The specific growth rate of *B. adolescentis* with MOS was not significantly different from those of glucose and Min Glu (Figure 4-6).

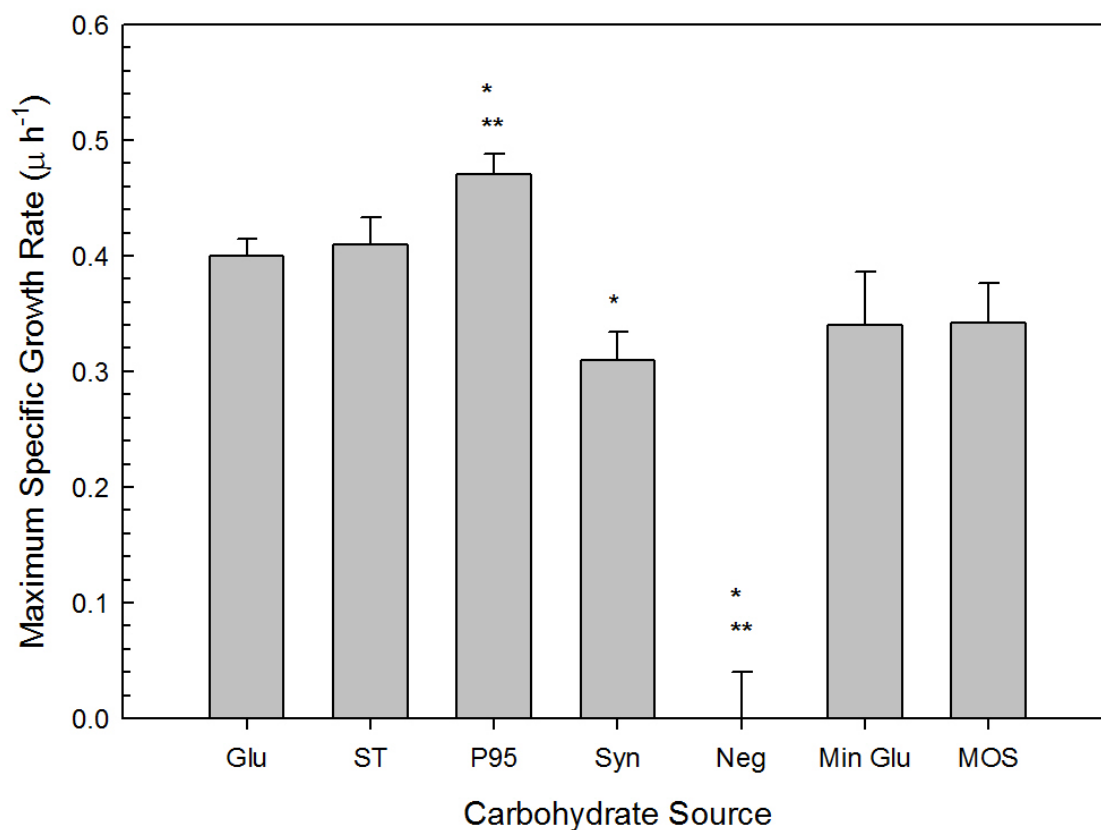


**Figure 4-6** Specific growth rates of *B. adolescentis* on different carbohydrate samples; Glu (10.0 g L<sup>-1</sup> glucose); ST (10.0 g L<sup>-1</sup> Orafti® ST); P95 (10.0 g L<sup>-1</sup> Orafti® P95); Syn (10.0 g L<sup>-1</sup> Orafti® Synergy1); Neg (no carbohydrate); Min Glu (0.85 g L<sup>-1</sup> glucose); MOS (10.0 g L<sup>-1</sup> glucose free maltooligosaccharide). Data represents the mean value  $\pm$  one standard deviation (n = 3). Notations (\*) and (\*\*) represent a significant change in specific growth rate from glucose and minimal glucose, respectively (p < 0.05).



The observed ability of *B. adolescentis* to utilise short chain FOS better than glucose and large chain FOS has been observed by others (Gibson & Wang, 1994b; Hopkins et al., 1998; Kaplan & Hutkins, 2000; Rossi et al., 2005; Vernazza et al., 2006; Huebner et al., 2007). However, in all of these published studies, the carbohydrate sources used were commercial and contained appreciable levels of monosaccharides (i.e., glucose/fructose) which leads to some confusion comparing specific growth rates on these substrates and oligosaccharide utilization. Gibson & Wang (1994b) reported *B. adolescentis* NCFB 2230 to have a significantly higher ( $p < 0.01$ ) specific growth rate ( $0.27 \pm 0.03 \text{ h}^{-1}$ ) for oligofructose (DP 2-4) than for glucose ( $0.20 \pm 0.05 \text{ h}^{-1}$ ), but no difference was observed when inulin ( $0.20 \pm 0.03 \text{ h}^{-1}$ , DP of 10) was used as the carbon source when compared to glucose. Huebner et al. (2007) reported that *B. adolescentis* ATCC# 15706 was able to utilise Raftilose® P95 (DP 2-7, 95% FOS) more effectively than inulin. In contrast, Vernazza et al. (2006), reported *B. adolescentis* DSM20083 had a lower specific growth rate on P95 ( $0.09 \pm 0.02 \text{ h}^{-1}$ ) and a higher specific growth rate on ST ( $0.24 \pm 0.01 \text{ h}^{-1}$ ) when compared to glucose ( $0.11 \pm 0.01 \text{ h}^{-1}$ ). Kaplan & Hutkins (2000) investigated the specific growth rate of *B. infantis* 17930 on a purified FOS and demonstrated that the growth was in fact due to the utilization of the FOS instead of any appreciable amount of monosaccharides found in the commercial sources; however, the pure FOS were added to basal MRS broth which contained 2.0% glucose. It has been reported that the ability and the extent of FOS utilization as a carbon source is highly species- and strain-specific, and can account for the published differences in specific growth rates observed (Gibson & Wang, 1994b; Hopkins et al., 1998; Kaplan & Hutkins, 2000; Rossi et al., 2005; Vernazza et al., 2006; Huebner et al., 2007).

In the present study, *B. adolescentis* was able to grow in a low concentration ( $0.85 \text{ g L}^{-1}$ ) of glucose at a rate that was not statistically different from GLU, ST and Syn. These results indicate that the specific growth rate for probiotics in literature may only represent the utilization of the monosaccharides present in the FOS samples, rather than oligosaccharide utilization. The prepared MOS material was used to confirm whether *B. adolescentis* was able to utilise oligosaccharides when glucose was present in minimal concentrations ( $<0.007\%$ ). The specific growth rate for MOS indicated that

*B. adolescentis* was able to utilise DP 2-7 oligosaccharides as effectively as glucose with rates of  $0.34 \pm 0.03$  and  $0.40 \pm 0.02 \text{ h}^{-1}$ , respectively.

#### **4.2.2 HPAE-PAD analysis of the carbohydrate profile of the medium containing P95 (FOS) and MOS before and after incubation with *B. adolescentis***

The carbohydrate profile of P95 and MOS before (0 h) and after (24 h) incubation with *B. adolescentis* was determined by HPAE-PAD analysis of the medium (Table 4-2). A significant reduction in peak area for select oligosaccharides (DP 3-6) in medium containing P95 was observed with ranges of 33.7 to 49.8%, whereas the peak area for DP 2 increased by 15.2%. For MOS, the DP 2-4 oligosaccharides were completely utilized whereas DP 5-7 were not utilized at all as their peak areas/heights were virtually unchanged (Figure 4-7).

To confirm that *B. adolescentis* utilized the oligosaccharides in the samples and not just the monosaccharides, the carbohydrate profile of the growth medium containing P95 at time 0 and 24 h was determined by HPAE-PAD. The significant reduction in peak areas (Table 4-2) for DP 3-6 indicated that *B. adolescentis* utilized these oligosaccharides. The changes observed in carbohydrate peak area also show that *B. adolescentis* did not preferentially utilize a specific DP first. These results were in agreement with those of Rossi et al. (2005) and Ameratti et al. (2006) who reported simultaneous utilization of FOS by *B. adolescentis* MB 239. The peak area for DP 2 increased over the 24 h time period indicating its production during probiotic growth as a result of the breakdown of longer chain oligosaccharides. The enzymes inulinase or  $\beta$ -fructosidase are produced by *B. adolescentis* in the presence of P95 and cleave off fructose moieties from the non-reducing end of the oligosaccharide molecules creating shorter chain compounds (McKeller & Molder, 1989). The use of short chain FOS as a prebiotic for encapsulation with *Bifidobacterium* shows much promise as these organisms are able to utilize these compounds as a carbon source with specific growth rates close to or better than glucose (Gibson & Wang, 1994b; Hopkins et al., 1998; Kaplan & Hutkins, 2000; Rossi et al., 2005; Vernazza et al., 2006). Rossi et al., (2005) reported that out of 55 *Bifidobacterium* strains (representing 11 species), 52 were able to utilize FOS as a

**Table 4-2 Percent change in carbohydrate abundance in P95 after 24 h of *B. adolescentis* cell growth in a basal media containing P95 as the carbon source.**

Carbohydrate <sup>a</sup>	Mean Relative Retention Time (min)	% Change in peak area after 24 h <sup>b</sup>
F	6.14	-11.5 (5.5)
DP2	18.90	+15.2 (10.2)
DP3	24.86	-33.7 (6.2)
DP4	29.96	-49.8 (4.2)
DP5	36.22	-42.4 (5.6)
DP6	45.33	-38.0 (8.3)

<sup>a</sup> F, Fructose; G, glucose; DP 2-6 includes FOS with chemical structures of  $\text{Gal}1\rightarrow2[\beta\text{F}-1\rightarrow2]_n$ , and  $[\beta\text{F}-1\rightarrow2]_n$  (i.e. DP 3 includes  $\text{F}_3$  and  $\text{GF}_2$ )

<sup>b</sup> – Indicates a decrease in peak area, + indicates an increase in peak area. Standard deviation in brackets (n = 3)

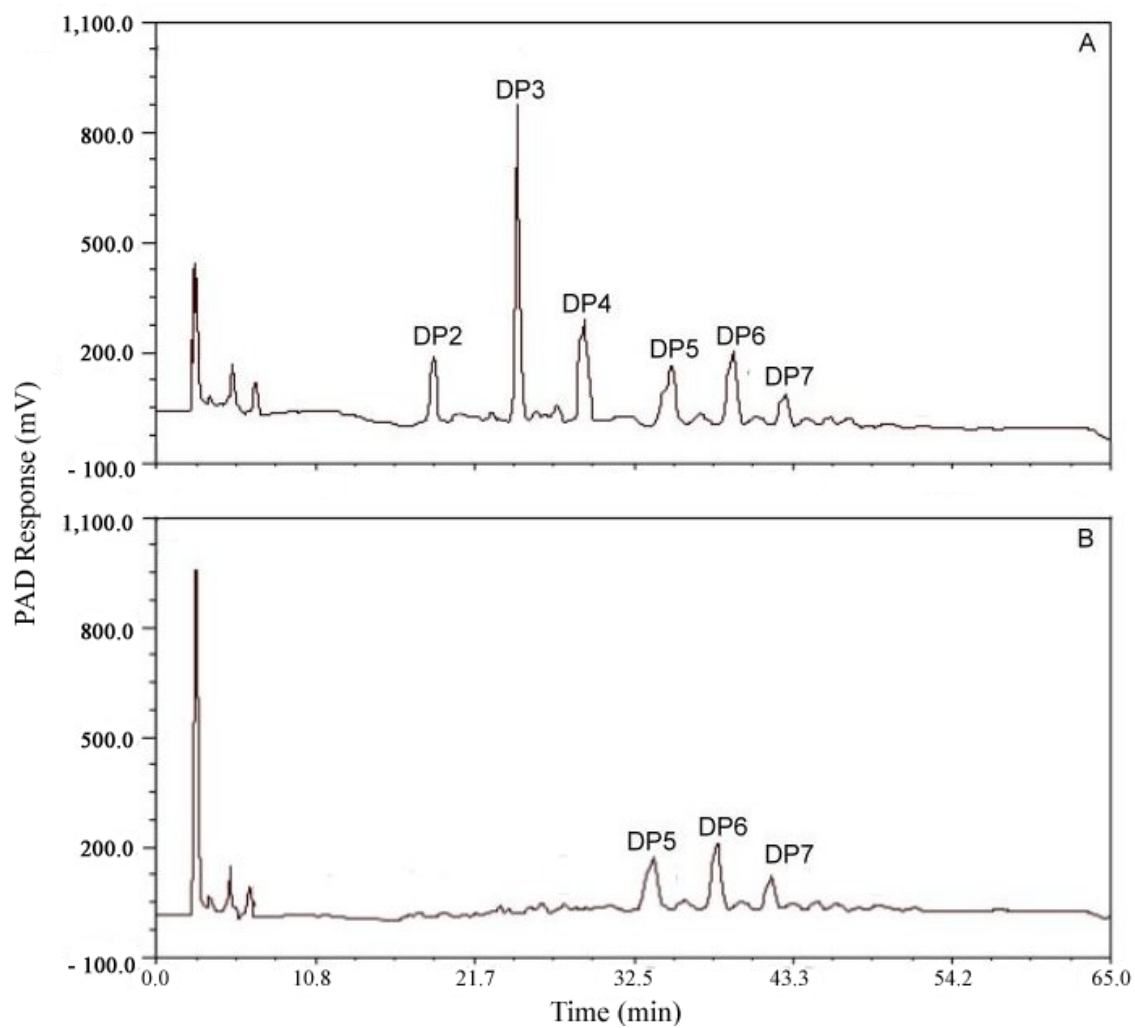


**Figure 4-7** HPAE-PAD carbohydrate elution patterns present at time 0 (A) and after 24 h of *B. adolescentis* growth (B). DP 2 = maltose, DP 3 = maltotriose, DP 4 = maltotetraose, DP 5 = maltopentaose, DP 6 = maltohexaose (glucose relative retention time ~ 6 min).

carbon source, whereas only 8 were able to utilize inulin (average DP of 25). Since FOS are nondigestible carbohydrates, they would transverse the GI tract and reach the colon intact and therefore be available to the bacteria for fermentation, whereas monosaccharides, such as glucose and fructose would be digested. The addition of FOS into the capsules would not substantially increase the caloric content of foods to which this material was added and would provide an appropriate carbon source for probiotic growth.

The HPAE-PAD analysis of the growth media containing MOS confirmed this materials ability to be utilized as a carbon source by *B. adolescentis* (Figure 4-7). After 24 h of *B. adolescentis* growth, the DP 2-4 oligomers, were completely utilized whereas the DP 5-7 oligomers were not. Although the MOS produced and used in this study would not be considered to be a prebiotic, it was clearly utilized as a carbon source by *B. adolescentis*.

#### **4.2.3 Synbiot encapsulation with FOS (P95) and its effect on the survival of *B. adolescentis* in SGJ**

The prebiotic, P95, was successfully encapsulated employing the extrusion method (see section 3.2.4.1). The mean percentage of the initial amount (0.1900 g) of P95 that was encapsulated was  $13.41 \pm 0.64 \%$ ,  $16.83 \pm 1.34\%$ , and  $10.87 \pm 0.32\%$  for 1.0% AL, 4.0% WPI + 0.5% AL, and 4.0% PPI + 0.5% AL, respectively (Table 4-3). Per gram of wet capsules, there was  $0.0044 \pm 0.0001$  g,  $0.0040 \pm 0.0003$  g and  $0.0044 \pm 0.0002$  g of P95 for 1.0% AL, 4.0% WPI + 0.5% AL, and 4.0% PPI + 0.5% AL, respectively. The carbohydrate profile of the encapsulated P95 was examined by homogenizing the capsules (5-8 g) in 30 mL of 0.1 M pH 7.0 phosphate buffer for 30 sec. HPAE-PAD chromatograms of a 0.04% P95 standard, and the extracted material from 1.0% AL + P95 (dilution factor of 10) capsules are shown in Figure 4-8.

The addition of P95 improved the survival of *B. adolescentis* in SGJ at pH 2.0 for all wall materials (Figure 4-9). The log CFU mL<sup>-1</sup> reduction after 2 h was 1.0 and 1.1 for 4.0% PPI + 0.5% AL and 4.0% WPI + 0.5% AL, respectively. The addition of P95 did

**Table 4-3 Percent P95 in extrusion-based capsules and supernatant.**

Wall Material <sup>a</sup>	Encapsulated <sup>b</sup>	Cross-linking Solution	Wash	Total
1.0% AL	13.41 ± 0.64	68.57 ± 4.20	13.16 ± 1.39	97.94 ± 3.70
4.0% WPI + 0.5% AL	16.83 ± 1.34	70.11 ± 2.07	14.72 ± 0.85	101.67 ± 4.12
4.0% PPI + 0.5% AL	10.87 ± 0.32	69.18 ± 2.60	16.32 ± 0.28	98.34 ± 2.04

<sup>a</sup>Alginate (AL), Whey Protein Isolate (WPI), Pea Protein Isolate (PPI)

<sup>b</sup> Values reported as mean ± SD (n = 3).

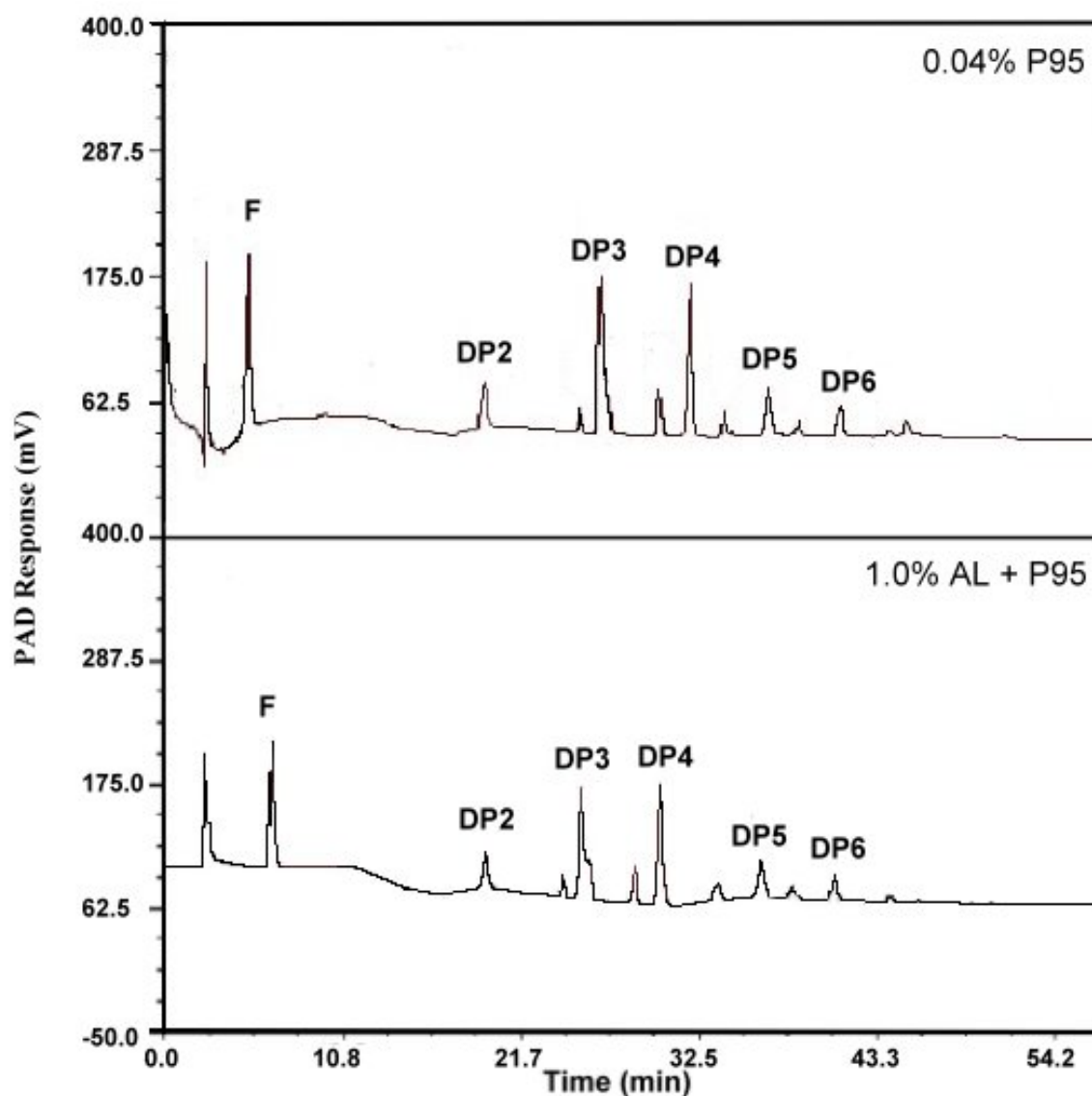
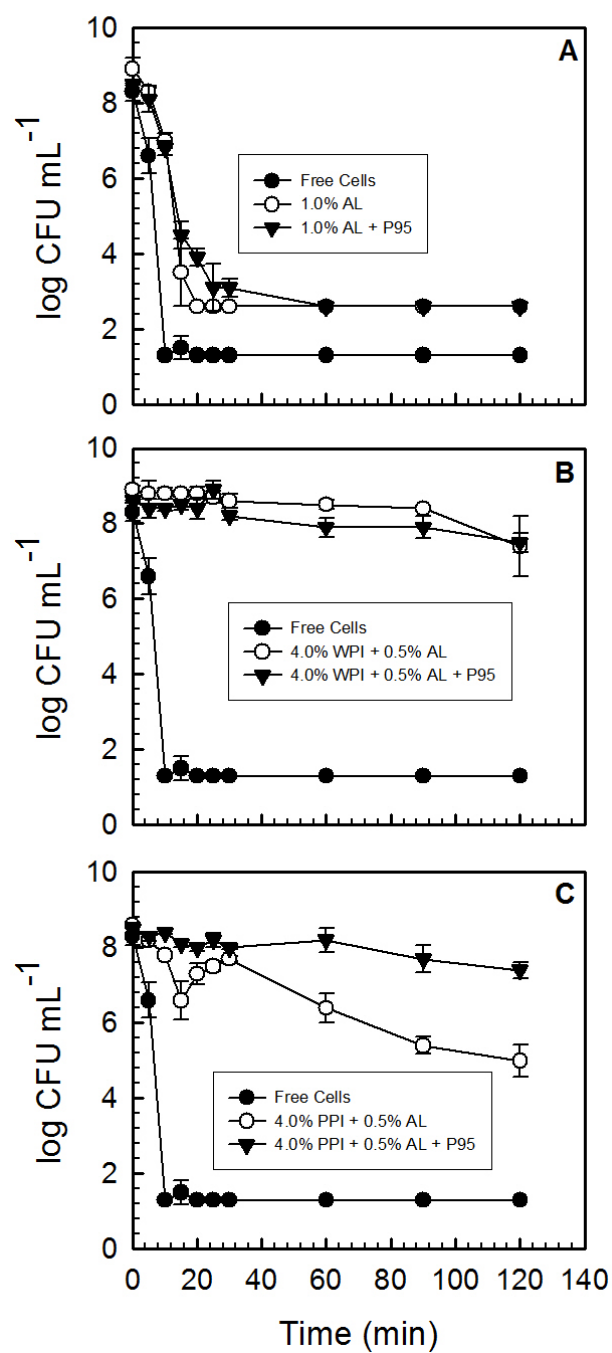


Figure 4-8 HPAE-PAD carbohydrate profiles for the P95 standard and the homogenized 1.0% AL + P95 extrusion-based capsules. (F= fructose, DP 2-6 =  $[\beta\text{F-1}\rightarrow\text{2}]_n$ ,  $n = 2-6$ ).



**Figure 4-9** Survival of free- and encapsulated *B. adolescentis* cells with and without P95 in SGJ at pH 2.0 for 1.0%AL (A), 4.0% WPI + 0.5% AL (B) 4.0% PPI + 0.5% AL (C). Data represents the mean value  $\pm$  one standard deviation (n = 3).



not appear to affect the structure of the capsules, as SEM images of capsules produced and without P95 were similar (results not shown). However the addition of P95 to the capsules could have caused some structural changes that were visualized using SEM, resulting in an increase in probiotic survival.

During capsule formation the water solubility of P95 facilitated its migration out of the capsules and into the cross-linking solution. Analysis (HPAE-PAD) of the cross-linking solution showed significant levels (68-70%) of the original P95 used with a further 13-16% in the capsule wash (PS) solution. The amount of carbohydrate encapsulated is important, as it must be sufficient to facilitate probiotic growth upon arrival at the colon. The amount of P95 encapsulated in one gram of wet capsules ranged from 4.0 to 4.4 mg. Growth studies from this research indicated that *B. adolescentis* was able to grow in a medium which contained as little as 0.085% carbohydrate (glucose). Therefore, one gram of capsules would contain sufficient carbohydrate to facilitate the growth of *B. adolescentis*. HPAE-PAD results show that the carbohydrate profile of the encapsulated P95 was similar to that of the P95 standard, indicating that no molecular sieving of this material by the pores present in the AL capsules occurred (Figure 4-8). This was also observed for capsules composed of PPI and WPI (results not shown). Therefore, *B. adolescentis* would have direct access to the FOS required for growth and proliferation upon arrival into the large intestine if the FOS is available to the bacteria and not cross-linked into the wall materials. The addition of P95 to the capsules may have increased the survival of *B. adolescentis* cells by increasing the physical barrier (wall) to SGJ diffusion into the capsule. The co-encapsulation of probiotics with prebiotics (synbiot) has been shown in literature to increase probiotic survival (Chen et al., 2005; Iyer & Kailasapathy, 2005).

#### **4.2.4 Enumeration of *B. adolescentis* before and after drying**

The moisture content in capsules produced by the extrusion method containing P95 was reduced by freeze and air-drying to investigate the effect of drying on probiotic viability after these treatments. Freeze-drying resulted in better survival of *B. adolescentis* than air-drying, with cell count of approximately (dried capsule weights

not determined)  $8.0 \pm 0.3 \log \text{CFU mL}^{-1}$  and  $6.6 \pm 0.3 \log \text{CFU mL}^{-1}$  for the 4.0% PPI + 0.5% AL capsules, respectively (Figure 4-10). *Bifidobacterium adolescentis* has been reported to have low oxygen tolerance with 24 h of exposure resulting in a 95% reduction in cell viability (Simpson et al., 2005). In this study, the observed significant differences in probiotic survival for WPI and PPI + AL versus AL capsules may be explained by the structural differences between the protein + AL capsules and the AL capsules (Figure 4-3). The addition of protein to the wall material may have provided an increased barrier to  $\text{O}_2$  diffusion.

#### 4.2.5 Summary and conclusions

*Bifidobacterium adolescentis* was able to utilise the commercial FOS and inulin sources as well as glucose, with short chain FOS (P95) resulting in the best growth rate. It was shown that *B. adolescentis* was able to grow on the low concentrations of glucose/fructose/sucrose (0.085%) present in the FOS sources. However, the growth of *B. adolescentis* on MOS and analysis of the growth media containing P95 and MOS by HPAE-PAD confirmed that the probiotic was able to grow and utilise oligosaccharides.

A concentration of P95 suitable for probiotic growth was successfully encapsulated by the extrusion method. Analysis by HPAE-PAD also demonstrated that the capsule matrix did not result in molecular sieving of the P95, in that the large DP FOS were not preferentially encapsulated over the low DP FOS. The addition of P95 to the capsules showed an increase in probiotic survival for the protein + AL capsules. The entrapment of both *B. adolescentis* and P95 within the protein-AL capsules created a synbiotic that protected the probiotics from SGJ and could potentially deliver both the organism and its carbon source to the large intestine. However, the availability of the prebiotic to *B. adolescentis* was not determined.

The protein-based capsules showed better survival than AL capsules for the probiotic for both drying techniques. Of the two protein-based capsules, the PPI + AL + P95 exhibited the best probiotic protection. Freeze drying resulted in higher survival rates than air drying which was mostly likely due to the decreased exposure to oxygen encountered for this technique.

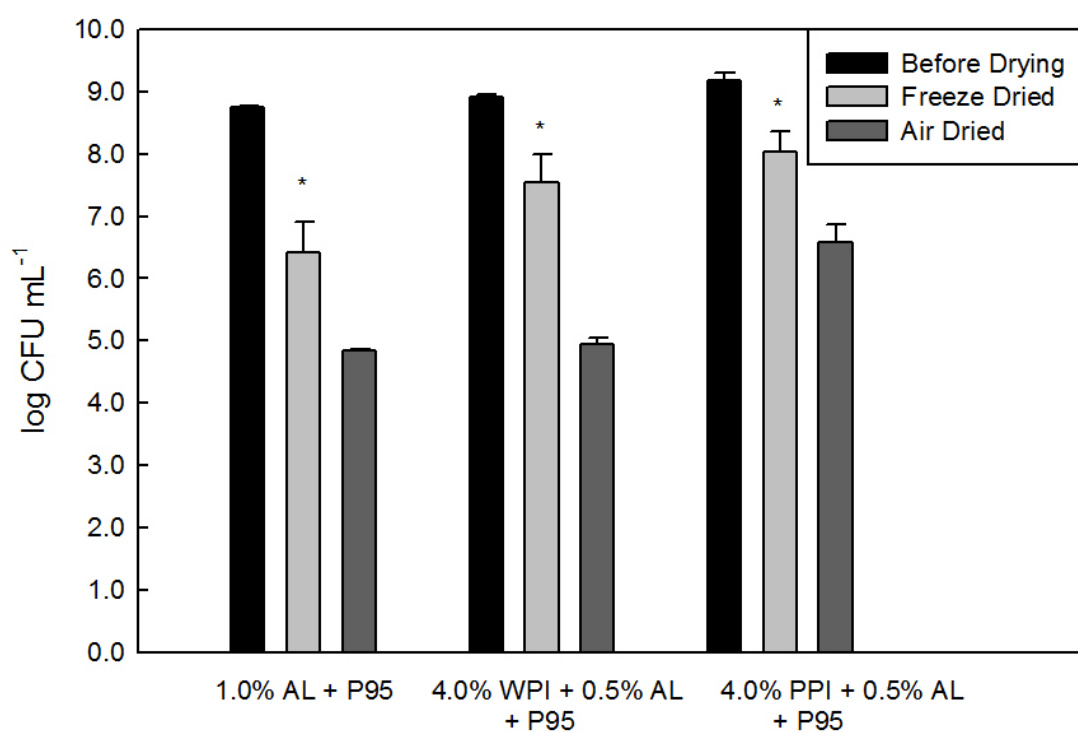


**Figure 4-10** *B. adolescentis* cell counts before and after drying in the extrusion-based capsules containing P95. Data represents the mean value  $\pm$  one standard deviation (n = 3).

\* Statistically significant ( $p < 0.05$ ) change in cell viability from air drying in respective wall material.

### **4.3 Study 3: Investigation of the external and internal structures, size and shapes of the pea protein-alginate capsules, and determination of the spatial distribution of prebiotics and probiotics within these capsules**

#### **4.3.1 Examination of the external surface, size and shape of capsules**

The external surface, size and shape of PPI + AL capsules were examined using both cryo-SEM and AFM imaging techniques. Overall, capsules ranged in size from 1.5 to 2.0 mm in diameter under cryo-SEM, which were comparable to the values observed by particle sizing (~2.0 mm – geometric mean diameter; Table 4-1). Capsules prepared for cryo-SEM imaging maintained their spherical shape with no evidence of structural collapse or excessive shrinkage. This is in contrast to capsules prepared for conventional SEM, which resulted in structural collapse (i.e., loss of their spherical structure within the native hydrated state) and a more porous surface (Figure 4-3). Cryo-SEM has been shown to maintain structural integrity for a pectin-AL based capsule (Zohar-Perez et al., 2004; Sriamornsak et al., 2008).

The external surface of the PPI + AL capsules appeared smooth and relatively non-porous (Figure 4-11 A, C) with the exception of a few tiny black patches on the surface (Figure 4-11 B, D). The latter were presumed to be small pores that ranged in diameter from 0.25 to 1.0  $\mu\text{m}$ , and occurred regardless of the presence or absence of *B. adolescentis*. Topographical images by AFM also suggested the presence of external pores on the capsules, observed as low-lying areas ranging in diameter from 0.5 to 1.0  $\mu\text{m}$  (Figure 4-12). Surface roughness or the deviation of the vertical height of the capsules surface, as measured by AFM, was found to be  $119.02 \pm 35.40$  nm. The addition of P95 had no significant effects on the external surface morphology or surface roughness of the capsules as determined by AFM ( $76.35 \pm 16.49$  nm;  $p > 0.05$ ).

Scanning electron microscopy of capsules containing *B. adolescentis* showed partially- or completely-exposed bacteria on their surfaces (Figure 4-13). Exposed bacteria had lateral and longitudinal lengths of 0.9 and 1.6-2.3  $\mu\text{m}$ , respectively and were spatially oriented near or at surface pockets (Figure 4-13). The presence of bacteria on, or integrated within the surface was expected because in capsule processing both the wall

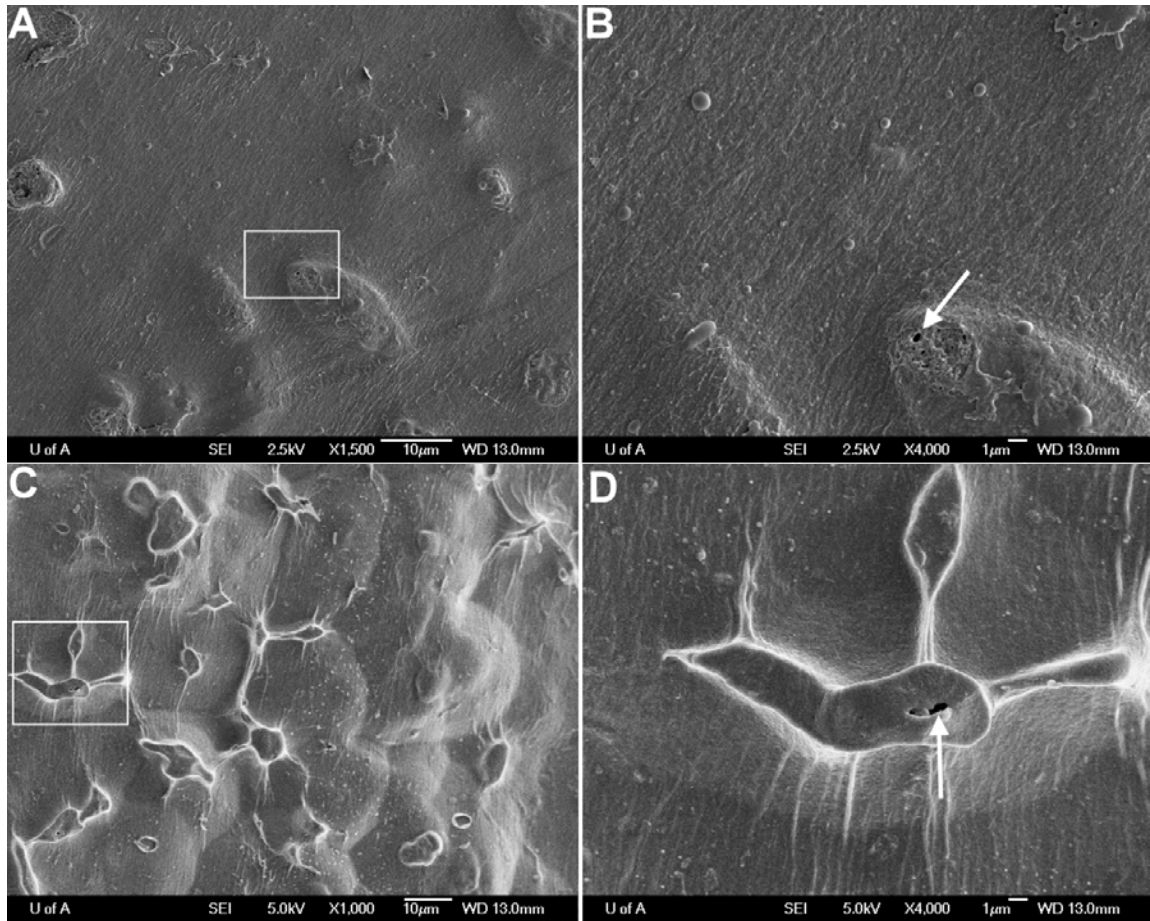


**Figure 4-11** Cryo-SEM micrographs of the external surface of 4.0% PPI + 0.5% AL capsules in the absence (A, B) and presence (C, D) of *B. adolescentis*. Rectangles indicate the areas in A and C that are magnified in B and D, respectively, and white arrows indicate pores.

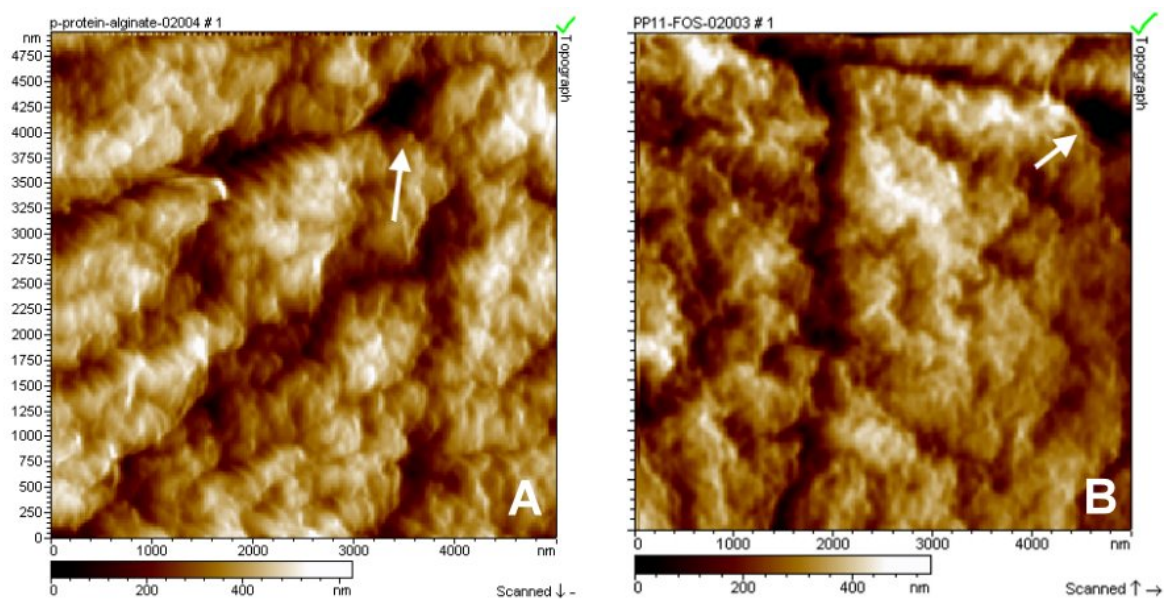


**Figure 4-12** AFM topographical images (5.0 x 5.0  $\mu\text{m}$ ) of 4.0% PPI + 0.5% AL capsules in the absence (A), and presence (B) of P95. Arrows indicate possible external pores.

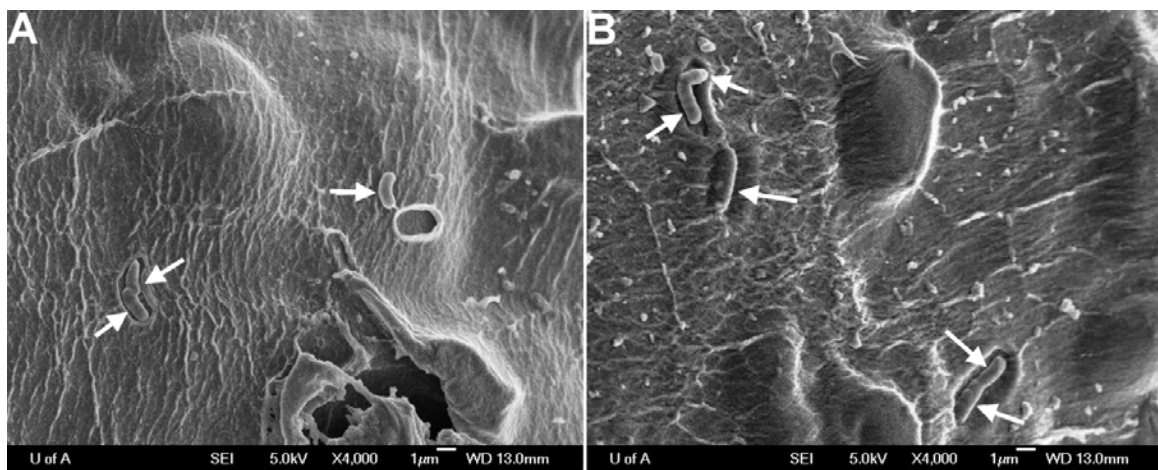


**Figure 4-13** Cryo-SEM micrographs showing the exterior surface of: 4.0% PPI + 0.5% AL + *B. adolescentis* (A); and 4.0% PPI + 0.5% AL + *B. adolescentis* + P95 (B) capsules. White arrows indicate presumptive *B. adolescentis* cells.

material and probiotic were homogenously mixed prior to ionic cross-linking. The presence of probiotics on the surface of the capsules and the small pores observed helps to explain the loss in viable cell counts during capsule exposure to SGJ. Allan-Wojtas et al. (2008), and Truelstrup-Hansen et al. (2002) studied the entrapment of probiotics within calcium-linked alginate capsules, and found visible surface impressions of probiotics. The authors hypothesized that the presence of bacteria may induce localized gelation of the AL polymer around their outer cell membrane.

The external wall thickness (the wall separating the interior of the capsule from the external environment) of the 4.0% PPI + 0.5% AL capsules without pre- or probiotics was found to be  $2.1 \pm 0.7 \mu\text{m}$  (Table 4-4). In contrast, wall thicknesses were found to be lower with their addition, where capsules with *B. adolescentis* and *B. adolescentis* + P95 had values of  $0.8 \pm 0.1$  and  $1.2 \pm 0.2 \mu\text{m}$ , respectively. If the presence of bacteria induces localized gelation of the AL polymer this could decrease the amount of AL available for capsule formation decreasing the thickness of the external wall. Capsules containing the prebiotic and the probiotic had a thicker external wall than capsules contain the probiotic alone (Table 4-4). The addition of the prebiotic therefore increased the physical barrier to the diffusion of the SGJ into the capsules, helping to explain the increased probiotic survival observed with the addition of P95. The addition of DMSO in the wall material solution for PPI + AL capsule production decreased the external wall thickness. However, with the addition of GLU-FA the wall thickness increased to measurements similar to those of the capsules without DMSO.

For comparison, the external surface of the AL capsules was examined using cryo-SEM. The diameter of AL capsules observed by cryo-SEM was approximately 2.4 mm, which was comparable to that observed by particle sizing (Table 4-1). These capsules were spherical in shape and experienced no structural collapse or excessive shrinkage under cryo-SEM. The surface of the AL capsules as examined by cryo-SEM was found to be smooth with no visible external pores. The absence of external pores for the AL capsules is interesting as these capsules were unable to provide any probiotic



**Table 4-4 Internal and external wall and pore sizes for AL and PPI + AL capsules.**

Sample	Wall Thickness		Pore Size		
	Internal (μm)	External (μm)	Long axis diameter (μm)	Short axis diameter (μm)	Aspect ratio
1.0% AL	0.9 ± 0.3	N/A			
Large pores			85.6 ± 13.4	75.9 ± 10.1	1.2 ± 0.2
Small pores			14.9 ± 5.0	13.0 ± 3.4	1.2 ± 0.1
4.0% PPI + 0.5% AL	0.4 ± 0.1	2.1 ± 0.7	13.9 ± 2.7	13.2 ± 1.6	1.2 ± 0.2
4.0% PPI + 0.5% AL + <i>B. adolescentis</i>	0.4 ± 0.1	0.8 ± 0.2	20.4 ± 7.1	18.1 ± 6.8	1.4 ± 0.3
4.0% PPI + 0.5% AL + <i>B. adolescentis</i> + P95	0.4 ± 0.1	1.2 ± 0.2	21.9 ± 4.9	21.1 ± 4.6	1.2 ± 0.2
4.0% PPI + 0.5% AL + DMSO	0.2 ± 0.1	1.4 ± 0.6	12.2 ± 3.0	10.6 ± 3.0	1.3 ± 0.4
4.0% PPI + 0.5% AL + DMSO + GLU-FA	0.5 ± 0.3	N/A			
Large pores			15.8 ± 7.0	11.9 ± 4.6	1.4 ± 0.3
Small pores			8.6 ± 3.7	6.5 ± 2.8	1.4 ± 0.3

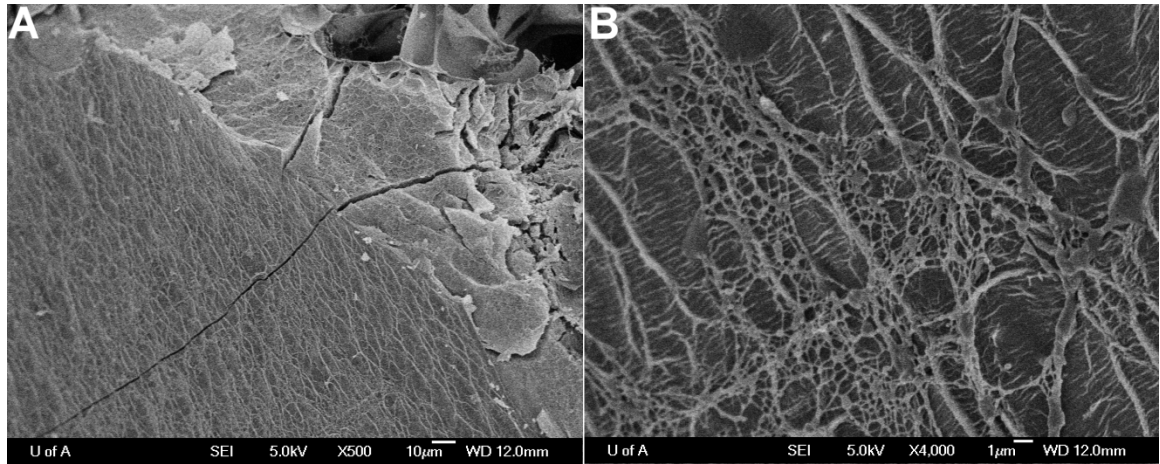


**Figure 4-14** Cryo-SEM micrographs showing the exterior surface of 1.0% AL capsules.

protection against the SGJ (Figure 4-4). This indicates that the presence of external pores may not explain whether or not a capsule will provide probiotic protection. It is possible that external pores were present but the cryo-SEM images failed to show them. The external wall thickness of the AL capsules was not determined as freeze fracturing was unsuccessful in producing a clean edge.

#### **4.3.2 Examination of the internal structure of the capsules**

The internal morphology of both the 1.0% AL and 4.0% PPI + 0.5% AL capsules by cryo-SEM revealed a honeycomb-like structure (Figure 4-15 and Figure 4-16). In the case of the AL capsules two distinct structures were evident (Table 4-4 and Figure 4-15). The first, consisted of large hollow honeycomb shaped pores (average short and long axis of  $75.9 \pm 10.1$  and  $85.6 \pm 13.4$   $\mu\text{m}$ , respectively), whereas in the second, smaller honeycomb pores (average short and long axis of 13.0 to 14.9  $\mu\text{m}$ , respectively) were present with filamentous structures inside. The honeycombs were not of consistent shape, varying from rectangular to square to oval. Both honeycomb structures had distinct walls separating individual pores within the internal structure. The aspect ratio of the individual honeycomb pores, determined by dividing the long by the short axis measurements, for both the small and large pores were the same at 1.2 (Table 4-4). The 4.0% PPI + 0.5% AL capsules produced with or without probiotics or the synbiot, all exhibited a honeycomb structure. The individual honeycomb pores were smaller than those observed in the 1.0% AL capsules as their long and short axis diameters ranged from 13.2 to 21.9  $\mu\text{m}$  (Table 4-4 and Figure 4-16 A, B). The aspect ratio of the 4.0% PPI + 0.5% AL capsules was similar to the 1.0% AL capsules ranging from 1.2 to 1.4, indicating that the pores were slightly elongated.

In the core of the 4.0% PPI + 0.5% AL capsules, both thick and thin filaments were evident within the pores (Figure 4-16 C, D). Although filaments were seen in capsules with or without entrapped *B. adolescentis* and P95, thin filaments were more prevalent in the presence of the prebiotic. The interior wall thickness for these capsules was not affected by the presence or absence of *B. adolescentis* and/or P95 and DMSO, as values were not significantly different (Table 4-4).

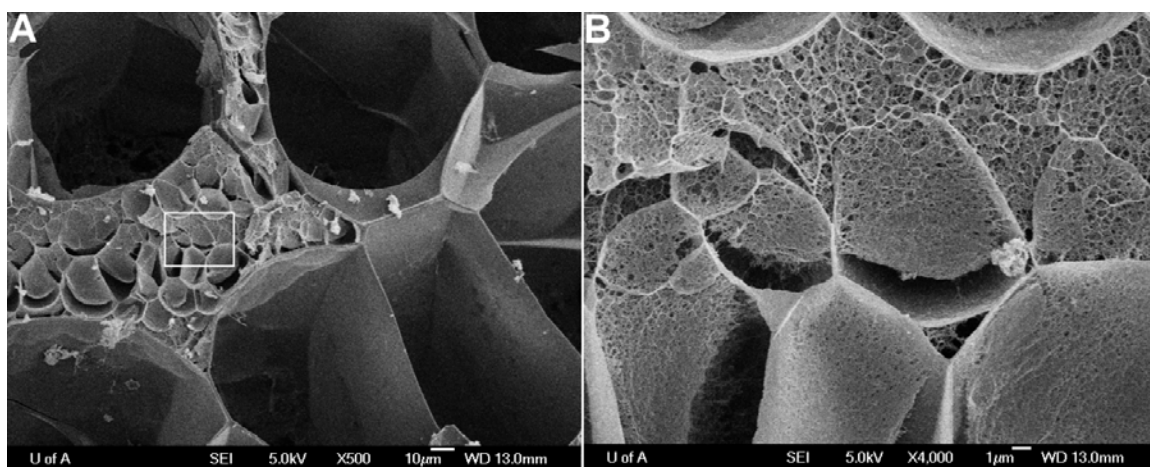


**Figure 4-15** Cryo-SEM micrographs of the internal structures of 1.0% AL capsules illustrating the large hollow (A) and small filamentous containing (B) honeycomb pores. The rectangle indicates the area in A magnified in B.

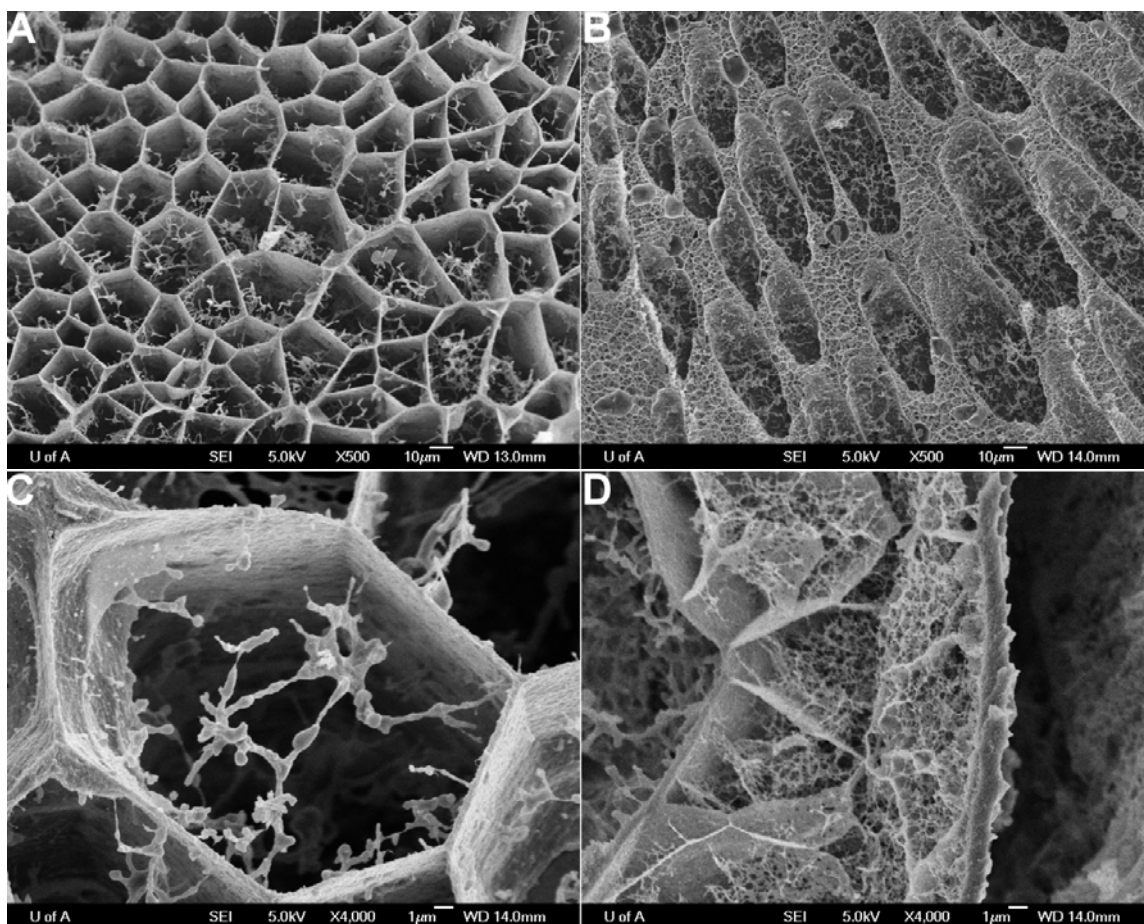


**Figure 4-16** Cryo-SEM micrographs showing the internal structures of capsules composed of: 4.0% PPI + 0.5% AL + *B. adolescentis* (A, B); and 4.0% PPI + 0.5% AL + *B. adolescentis* + P95 (C, D).

The internal porous structure of the 4.0% PPI + 0.5% AL and 1.0% AL capsules observed with cryo-SEM agreed with those reported in literature for capsules produced with 2.0% (w/w) AL in a 1.0% CaCl<sub>2</sub> solution (Zohar-Perez et al., 2004). In this study, the aspect ratio determined for the internal pores were not significantly different for any of the capsules examined. Although similar internal structures were observed for the 4.0% PPI + 0.5% AL and 1.0% AL capsules, the size of the internal pores were much larger and less uniform in the latter. The concentration of wall materials may have been a contributing factor to the size difference observed in the internal pores of the capsules. The concentration of the wall materials was 1.0% (w/w) for the AL, and 4.5% (w/w) for the PPI + AL capsules, respectively.

The thick filamentous structures observed within the pores of the 4.0% PPI + 0.5% AL capsules are thought to arise from the commercial pea protein isolate material as they were not present in the capsules comprised of AL alone. These structures could consist of protein, fiber and/or carbohydrate as these compounds were all present at relatively high concentration in the starting material. The thin filamentous structures were observed in all the capsules but were more prevalent in the capsules containing P95 and are thought to be artifacts of salts or carbohydrates created by the cryo-SEM technique. Published research examining artifacts created by cryo-SEM have reported that solutions commonly used as storage reagents, such as sucrose, tris and NaCl, produced filament-like structures when observed under cryo-SEM (Miller et al., 1983). Also, fibrillar networks and membranous structures have been observed in sugar solutions ranging in concentration from 2 to 50 mM (Moss et al., 1989). These structures form as a result of ice crystal growth for soluble compounds that concentrate between the crystals, forming a network of eutectic regions. When the ice is sublimed, it leaves behind the less volatile eutectic regions and produces a lattice-like appearance (Moss et al., 1989).

#### **4.3.3 Prebiotic and probiotic distribution within the capsules**

*Bifidobacterium adolescentis* were found to be present on the external surface of capsules and within the internal honeycomb pores as determined by cryo-SEM

(Figures 4-13 and 4-17). The presence of probiotics within the internal pores of the biopolymer-based capsules has been reported by others (Sultana et al., 2000; Truelstrup-Hansen et al., 2002; Allan-Wojtas et al., 2008). The use of CLSM to observe probiotic distribution within the capsules was unsuccessful because both the PPI + AL matrix and *B. adolescentis* labeled with PI were excited at 488 nm and emitted light at the same bandwidth (610-675 nm, Figure 4-18). This created background fluorescence that made it impossible to distinguish probiotic cells from the capsule matrix.

Visualization of the distribution of prebiotic within the 4.0% PPI + 0.5% AL capsules was accomplished by fluorescent tagging (FA) of the carbohydrate prior to CLSM analysis. Glucose was used in these studies because of the better water solubility of the GLU-FA derivative compared to P95. Also, the molecular mass of GLU-FA ( $\sim 530 \text{ g mol}^{-1}$ ) is approximately the same as that of a DP 3 FOS, which was the most abundant oligosaccharide present in P95 (Table 4-2). The fact that glucose had similar chemical/reaction properties (reducing carbohydrate; conversion to an amine via reductive amination) to P95 also supported its use. Preliminary work involved a reductive amination reaction with glucose and FA (glu-FA), where FA was employed as the limiting reagent (4:1, glucose to FA). Thin layer chromatography (TLC) of the reaction mixture showed no unbound FA. The lowest concentration of FA to be visualized by TLC was 0.005 M. The GLU-FA (0.3% w/w) was encapsulated without purification (impure GLU-FA) within the 4.0% PPI + 0.5% AL capsule; in addition the same protein-based capsules were prepared with 0.005M FA. CLSM images of representative capsules showed fluorescence for each which was homogeneously distributed (Figure 4-19). Based on these results, it was unclear whether the fluorescence within the protein-based capsules was due to the GLU-FA or unbound FA. However, these experiments showed that background fluorescence of the protein-based + DMSO was negligible (Figure 4-19). A GLU-FA sample was produced using glucose as the limiting reagent (5:1, FA to glucose) so as to reduce the concentration of unbound FA in the reaction mixture. Chromatographic separation was used to isolate GLU-FA from FA, and this purified material was used in subsequent protein-based + prebiotic encapsulation experiments.

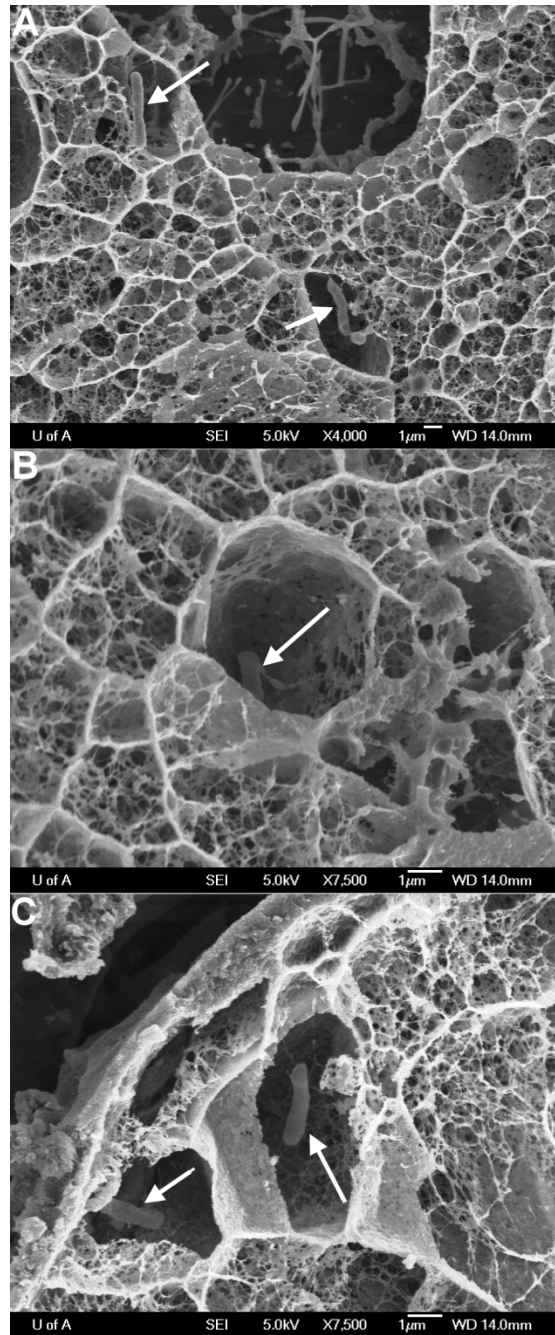


**Figure 4-17** Cryo-SEM micrographs showing the presence of bacteria in capsules composed of: 4.0% PPI + 0.5% AL + *B. adolescentis* (A,B); and 4.0% PPI + 0.5% AL + *B. adolescentis* + P95 (C). White arrows indicate *B. adolescentis* cells.



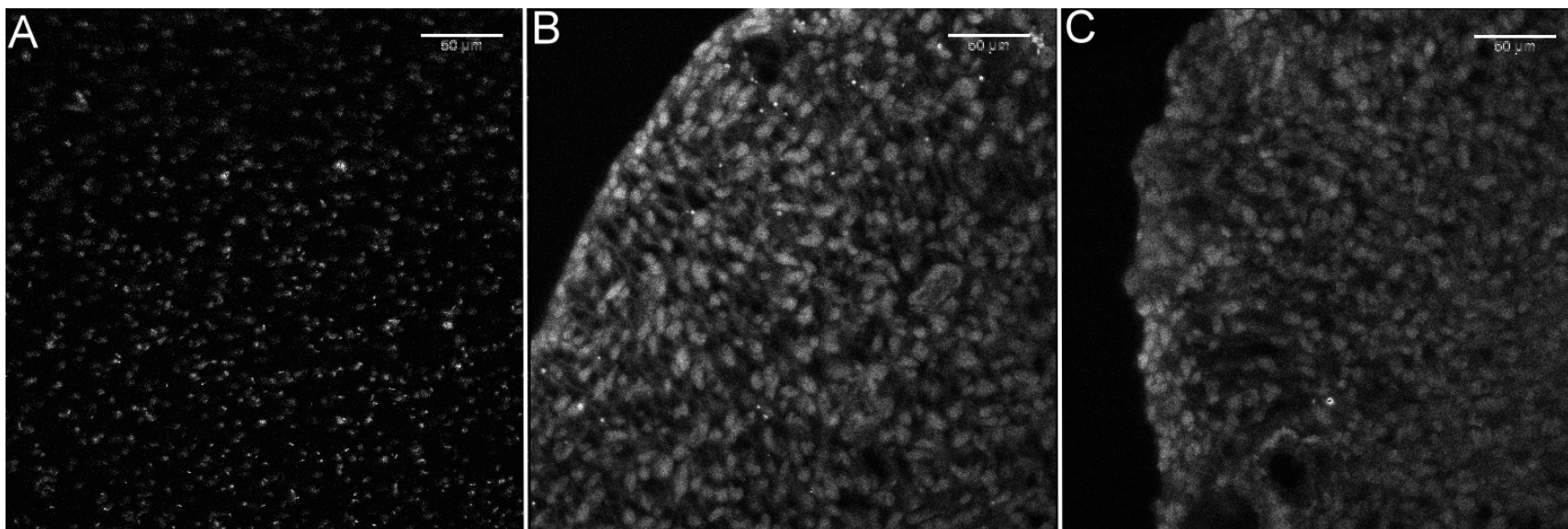


**Figure 4-18** CLSM images of: *B. adolescentis* labelled with PI (A); 4.0% PPI + 0.5% AL capsules (B); and 4.0% PPI + 0.5% AL + *B. adolescentis* labelled with PI (C) capsules. Images taken with a 40x objective lens, attenuation, brightness and contrast for all images were the same.  $\lambda_{\text{ex}} = 488 \text{ nm}$   $\lambda_{\text{em}} = 573\text{-}647 \text{ nm}$

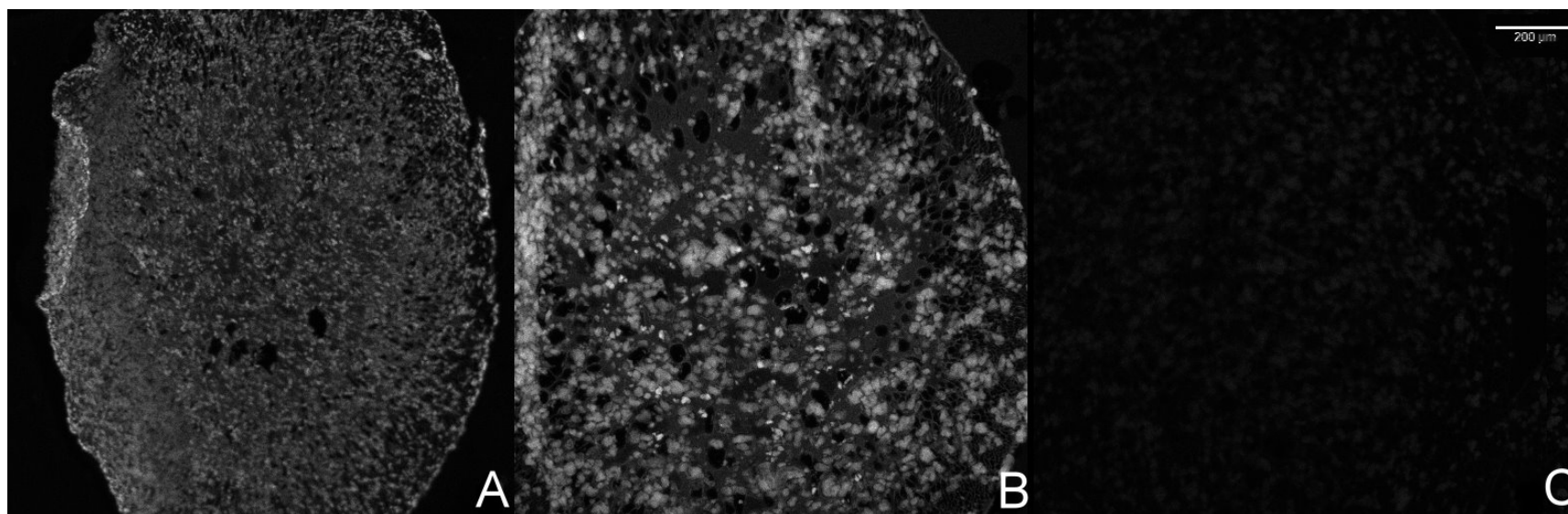


**Figure 4-19** CLSM images of capsules comprised of: 4.0% PPI + 0.5% AL + impure GLU-FA (A); 4.0% PPI + 0.5% AL + 0.005 M FA (B) and 4.0% PPI + 0.5% AL + DMSO (C). Attenuation, brightness and contrast for all images were the same.  $\lambda_{\text{ex}} = 488 \text{ nm}$   $\lambda_{\text{em}} = 495\text{-}525 \text{ nm}$ .

Images (CLSM) of 4.0% PPI + 0.5% AL + DMSO + GLU-FA capsules showed fluorescence throughout, as cross sections near the top/bottom and middle of the capsules all showed fluorescence (Figure 4-20). These results indicated that GLU-FA was distributed throughout the capsule.

However, the GLU-FA was not completely soluble in the 4.0% PPI + 0.5% AL solution, therefore DMSO was added to solubilize this derivative. The addition of DMSO resulted in changes to the structure of the protein-based capsules, in that the external walls were more porous, there was some flattening of the internal pores and these pores were smaller (Figure 4-21 and Table 4-4) than those without added DMSO. These results indicated that the presence of DMSO in the amount used (0.4 g or 16.7%) to solubilize the GLU-FA impacted capsule structure. When DMSO was added at concentrations >50%, the wall material gelled, however, this phenomenon was not observed at the 16.7% concentration used in this study. Studies have shown that DMSO can affect proteins when used at high and low concentrations. A study examining DMSO concentrations (0.1 to 5% (v/v)) on a human growth hormone receptor and the phosphatase domain of PFKFB1 found that it could change the properties of proteins in solution, leading to protein denaturation, aggregation or degradation (Tjernberg et al., 2005). Therefore, structural changes and aggregation of PPI in 16.7% DMSO could have occurred prior to complexation with  $\text{CaCl}_2$  affecting capsule structure.

In contrast, the addition of DMSO did not significantly change the internal wall thickness or aspect ratio of the internal pores (Table 4-4). The 4.0% PPI + 0.5% AL + DMSO  $\pm$  GLU-FA capsules also had the same spherical shape and capsule diameter (1.7 to 2.0  $\mu\text{m}$ ) as the protein-based capsules without DMSO. It was assumed that P95 would have the same distribution within the PPI + AL capsules as seen with GLU-FA. The even distribution of the GLU-FA in the capsules show that P95 would also be evenly distributed throughout the capsule wall, making the prebiotic readily available to the probiotic as a carbon source to promote growth.

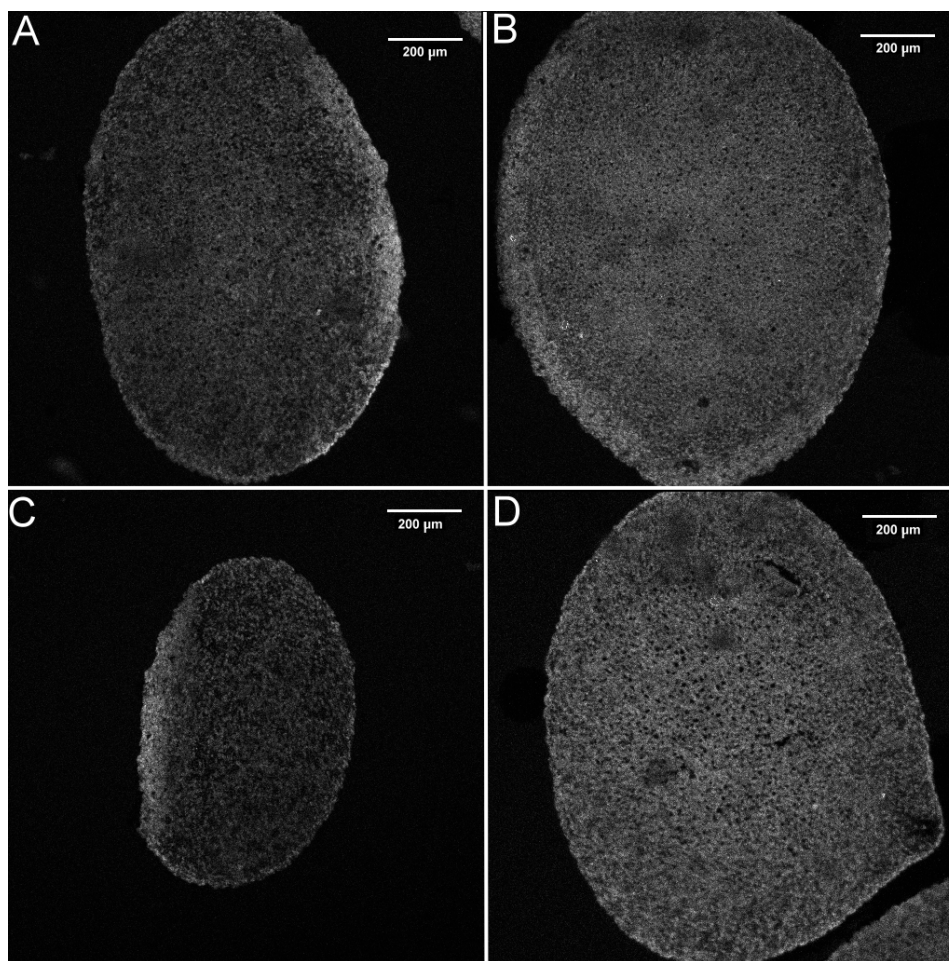


**Figure 4-20** CLSM images of 4.0% PPI + 0.5% AL + DMSO + GLU-FA capsules showing carbohydrate distribution in centre cross-sections (A, B, and D) and peripheral cross-section (C) of the capsules. Images were taken with a 10x objective lens.  $\lambda_{\text{ex}} = 488 \text{ nm}$   $\lambda_{\text{em}} = 495\text{-}525 \text{ nm}$ .

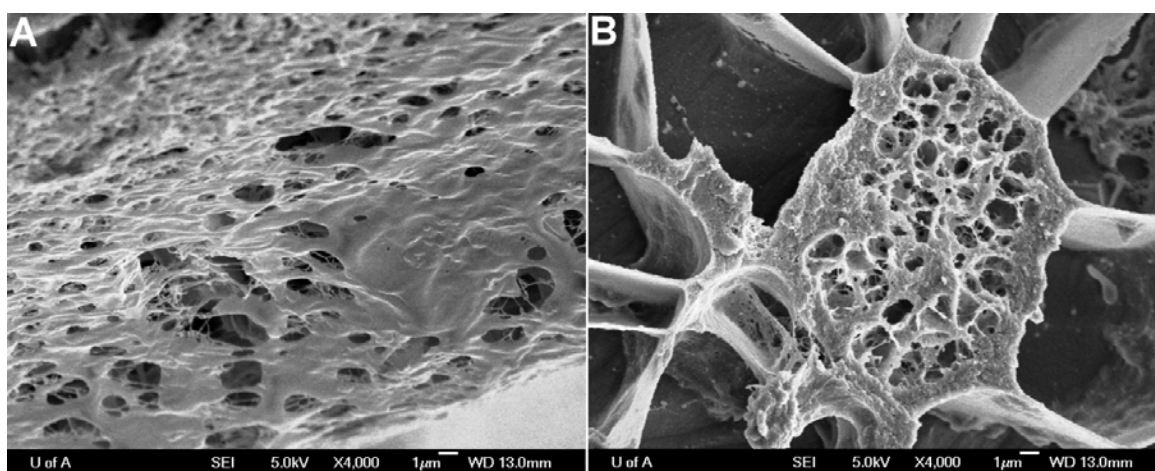


**Figure 4-21** Cryo-SEM micrographs showing the porous external surface of 4.0% PPI + 0.5% AL + DMSO + GLU-FA (A) and the flattening of the internal pores of 4.0% PPI + 0.5% AL + DMSO (B), capsules.

#### 4.3.4 Summary and conclusions

The external and internal morphologies of the 4.0% PPI + 0.55 AL capsules were examined to better understand the encapsulation matrix and its ability to protect *B. adolescentis* against the harsh conditions in the GI tract. The external surface of the 4.0% PPI + 0.5% AL capsules as determined by cryo-SEM and AFM showed a relatively smooth surface with the presence of pores. The presence of these surface pores indicated that gastric juices would be able to penetrate the surface of the capsules and could potentially destroy encapsulated probiotics.

The internal structure of the 4.0% PPI + 0.5% AL capsules was observed using cryo-SEM; alginate capsules were observed for comparison. A porous honeycomb internal structure was observed for both the 1.0% AL and 4.0% PPI + 0.5% AL capsules with the AL capsules having larger internal diameters than the PPI + AL capsules. The large internal pores of the AL capsules helped to explain why no survival of *B. adolescentis* was observed with this wall material. If SGJ entered the capsules through the pores on the external surface then diffusion through the AL capsule internal matrix would be faster due to their larger internal diameter.

*Bifidobacterium adolescentis* cells were randomly distributed on the external surface and within the internal pores of the capsules. Fluorescently tagged glucose encapsulated in the PPI + AL capsules as observed by CLSM showed fluorescence throughout the capsule matrix. This result indicated that the prebiotic would be in the vicinity of the probiotic and would be available for use as a growth substrate.

## 5. Conclusions

Although encapsulation of probiotics to improve survival in SGJ has been extensively researched in literature, the examination of WPI-AL and PPI-AL as wall materials have not. The use of protein-based capsules by extrusion was shown to provide excellent protection to *B. adolescentis*, as numbers were only reduced by 1.1 and 3.6 log CFU mL<sup>-1</sup> in SGJ at pH 2.0 for 2 h whereas capsules produced from AL alone showed no survival. The increase in probiotic survival exhibited by the protein-based capsules over AL was due in part to their having a higher wall material concentration, 4.5% for the protein-based capsules and 1.0% for the AL capsules, and a smoother, less porous external surface as shown by SEM. The higher wall material concentration and the less porous nature of the protein-AL capsules indicated that the diffusion of SGJ into these capsules would be slower than in the case of the AL capsules. The creation of a capsule that successfully protects probiotics from the acidic environment of the stomach is important to allow for the delivery of probiotic strains associated with health benefits rather than the delivery of probiotic strains associated with increased acid resistance.

The size of the capsules was also determined to be a possible factor in probiotic survival. Capsules composed of 4.0% WPI + 0.5% AL were produced by the emulsion and the extrusion methods of encapsulation. The emulsion capsule had a geometric mean diameter of 53 µm and the extrusion capsules had a geometric mean diameter of 2.2 mm. The emulsion produced capsules showed no probiotic survival. Reducing capsule size to where the texture/sensory of a food would not be adversely affected, as in the case for the emulsion capsules, removed the capsule's ability to protect the probiotic against SGJ. Another factor that could potentially be a factor in probiotic survival is the structure of the capsule. The structure of the emulsion-based capsules may have been different from the extrusion-based capsules therefore allow SGJ to penetrate the capsules more readily.

*Bifibacterium adolescentis* was found to have a significantly higher growth rate with P95 than with glucose. The growth of the probiotic on P95 and Syn was a result of

oligosaccharide and monosaccharide utilization as determined by HPAE-PAD. Growth rates of probiotics with prebiotics have been studied; however, the ability of a probiotic to utilise a monosaccharide free oligosaccharide source had yet to be researched. Results of this study showed *B. adolescentis* is capable of utilizing glucose-free maltooligosaccharides as a carbon source.

The probiotic and prebiotic were encapsulated by extrusion in 1.0% AL + P95 and 4.0% PPI and 4.0% WPI + 0.5% AL + P95 with a final carbohydrate concentration of 4.0 to 4.4 mg per gram of capsules, although exhibited low retention (<15%). The addition of P95 into the capsules resulted in improved survival for the 4.0% PPI + 0.5% AL capsules in SGJ at pH 2.0 for 2 h. It is important to deliver the prebiotic in an encapsulated form along with the probiotic to ensure that they are in proximity to one another and to decrease acidic hydrolyse of the prebiotic. This research was able to create a possible synbiot to improve probiotic survival in SGJ at pH 2.0. The creation of a successful synbiot can be stated if the availability of the encapsulated P95 was determined.

Extrusion-based capsules employing 4.0% PPI + 0.5% AL were examined for their morphological properties and prebiotic and probiotic distribution. Morphological studies using cryo-SEM and AFM showed that the protein-based capsules had small surface pores (0.25 to 1.0  $\mu\text{m}$  in diameter). The addition of P95 and *B. adolescentis* appeared to have no effect on the external surface of the capsules. The internal structure of the 4.0% PPI + 0.5% AL capsules was observed to have a porous honeycomb structure with internal pore diameters ranging for 13.2 to 21.9  $\mu\text{m}$ . Alginate capsules viewed under cryo-SEM showed a porous honeycomb structure with two internal pore sizes; one large (75.9 to 85.6  $\mu\text{m}$ ) and one small (13.0 to 14.9  $\mu\text{m}$ ). The presence of pores on the external surface and the smaller internal porous structure of the 4.0% PPI + 0.5% AL capsules helps explain the increased probiotic survival observed when compared to the AL capsules. The SGJ entering the capsules through the small external pores would diffuse more rapidly throughout the AL capsule with large internal pores than through the protein-based capsule with small internal pores. The distribution of the probiotic and prebiotic was found to be randomly and evenly distributed throughout the capsules,



respectively. This indicates that the probiotic would have access to the prebiotic for growth.

## 6. Future Directions

This study has shown that the production of extrusion-based capsules composed of WPI + AL and PPI + AL shows much promise for increasing probiotic survival in SGJ at pH 2.0. It has also shown that P95 can be added to create a synbiotic in concentrations that could facilitate growth of the probiotic. However, the availability of the P95 to the probiotics was not determined. The P95 may have been incorporated into the wall structure making it unavailable. To confirm the successful creation of a synbiotic access to the encapsulated P95 must be determined. Also the amount of P95 encapsulated was <15% and would not be commercially viable, therefore ways to increase the amount of P95 encapsulated must be investigated. A potential approach would be to add P95 to the cross-linking solution at a concentration desired within the capsule to prevent the diffusion of the P95 out along the concentration gradient.

Morphological studies showed that the prebiotic and probiotic would be in close proximity and the internal small pore honeycomb structure of the 4.0% PPI + 0.5% AL capsules help explain the increase in probiotic survival of this wall material when compared to AL alone. With this data, it would be valuable to investigate ways to decrease the size of the extrusion-based capsules by using a smaller gauge needle or changing the polymer concentration. Also morphological studies determined the structure of the extrusion-produced capsules, and it would be valuable to determine the structure of the emulsion-produced capsules to determine the extent of size and structure on the capsules ability to protect the probiotic.

Although this study examined probiotic survival in SGJ, no research was conducted on the ability of these capsules to provide protection against the bile acids present in the small intestine. In addition, probiotic and prebiotic release from the capsules were not investigated. These two studies would provide valuable information on whether not these capsules could deliver and release the active ingredients to their target destination. These studies could be conducted *in vivo* with the use of a simulator of the human intestinal

microbial ecosystem (SHIME). Also the investigation of these capsules in an animal model would be very useful if one was to market the capsules as an animal feed supplement instead of a functional food ingredient.

## 7. References

- Adhikari, K., Mustapha, A., Grun, I. U., & Fernando, L. (2000). Viability of microencapsulated bifidobacteria in set yogurt during refrigerated storage. *Journal of Dairy Science*, 83, 1946-1951.
- Agerbaek, M., Gerdes, L. U., & Richelsen, B. (1995). Hypocholesterolaemic effect of a new fermented milk product in healthy middle-aged men. *European Journal of Clinical Nutrition*, 49, 346-352.
- Alcamo, E. I. (1997). Anatomy and growth of bacteria. In, *Fundamentals of Microbiology* (5<sup>th</sup> ed., pp. 87-122). Menlo Park, CA: The Benjamin/Cummings Publishing Company.
- Allan-Wojtas, P., Truelsrup-Hansen, L., & Paulson, A. T. (2008). Microstructural studies of probiotic bacteria-loaded alginate microcapsules using standard electron microscopy techniques and anhydrous fixation. *Lebensmittel-Wissenschaft und Technology*, 41, 101-108.
- Ameratti, A., Tamburine, E., Bernardi, T., Pompei, A., Zanoni, S., & Vaccari, G. (2006). Substrate preference of *Bifidobacterium adolescentis* MB 239: Compared growth on single and mixed carbohydrates. *Applied Microbiology and Biotechnology*, 73, 654-662.
- Anal, A. K., & Singh, H. (2007). Recent advances in microencapsulation of probiotics for industrial applications and targeted delivery. *Trends in Food Science & Technology*, 18, 240-251.
- Apajalahti, J. H. A., Kettunen, A., Nurminen, P. H., Jatila, H., & Holben, W. E. (2003). Selective plating underestimates abundance and shows differential recovery of bifidobacterial species in human feces. *Applied and Environmental Microbiology*, 69, 5731-5735.
- Arndt-Jovin, D. J., & Jovin, T. M. (1989). Fluorescence labeling and microscopy of DNA. *Methods in Cell Biology*, 30, 417-448.
- Arnosti, C. (2003). Fluorescent derivatization of polysaccharides and carbohydrate-containing biopolymers for measurement of enzyme activities in complex media. *Journal of Chromatography B*, 793, 181-191.

- Arnosti, C., Keith, S. C., & Blough, N. V. (2000). Application of fluorescence spectroscopic techniques and probes to the detection of biopolymer degradation in natural environments. *Marine Chemistry*, 71, 321-330.
- Barbut, S. (1995). Effects of calcium level on the structure of pre-heated whey protein isolate gels. *Lebensmittel-Wissenschaft and Technology*, 28, 598-603.
- Batista, A. P., Portugal, C. A. M., Sousa, I., Crespo, J. G. & Raymundo, A. (2005). Accessing gelling ability of vegetable proteins using rheological and fluorescence techniques. *International Journal of Biological Macromolecules*, 36, 135-143.
- Benno, Y., & Mitsuoka, T. (1992). Impact of *Bifidobacterium longum* on human fecal microflora. *Microbiology and Immunology*, 36, 683-694.
- Bielecka, M., Biedrzycka, E., & Majkowska, A. (2002). Selection of probiotics and prebiotics for synbiotics and confirmation of their in vivo effectiveness. *Food Research International*, 35, 125-131.
- Borch, R. F., Bernstein, M. D., & Durst, H. D. (1971). The cyanohydrinborate anion as a selective reducing agent. *Journal of the American Chemical Society*, 93, 2897-2904.
- Bouhnik, Y. (1993). Survival and effects in humans of bacteria ingested cultures in milk. *Lait*, 73, 241-247.
- Bouhnik, Y., Pochart, P., Marteau, P., Arlet, G., Goderel, I., & Rambaud, J. C. (1992). Fecal recovery in humans of viable *Bifidobacterium sp.* ingested in fermented milk. *Gastroenterology*, 102, 875-878.
- Bryant, C. M., & McClements, D. J. (2000). Optimizing preparation conditions for heat-denatured whey protein solutions to be used as cold-gelling ingredients. *Journal of Food Science*, 65, 259-263.
- Chandramouli, V., Kailasapathy, K., Peiris, P., & Jones, M. (2004). An improved method of microencapsulation and its evaluation to protect *Lactobacillus sp.* in simulated gastric conditions. *Journal of Microbiological Methods*, 56, 27-35.
- Charteris, W. P., Kelly, P. M., Morelli, L., & Collins, J. K. (1998). Development and application of an in vitro methodology to determine the transit tolerance of potentially probiotic *Lactobacillus* and *Bifidobacterium* species in the upper human gastrointestinal tract. *Journal of Applied Microbiology*, 84, 759-768.

- Chen, K., Chen, M., Liu, J., Lin, C., & Chiu, H. (2005). Optimization of incorporated prebiotics as coating materials for probiotic microencapsulation. *Journal of Food Science*, 70, M260-M266.
- Corcoran, B. M., Ross, R. P., Fitzgerald, G. F., & Stanton, C. (2003). Comparative survival of probiotic lactobacilli spray-dried in the presence of prebiotic substances. *Journal of Applied Microbiology*, 96, 1024-1039.
- Crittenden, R., & Playne, M. J. (1996). Production, properties and applications of food-grade oligosaccharides. *Trends in Food Science & Technology*, 7, 353-361.
- De Belder, A. N., & Granath, K. (1973). Preparation and properties of fluorescein-labelled dextrans. *Carbohydrate Research*, 30, 375-378.
- Deguchi, Y., Morishita, T., & Mutai, M. (1985). Comparative studies on synthesis of water-soluble vitamins among human species of *Bifidobacteria*. *Agricultural Biology and Chemistry*, 49, 13-19.
- Delzenne, N. M., & Roberfroid, M. B. (1994). Physiological effects of non-digestible oligosaccharides. *Lebensmittel-Wissenschaft and Technology*, 27, 1-6.
- Derbyshire, E., Wright, D. J., & Boulter, D. (1976). Legumin and vicilin, storage proteins of legume seeds. *Phytochemistry*, 15, 3-24.
- Ducel, V., Richard, J., Popineau, Y., & Boury, F. (2004). Adsorption kinetics and rheological interfacial properties of plant proteins at the oil-water interface. *Biomacromolecules*, 5, 2088-2093.
- Dykstra, M. J. (1992). *Biological Electron Microscopy: Theory, techniques, and troubleshooting* (pp. 209-272). New York, NY: Plenum Press.
- Favaro-Trindade, C. S., & Grosso, C. R. F. (2002). Microencapsulation of *L. acidophilus* (la-05) and *B. lactis* (bb-12) and evaluation of their survival at the pH values of the stomach and in bile. *Journal of Microencapsulation*, 19, 485-494.
- Fiordaliso, M. F., Knock, N., Desager, J. P., Goethals, F., Deboyser, D., & Roberfroid, M. B. (1995). Dietary oligofructose lowers triglycerides, phospholipids and cholesterol in serum and very low density lipoproteins of rats. *Lipids*, 30, 163-167.
- Fooks, L. J., Fuller, R., & Gibson, G. R. (1999). Prebiotics, probiotics and human gut microbiology. *International Dairy Journal*, 9, 53-61.

- Franco, J. M., Partal, P., Ruiz-Marquez, D., Conde, B., & Gallagos, C. (2000). Influence of pH and protein thermal treatment on the rheology of pea protein-stabilized oil-in-water emulsions. *Journal of the American Oil Chemists' Society*, 77, 975-984.
- Fuller, R. (1992). History and development of probiotics. In, *Probiotics the Scientific Basis* (first ed., pp. 1-7) R. Fuller (Ed.). Boundary Row, London: Chapman & Hall.
- Fuller, R. (1989). Probiotics in man and animals. *Journal of Applied Bacteriology*, 6, 365-378.
- Gibson, G. R., Saavedra, J. M., Macfarlene, S., & Macfarlene, G. T. (1997). Probiotics and intestinal infections. In, *Probiotics 2 Applications and Practical Aspects* (pp. 10-39) R. Fuller (Ed.). Boundary Row, London: Chapman and Hall.
- Gibson, G., R., & Roberfroid, M., B. (1995). Dietary modulation of the human colonic microbiota: Introducing the concept of prebiotics. *Journal of Nutrition*, 125, 1401-1412.
- Gibson, G. R., Beatty, E. R., Wang, X., & Cummings, J. H. (1995). Selective stimulation of bifidobacteria in the human colon by oligofructose and inulin. *Gastroenterology*, 108, 975-982.
- Gibson, G. R., & Wang, X. (1994a). Regulatory effects of bifidobacteria on the growth of other colonic bacteria. *Journal of Applied Bacteriology*, 77, 412-420.
- Gibson, G. R., & Wang, X. (1994b). Bifidogenic properties of different types of fructo-oligosaccharides. *Food Microbiology*, 11, 491-498.
- Guerin, D., Vuilleumard, J., & Subirade, M. (2003). Protection of bifidobacteria encapsulated in polysaccharide-protein gel beads against gastric juice and bile. *Journal of Food Protection*, 66, 2076-2084.
- Guttman, A., & Pritchett, T. (1995). Capillary gel electrophoresis separation of high-mannose type oligosaccharides derivatized by 1-aminopyrene-3,6,8-trisulfonic acid. *Electrophoresis*, 16, 1906-1911.
- Hagler, H. K. (1988). Artifacts in cryoelectron microscopy. In, *Artifacts in Biological Electron Microscopy* (1<sup>st</sup> ed., pp. 205-217) R. F. E. Crang, & K. L. Klomparens (Eds.). New York, NY: Plenum Press.
- Hahn, M. A., Keng, P. C., & Krauss, T. D. (2008). Flow cytometric analysis to detect pathogens in bacterial cell mixtures using semiconductor quantum dots. *Analytical Chemistry*, 70, 864-872.

- Hansma, P. K., Elings, V. B., Marti, O. & Bracker, C. E. (1988). Scanning tunneling microscopy and atomic force microscopy: Application to biology and technology. *Science*, 242, 209-242.
- Hartke, A., Bouché, S., Giard, J. , Benachour, A., Boutibonnes, P., & Auffray, Y. (1996). The lactic acid stress response of *Lactococcus lactis* subsp. *lactis*.. *Current Microbiology*, 33, 194-199.
- Hibbs, A. R. (2004a). What is confocal microscopy? In, *Confocal Microscopy for Biologists* (pp. 1-29), A. R. Hibbs (Ed.). New York: Springer.
- Hibbs, A. R. (2004b). Fluorescent probes. In, *Confocal Microscopy for Biologists* (pp. 201-238), A. R. Hibbs (Ed.). New York: Springer.
- Hongsprabhas, P., & Barbut, S. (1997). Protein and salt effects on  $\text{Ca}^{+2}$  -induced cold gelation of whey protein isolate. *Journal of Food Science*, 62, 382-385.
- Hopkins, M. J., Cummings, J. H., & Macfarlane, G. T. (1998). Inter-species differences in maximum specific growth rates and cell yields of bifidobacteria cultured on oligosaccharides and other simple carbohydrate sources. *Journal of Applied Microbiology*, 85, 381-386.
- Huebner, J., Wehling, R. L., & Hutkins, R. W. (2007). Functional activity of commercial prebiotics. *International Dairy Journal*, 17, 770-775.
- Iyer, C., & Kailasapathy, K. (2005). Effect of co-encapsulation of probiotics with prebiotics on increasing the viability of encapsulated bacteria under in vitro acidic and bile salt conditions and in yogurt. *Journal of Food Science*, 70, M18-M23.
- Jost, R. (1993). Functional characteristics of dairy proteins. *Trends in Food Science & Technology*, 4, 283-288.
- Kaplan, H., & Hutkins, R. W. (2000). Fermentation of fructooligosaccharides by lactic acid bacteria and bifidobacteria. *Applied and Environmental Microbiology*, 66, 2682-2684.
- Kaupp, G. (2006). Atomic force microscopy. In, *Atomic Force Microscopy, Scanning Nearfield Optical Microscopy and Nanoscratching Application to Rough and Natural Surfaces* (pp. 1-86) P. Avouris, B. Bhushan, D. Klaus von Klitzing, H. Sakaki & R. Wiesendanger (Eds.). Berlin, Heidelberg: Springer-Verlag Berlin Heidelberg.
- Khalil, A. H., & Mansour, E. H. (1998). Alginate encapsulated bifidobacteria survival in mayonnaise. *Journal of Food Science*, 63, 702-705.



- Kilara, A., & Vaghela, M. N. (2004). Whey proteins. In, *Proteins in Food Processing* (1st ed., pp. 72-99) R. Y. Yada (Ed.). Boca Raton, FL: Woodhead Publishing Limited.
- Krasaekoopt, W., Bhandari, B., & Deeth, H. (2004). The influence of coating materials on some properties of alginate beads and survivability of microencapsulated probiotic bacteria. *International Dairy Journal*, 14, 737-743.
- Krasaekoopt, W., Bhandari, B., & Deeth, H. (2003). Evaluation of encapsulation techniques of probiotics for yogurt. *International Dairy Journal*, 13, 3-13.
- Kulkarni, N., & Reddy, B. S. (1994). Inhibitory effect of *Bifidobacterium longum* cultures on the azoxymethane-induced aberrant crypt foci formation and fecal bacterial  $\beta$ -glucuronidase. *Proceedings of the Society of Experimental Biology and Medicine*, 207, 278-283.
- Jensen, W. A. (1962). *Botanical histochemistry - principles and practice* (p 408). San Francisco: Freeman and Company.
- Lee, K., & Heo, T. (2000). Survival of *Bifidobacterium longum* immobilized in calcium alginate beads in simulated gastric juices and bile salt solution. *Applied and Environmental Microbiology*, 66, 869-873.
- Lekka, M., Sainz-Serp, D., Kulik, A. J., & Wandrey, C. (2004). Hydrogel microspheres: Influence of chemical composition on surface morphology, local elastic properties, and bulk mechanical characteristics. *Langmuir*, 20, 9968-9977.
- Lin, J. K., Jacobson, B. J., Pereira, A. N., & Ladisch, M. R. (1988). Liquid chromatography of carbohydrate monomers and oligomers. *Methods in Enzymology*, 160, 145-159.
- Lorca, G. L., & de Valdez, G. F. (2001). A low-pH-inducible, stationary-phase acid tolerance response in *Lactobacillus acidophilus* CRL 639. *Current Microbiology*, 42, 21-25.
- Magonov, S. N., & Yerina, N. A. (2005). Visualization of nanostructures with atomic force microscopy. In, *Handbook of Microscopy for Nanotechnology* (pp. 113) Z. L. Wang, & N. Yao (Eds.). Boston, MA: Kluwer Academic Publishers.
- Marteau, P., Minekus, M., Havenaar, R., & Huis In't Veld, J. H. J. (1997). Survival of lactic acid bacteria in a dynamic model of the stomach and small intestine: validation and the effects of bile. *Journal of Dairy Science*, 80, 1031-1037.

- Mattila-Sandholm, T., Myllarinen, P., Crittenden, R., Mogensen, G., Fonden, R., & Saarela, M. (2002). Technological challenges for future probiotic foods. *International Dairy Journal*, 12, 173-182.
- McKeller, R. C., & Molder, H. W. (1989). Metabolism of fructo-oligosaccharides by *Bifidobacterium spp.* *Applied Microbiology and Biotechnology*, 31, 537-541.
- Miller, K. R., Prescott, C. S., Jacobs, T. L., & Lassignal, N. L. (1983). Artifacts associated with quick-freeze and freeze-drying. *Journal of Ultrastructure Research*, 82, 123-133.
- Moss, P. A., Howard, R. C., & Sheffield, E. (1989). Artifacts arising during preparation of hydrated paper pulp samples for low-temperature SEM. *Journal of Microscopy*, 156, 343-351.
- Muthukumarasamy, P., Allan-Wojtas, P., & Holley, R. A. (2006). Stability of *Lactobacillus reuteri* in different types of microcapsules. *Journal of Food Science*, 71, M20-M24.
- Noda, H., Akasaka, N., & Ohsugi, M. (1994). Biotin production by bifidobacteria. *Journal of Nutritional Science and Vitaminology*, 40, 181-188.
- Olano-Matrin, E., Gibson, G. R., & Rastall, R. A. (2002). Comparison of the *in vitro* bifidogenic properties of pectins and pectic-oligosaccharides. *Journal of Applied Microbiology*, 93, 505-511.
- Penders, J., Vink, C., Driessen, C., London, N., Thijs, C., & Stobberingh, E. E. (2005). Quantification of *Bifidobacterium spp.*, *Escherichia coli* and *Clostridium difficile* in faecal samples of breast-fed and formula-fed infants by real-time PCR. *FEMS Microbiology Letters*, 243, 141-147.
- Picot, A., & Lacroix, C. (2004). Encapsulation of bifidobacteria in whey protein-based microcapsules and survival in simulated gastrointestinal conditions and in yogurt. *International Dairy Journal*, 14, 505-515.
- Pool-Zobel, B., Van Loo, J., Rowland, I. & Roberfroid, M. B. (2002). Experimental evidences on the potential of prebiotic fructans to reduce the risk of colon cancer. *British Journal of Nutrition*, 87, S273-S281.
- Rao, A. V., Shiwnarian, N., & Maharaj, I. (1989). Survival of microencapsulated *Bifidobacterium pseudolongum* in simulated gastric and intestinal juices. *Canadian Institute of Food Science and Technology Journal*, 22, 345-349.

- Rastell, R. A. & Maitin, V. (2002). Prebiotics and synbiotics: towards the next generation. *Current Opinion in Biotechnology*, 13, 490-498.
- Reid, A. A., Vuilleumard, J. C., Britten, M., Arcand, Y., Farnworth, E., & Champagne, C. P. (2005). Microentrapment of probiotic bacteria in a  $\text{Ca}^{2+}$ -induced whey protein gel and effects on their viability in a dynamic gastro-intestinal model. *Journal of Microencapsulation*, 22, 603-619.
- Reid, G. (2002). The potential role of probiotics in pediatric urology. *The Journal of Urology*, 168, 1512-1517.
- Risch, S. J. (1995). Encapsulation: Overview of uses and techniques. In, *Encapsulation and Controlled Release of Food Ingredients* (1<sup>st</sup> ed., pp. 2-7) S. J. Risch, & G. A. Reineccius (Eds.). Washington, DC: American Chemical Society. .
- Roberfroid, M., B. (2000). Nondigestible oligosaccharides. *Critical Reviews in Food Science and Nutrition*, 40, 461-480.
- Rossi, M., Corradini, C., Ameratti, A., Nicolini, M., Pompei, A., & Zanoni, S. (2005). Fermentation of fructooligosaccharides and inulin by bifidobacteria: a comparative study of pure and fecal cultures. *Applied and Environmental Microbiology*, 71, 6150-6158.
- Rugar, D., & Hansma, P. (1990). Atomic force microscopy. *Physics Today*, 43, 23-30.
- Sabra, W., & Deckwer, W. (2005). Alginate a polysaccharide of industrial interest and diverse biological functions. In, *Polysaccharides Structural Diversity and Functional Versatility* (2<sup>nd</sup> ed., pp. 515-533) S. Dumitriu (Ed.). New York, NY: Marcel Dekker.
- Simpson, P. J., Stanton, C., Fitzgerald, G. F., & Ross, R. P. (2005). Intrinsic tolerance of bifidobacterium species to heat and oxygen and survival following spray drying and storage. *Journal of Applied Microbiology*, 99, 493-501.
- Sperti, G. S. (Ed.). (1971). *Probiotics* (1<sup>st</sup> ed.). West Point, CT: Avi Publishing Co.
- Sriamornsak, P., Thirawong, N., Cheewatanakornkool, K., Burapapadh, K., & Sae-Ngow, W. (2008). Cryo-scanning electron microscopy (cryo-SEM) as a tool for studying the ultrastructure during bead formation by ionotropic gelation of calcium pectinate. *International Journal of Pharmaceutics*, 353, 115-122.
- Sultana, K., Godward, G., Reynolds, N., Arumugaswamy, R., Peiris, P., & Kailasapathy, K. (2000). Encapsulation of probiotic bacteria with alginate-starch and evaluation of

- survival in simulated gastrointestinal conditions and in yogurt. *International Journal of Food Microbiology*, 62, 47-55.
- Tjernberg, A., Markova, N., Griffiths, W. J., & Hallen, D. (2005). DMSO-related effects in protein characterization. *Journal of Biomolecular Screening*, 11, 131-137.
- Tomomatsu, H. (1994). Health effects of oligosaccharides. *Food Technology*, 48, 61-65.
- Truelstrup-Hansen, L., Allan-Wojtas, P. M., Jin, Y., & Paulson, A. T. (2002). Survival of Ca-alginate microencapsulated *bifidobacterium* sp. in milk and simulated gastrointestinal conditions. *Food Microbiology*, 19, 35-45.
- Truernit, E., & Haseloff, J. (2008). A simple way to identify non-viable cells within living plant tissue using confocal microscopy. *Plant Methods*, 4, 15-21.
- van Dokkum, W., & van den Heuvel, E. (2001). Nondigestible oligosaccharides and mineral absorption. In, *Handbook of Dietary Fiber* (1st ed., pp. 259-268) S. S. Cho, & M. L. Dreher (Eds.). New York, NY: Marcel Dekker, Inc.
- Vernazza, C. L., Gibson, G. R., & Rastall, R. A. (2006). Carbohydrate preference, acid tolerance and bile tolerance in five strains of *bifidobacterium*. *Journal of Applied Microbiology*, 100, 846-853.
- Walter, R. H. (Ed.). (1991). *The Chemistry and Technology of Pectin* (1<sup>st</sup> ed.). San Diego, CA: Academic Press, Inc.
- Zimmermann, H., Hillgartner, M., Manz, B., Feilen, P., Brunnenmeier, F., & Leinfelder, U. (2003). Fabrication of homogeneously cross-linked functional alginate microcapsules validated by NMR-, CLSM- and AFM-imaging. *Biomaterials*, 24, 2083-2096.
- Zohar-Perez, C., Chet, I., & Nussinovitch, A. (2004). Irregular textural features of dried alginate–filler beads. *Food Hydrocolloids*, 18, 249-258.